REGULATION OF HYPOTHALAMIC-PITUITARY-INTERRENAL AXIS FUNCTION DURING CHRONIC SOCIAL STRESS IN RAINBOW TROUT (*Oncorhynchus mykiss*)

Carol Best, M.Sc.

Thesis submitted to the University of Ottawa
in partial fulfillment of the requirements for the
Doctorate in Philosophy degree in Biology

Department of Biology
Faculty of Science
University of Ottawa

Abstract

The hypothalamic-pituitary-interrenal (HPI) axis in fishes controls the production of cortisol in response to a stressor. To study HPI axis regulation during chronic stress, pairs of juvenile rainbow trout (*Oncorhynchus mykiss*) were allowed to form dominance hierarchies. Subordinate trout experience chronic social stress associated with a sustained elevation in circulating cortisol levels. Circulating cortisol levels reflect the balance between negative feedback regulation of the HPI axis and cortisol clearance, both of which lower cortisol levels, and cortisol production via HPI axis activation. The capacity for negative feedback and cortisol clearance appeared to be intact in subordinate fish, based on the rapid decline in cortisol after cortisol injection or during recovery from social stress. In addition, corticosteroid receptor transcript and protein abundances throughout the HPI axis did not differ between dominant and subordinate trout. Elevated transcript abundances of 11β-hydroxysteroid dehydrogenase type 2 (*11βhsd2*) in the preoptic area (POA) and pituitary of subordinate fish suggested an enhanced role for this cortisol-inactivating enzyme during chronic social stress. Steroidogenesis occurs in the interrenal cells of the head kidney, and appeared to be a primary driver of increased plasma cortisol levels in subordinate trout. Transcript abundances of the HPI axis effectors corticotropin releasing factor (*crf*) and pro-opiomelanocortin (*pomc*) were not elevated in the POA or pituitary, respectively, of subordinate trout. However, rate-limiting components of head kidney steroidogenesis were elevated, including steroidogenic acute regulatory protein (*star*) and P450 side chain cleavage enzyme (*p450scc*). A novel finding in the head kidney was increased transcript abundance of steroidogenic factor 1, which regulates steroidogenic enzyme transcription in mammals. Accordingly, head kidney preparations from subordinate trout exhibited increased basal cortisol production *in vitro*. Despite this elevation in basal

steroidogenesis, subordinate rainbow trout demonstrated attenuated cortisol production in response to stimulation by exogenous adrenocorticotropic hormone (ACTH) both *in vivo* and *in vitro*. A similar attenuation was observed with cAMP, suggesting that impairment of acute cortisol production arises downstream of cAMP in the ACTH signalling pathway. The regulation of *crf* in the POA during chronic social stress was probed in more detail by measuring the abundance of selected microRNAs (miRNA) predicted to target and reduce *crf* or *11βhsd2* mRNA, but these were not found to play a role. Methylation of the *crf* promoter revealed significantly decreased methylation at two loci in dominant trout, but the functional significance of this methylation pattern requires further study. Collectively, the present thesis used an array of experimental approaches to provide a comprehensive picture of HPI axis regulation during chronic social stress in rainbow trout.

Résumé

Chez les téléostéens, l'axe hypothalamo-pituitaire-interrénal (HPI) contrôle la production de cortisol en réponse à un stresseur. Pour étudier la régulation de l'axe HPI pendant un stress chronique, on a permis à des paires de truites arc-en-ciel juvéniles (*Oncorhynchus mykiss*) de former des hiérarchies de dominance. Les truites subordonnées subissent un stress social chronique associé à une élévation soutenue des niveaux de cortisol circulant. Les niveaux de cortisol circulant reflètent l'équilibre entre la régulation par rétroaction négative de l'axe HPI et la clairance du cortisol, qui abaissent les niveaux de cortisol, et la production de cortisol par l'activation de l'axe HPI. La capacité de rétroaction négative et de clairance du cortisol semble être intacte chez les poissons subordonnés, d'après le déclin rapide du cortisol après l'injection de cortisol ou pendant la récupération après un stress social. De plus, l'abondance de l'ARNm et des protéines des récepteurs corticostéroïdes dans l'ensemble de l'axe HPI ne différait pas entre les truites dominantes et subordonnées. L'abondance élevée de l'ARNm de la 11β-hydroxystéroïde déshydrogénase de type 2 (*11βhsd2*) dans la zone préoptique (POA) et la pituitaire des poissons subordonnés a suggéré un rôle important pour cette enzyme cortisol-inactivant pendant le stress social chronique. La stéroïdogénèse se produit dans les cellules interrénales du rein antérieur, et semble être le principal facteur de l'augmentation des niveaux de cortisol plasmatique chez les truites subordonnées. L'abondance des products de la transcription des effecteurs de l'axe HPI, le facteur de libération de la corticotropine (*crf*) et la pro-opiomélanocortine (*pomc*), n'était pas élevée dans la POA ou la pituitaire, respectivement, des truites subordonnées. Cependant, les composants limitant la vitesse de la stéroïdogenèse dans le rein antérieur étaient élevés, y compris la protéine régulatrice aiguë stéroïdogène (*star*) et l'enzyme de clivage de la chaîne latérale P450 (*p450scc*). L'abondance élevée de la transcription du facteur stéroïdogénique 1, qui

régule la transcription des enzymes stéroïdogénique chez les mammifères, a été une nouvelle découverte dans le rein antérieur. En conséquence, les préparations de reins antérieurs provenant de truites subordonnées ont présenté une production accrue de cortisol basal *en vitro*. Malgré cette augmentation de la stéroïdogenèse basale, la truite arc-en-ciel subordonnée a démontré une production atténuée de cortisol en réponse à une stimulation par l'hormone adrénocorticotrope (ACTH) exogène, à la fois *en vivo* et *en vitro*. Une atténuation similaire a été observée avec l'AMPc, ce qui suggère que l'altération de la production aiguë de cortisol se produit en aval de l'AMPc dans la voie de signalisation de l'ACTH. La régulation de *crf* dans la POA au cours d'un stress social chronique a été étudiée plus en détail en mesurant l'abondance de certains microARN (miARN) dont on a prédit qu'ils ciblaient et réduisaient l'ARNm de *crf* ou de *11βhsd2*, mais ils ne se sont pas avérés jouer un rôle. La méthylation du promoteur de *crf* a révélé une diminution significative de la méthylation à deux loci chez la truite dominante, mais la signification fonctionnelle de ce profil de méthylation nécessite une étude plus approfondie. Collectivement, la présente thèse a utilisé un ensemble d'approches expérimentales pour fournir une image complète de la régulation de l'axe HPI pendant un stress social chronique chez la truite arc-en-ciel.

Acknowledgements

First and foremost, thank you to my supervisor Dr. Katie Gilmour. Your support, guidance, and composure in the face of adversity has been invaluable on this PhD journey. Whether I came to your office with good news or less good news, I always left feeling optimistic. Your enthusiasm about and dedication to both science and your students makes you an exemplary scientist, and I am thankful to have learned so much from you as a mentor. Thank you for all your hard work and support over these past years.

I would like to thank those with whom I have shared a lab over the course of my time at the University of Ottawa. Thank you to all past and present members of the Gilmour lab. When I first began in the lab, Jon Tea, Marie-Ève Bélair-Bambrick, Alex Hare, Julia Redfern, and Natalia Koudrina all made me feel immediately welcomed through our chats, outings, lab "sports" and many laughs. To Brittany Bard, Brenna Wilson, Emma Kunert and Liam Tigert, finishing a thesis during a pandemic is not straightforward, and I am not only thankful for your support but impressed by you all. I would also like to thank all the past and present members of the Perry and Mennigen labs, especially Dr. Kevin Pan, and Dan Kostyniuk. I feel like I have "shared a lab" with the whole comparative physiology group. In particular, thank you to the Standen, Pamenter, and Weber labs. Between the friendly chats, collaborations, and help with science, I could not ask for better lab neighbours. Thank you also to the support staff at uOttawa, particularly Bill Fletcher in the aquatics facility and all the folks at the science store.

I would like to thank the members of my thesis advisory committee, Dr. Jan Mennigen, Dr. Marc Ekker, and Dr. Ken Storey for your advice and guidance. Thank you to my external examiner, Dr. Nadia Aubin-Horth, for your valuable feedback and insight. A special thank you to Dr. Jan Mennigen. Your enthusiasm for science and positive attitude are infectious and I am

grateful for your support. Thank you also to Dr. Matt Vijayan for your mentorship since the very beginning.

Thank you to Drs. Milica Mandic and Alex Zimmer. I am so lucky to have met you and to call you my friends. I am grateful for your support and advice through these past years, both inside and outside the lab. To you both, and to Bazil, I am fairly certain our games nights and other outings kept me sane, but I am uncertain if I will ever improve my Dominion game. To Tiffany, Sindu, Herthana, Sarah, Sana, and Katie, thank you for your friendship despite the distance between us!

To my family, thank you for putting up with me when I said I would only be 15 more minutes in the lab, and it ended up being 2 hours. You have supported me in every sense of the word, and I am always thankful for you. To Brett, thank you first specifically for your help with this thesis, and thank you for always being there.

Table of Contents

List of Figures

List of Tables

List of Abbreviations

Abbreviation	Full Name
11βHSD1	11β hydroxysteroid dehydrogenase type 1
11βHSD2	11β hydroxysteroid dehydrogenase type 2
11KT	11-ketotestosterone
20βHSD2	20β hydroxysteroid dehydrogenase type 2
ACTH	adrenocorticotropic hormone
ANCOVA	analysis of covariance
ANOVA	analysis of variance
AVP	arginine vasopressin
AVT	arginine vasotocin
BCA	bicinchoninic acid
BSA	bovine serum albumin
cAMP	cyclic adenosine monophosphate
cDNA	complementary DNA
CLIP	corticotrophin-like intermediate lobe peptide
CNSS	caudal neurosecretory system
CpG	cytosine-phosphate-guanine
CpH	cytosine-phosphate-adenine/cytosine/thymine (H)
CRE	cAMP response element
CRF	corticotropin releasing factor
CRFR1/2	CRF receptor 1 or 2
CYP11A1	cholesterol side-chain cleavage enzyme (P450SCC)
DAPI	4′,6-diamidino-2-phenylindole
db-cAMP	dibutyryl-cAMP
DNA	deoxyribonucleic acid
DNMT1, 3A, 3B	DNA methyltransferase 1, 3A, or 3B
E2	estradiol
EF1α	elongation factor 1 alpha

FF1	fushi tarazu factor 1 (SF-1)
gDNA	genomic DNA
GNRH3	gonadotropin-releasing hormone 3
GR1/2	glucocorticoid receptor 1 or 2
GRE	glucocorticoid response element
HK	head kidney
HPA	hypothalamic-pituitary-adrenal
HPI	hypothalamic-pituitary-interrenal
HRP	horseradish peroxidase
IP	intraperitoneal
IPTG	isopropyl β-d-1-thiogalactopyranoside
LB	lysogeny broth
LN_2	liquid nitrogen
LNA	locked nucleic acid
MC2R	melanocortin 2 receptor
miRNA	microRNA
MR	mineralocorticoid receptor
MRAP1/2	melanocortin 2 receptor accessory protein 1 or 2
mRNA	messenger RNA
MSH	melanocyte-stimulating hormone
MyoD	myoblast determination protein 1
ncRNA	non-coding RNA
NPO	nucleus preopticus
P450SCC	cholesterol side-chain cleavage enzyme (CYP11A1)
PBS	phosphate buffered saline
PBST	PBS + 0.2% Triton X-100
PC	prohormone convertase
PCA	principal component analysis
PCR	polymerase chain reaction
PFA	paraformaldehyde

PKA	protein kinase A
POA	preoptic area
POMC	pro-opiomelanocortin
pri-miRNA	primary miRNA
PVDF	polyvinylidene fluoride
PVN	paraventricular nucleus
RIPA	radioimmunoprecipitation assay
RISC	RNA-induced silencing complex
RNA	ribonucleic acid
RT-PCR	reverse transcription polymerase chain reaction
RU-486	Roussel-Uclaf 486
SDS-PAGE	sodium dodecyl sulphate–polyacrylamide gel electrophoresis
SEM	standard error of the mean
SF-1	steroidogenic factor-1 (FF1)
snRNA	small nuclear RNA
StAR	steroidogenic acute regulatory (protein)
TBST	Tris-buffered saline with 0.05% Tween-20
TH	tyrosine hydroxylase
UTR	untranslated region

Note on nomenclature:

Gene and protein symbol nomenclature will follow the convention for zebrafish, *Danio rerio* (Mullins et al., 1998): lowercase italics for gene, title case for protein (e.g. *crf* and Crf for gene and protein, respectively). Uppercase (e.g. CRF) will be used for general reference.

Chapter 1: General Introduction

Parts of this section are also present as part of a review in preparation for submission to the *Journal of Experimental Biology* in collaboration with Dr. S. Currie (Acadia University, NS, CA):

Best, C., Currie, S., and Gilmour, K.M. "Social stress in fishes: physiological responses and the underlying mechanisms" (In preparation)

1.1 Overview of the thesis

In vertebrates, activation of the endocrine stress response is critical for animals to cope with stressors, and this stress response can manifest its effects on most aspects of an animal's physiology. Additionally, the animal's environment and physiology can impact the functioning of their stress response. In teleost fishes, the endocrine stress response is coordinated by the hypothalamic-pituitary-interrenal (HPI) axis (Bernier et al., 2009; Faught et al., 2016; Gorissen and Flik, 2016). The stress response of fishes has been studied in many species and contexts, and although general aspects of the response appear to be conserved, many factors can influence the timing and magnitude of HPI axis function. The present thesis addresses HPI axis activation and regulation in the context of chronic stress, when plasma cortisol levels are elevated for several days. The chronic stressor model used in this thesis is social subordination in juvenile rainbow trout (*Oncorhynchus mykiss*). This model is well established, with previous studies providing a robust foundation for the present research (Gilmour et al., 2005; Johnsson et al., 2006; Sørensen et al., 2013). Chapter 2 addresses mechanisms of HPI axis activation, negative feedback, and cortisol clearance during chronic social stress. Chapter 3 assesses the dynamics of cortisol production in the head kidney during chronic social stress, a context in which fish exhibit high basal cortisol levels and an attenuated ability to produce cortisol in response to an additional acute stressor. Chapter 4 explores regulation at the head of the HPI axis during chronic social stress, measuring endocrine and epigenetic factors that potentially regulate corticotropin releasing factor (CRF) in the preoptic area (POA) of the rainbow trout brain and/or activate the stress axis downstream of CRF. Together, these studies aimed to test the general hypothesis that chronic activation of the HPI axis by social stress modifies the normal regulation of the HPI axis with consequences for its function. This general introduction will provide background

information and context for the research, including a brief review of the HPI axis and its regulation, chronic stress, social hierarchies, and epigenetics. An outline of the specific objectives of the thesis also will be presented.

1.2 The HPI axis and its regulation in teleost fishes

Generally, stress is any perceived threat to an animal's homeostasis, and the stress response is the suite of behavioural and physiological reactions that enables the animal to cope with the stressor (Barton, 2002; Charmandari et al., 2005; Iwama, 1998; Romero et al., 2009; Schulte, 2014; Wendelaar Bonga, 1997). Many definitions also include the caveat that a prolonged stress response may lose its adaptive value (Barton, 2002; Charmandari et al., 2005; Wendelaar Bonga, 1997). The HPI axis mediates the glucocorticoid stress response in vertebrates and is the focus of the present thesis, but the endocrine stress response also includes the catecholamine response. The catecholamine response has both a faster onset and a shorter duration than the glucocorticoid response (Faught et al., 2016). Acute stressors activate the sympathetic division of the autonomic nervous system, stimulating the release of norepinephrine from postganglionic neurons to elicit responses such as an increased heart rate and the redirection of blood flow, as well as the release of epinephrine and norepinephrine into the blood from chromaffin cells in the head kidney (Vijayan et al., 2010). In addition to supporting the cardiovascular effects of the postganglionic neurons, which ultimately maintain or increase oxygen delivery to the tissues, the circulating catecholamines also stimulate the mobilization of energy reserves to aid the animal in coping with the stressor (Fabbri et al., 1998; Reid et al., 1998; Vijayan et al., 2010).

The glucocorticoid response to a stressor centres on increased cortisol production via activation of the HPI axis in teleost fishes (Bernier et al., 2009; Faught et al., 2016; Gorissen and Flik, 2016; Vijayan et al., 2010). Briefly, stressor perception causes the release of CRF from neurons in the POA of the brain to the corticotropes of the anterior pituitary. The corticotropes release adrenocorticotropic hormone (ACTH) into the circulation, which promotes cortisol production by the interrenal cells of the head kidney. Cortisol is distributed throughout the body by the circulation, and given the relatively small size and hydrophobic nature of this steroid hormone, it passes through cell membranes directly by diffusion. Cortisol then exerts its effects on target tissues through the corticosteroid receptors, which include glucocorticoid and mineralocorticoid receptors (GR and MR, respectively) and serve as ligand-activated transcription factors. There is some evidence to support a role for nongenomic (i.e. independent of transcription and translation) cortisol signalling in fishes (Das et al., 2018), but this thesis will focus on the classical receptors. To bring cortisol back down to resting or unstressed (basal) levels, HPI axis activity is reduced through negative feedback regulation by its ultimate effector, cortisol. Cortisol levels are also brought down by catabolism, mainly through the hepato-biliary route. The HPI axis is discussed in more detail in the following sections, with special attention to evidence in fishes.

1.2.1 The hypothalamic-pituitary (HP) axis

Perception of the stressor is the initial step for activation of the HPI axis (Barton, 2002). These stressor signals are integrated by the brain, leading to stimulation of the CRF neurons within the POA of the brain (Cerdá-Reverter and Canosa, 2009), which is analogous to the paraventricular nucleus (PVN) in mammals (Herget and Ryu, 2015). In mammals, CRF neurons

are directly stimulated by glutamate and norepinephrine during stress, although other afferent neurotransmitters may modulate this response (Aguilera and Liu, 2012); less is known about CRF neuron stimulation in teleosts. CRF neurons terminate mainly on corticotropes which are located in the rostral pars distalis of the pituitary (Bernier et al., 2009; Cerdá-Reverter and Canosa, 2009). Initial CRF release is from stored vesicles, and although evidence supports *crf* transcript upregulation by stressors in fishes, responses have been inconsistent, possibly reflecting the use of different stressor models (Faught et al., 2016). Although there are four paralogues of *crf* in trout (Lai et al., 2021), most work on stress has focused on *crfb1* (Alderman et al., 2012; Backström et al., 2011; Bernier et al., 2008; Craig et al., 2005; Jeffrey et al., 2012; Jeffrey et al., 2014; Madison et al., 2013), which is also the case in the present thesis. Chapter 4 addresses the transcriptional regulation of *crf* during chronic social stress, in the context of previous studies, as well as in the light of potential epigenetic mechanisms of control. CRF action on the corticotropes of the pituitary is mediated by the CRF receptors CRFR1 and CRFR2 (Manuel et al., 2014). CRF binding protein may also modulate CRF signalling at the pituitary (Manuel et al., 2014). While central CRF has received more research attention, this neuropeptide is also found peripherally. The caudal neurosecretory system (CNSS) is located at the end of the spinal cord and has high *crf* transcript abundance (Bernier et al., 2008). Although the physiological function of the CNSS is not well established, it does not appear to upregulate *crf* transcription after 24 h of social stress (Bernier et al., 2008). CRF is also expressed in other peripheral tissues, although at lower levels, and therefore may have local functions in teleosts as it does in mammals, such as in the heart (Williams and Bernier, 2017) and head kidney (Huising et al., 2007).

In addition to CRF, there are several other corticotropic hormones that trigger release of ACTH from the pituitary (reviewed by Bernier et al., 2009). Although most of these are less potent than CRF, arginine vasotocin (AVT) may be important in chronic stress responses. The mammalian homologue of AVT, arginine vasopressin (AVP), has been shown to be elevated during chronic stressors and can act to potentiate the action of CRF while being less susceptible to negative feedback (Aguilera and Rabadan-Diehl, 2000). In rainbow trout, AVT causes the release of ACTH from the pituitary, and also does so synergistically with CRF (Baker et al., 1996). The role of AVT during chronic social stress is addressed in Chapter 4.

CRF stimulates the corticotropes of the anterior pituitary to release ACTH into the systemic circulation. The teleost pituitary, as in mammals, consists of the adenohypophysis (anterior pituitary) and the neurohypophysis (posterior pituitary), and corticotropes are located in the pars distalis of the anterior pituitary (Bernier et al., 2009; Gorissen and Flik, 2016). A key difference between the mammalian and teleost systems is the absence of a hypophyseal portal system in teleost fishes (Gorissen and Flik, 2016). In mammals, releasing hormones enter a capillary network (the median eminence) and reach their target cells in the pituitary via a local circulation, the hypophyseal portal system (Aguilera and Liu, 2012; Charmandari et al., 2005). In teleosts, the neurosecretory cells containing the releasing hormones innervate the pituitary directly, which avoids dilution of the signalling molecule in the blood and likely changes signalling and receptor dynamics (Gorissen and Flik, 2016). CRF receptors in fishes, as in other taxa, are G-protein coupled receptors that bring about an elevation in cAMP that serves to release ACTH into the circulation (Abou-Samra et al., 1987; Huising et al., 2004). CRF also plays a role in upregulating transcription of pro-opiomelanocortin (POMC), the precursor protein for ACTH, but transcript levels can vary with stressor type (Aguilera, 1994). There are three paralogues of

POMC in rainbow trout, owing to both the teleost (A and B) and salmonid (A1 and A2) whole genome duplications (Leder and Silverstein, 2006). There is insufficient information to assign these paralogues functional differences in the HPI axis, so all three were examined in this thesis. POMC is processed by prohormone convertase (PC) 1/3 in corticotropes to yield ACTH and β-lipotropin, which together can be further processed by PC2 to yield melanocyte-stimulating hormone (α and β-MSH), corticotrophin-like intermediate lobe peptide (CLIP), γ-lipotropin, and β-endorphin (Chrétien and Mbikay, 2016; Leder and Silverstein, 2006). ACTH is then packaged into secretory granules to be released upon stimulation by CRF (Cawley et al., 2016). Once in the blood stream, ACTH stimulates glucocorticoid production in steroidogenic cells.

1.2.2 Head kidney and steroidogenesis of cortisol

Mammalian glucocorticoid-producing cells are consolidated in a layer (zona fasciculata) within the adrenal cortex whereas in teleosts these cells are dispersed in clusters throughout the anterior (head) kidney (Gallo and Civinini, 2003). The steroidogenic cells, also termed interrenal cells, comprise about 1 out of every 8000 cells in the rainbow trout head kidney (HK) (Hontela et al., 2008). Steroidogenesis of cortisol begins with cholesterol. The rate of steroid production is thought to be limited by shuttling of cholesterol from the outer to the inner mitochondrial membrane and initial processing of cholesterol, steps that are facilitated by steroidogenic acute regulatory protein (StAR) and cholesterol side-chain cleavage enzyme (CYP11A1, or P450scc), respectively (Aluru and Vijayan, 2008; Tokarz et al., 2015). A key difference from mammals is that fishes do not have the enzyme required to synthesize aldosterone, and thus lack this mineralocorticoid hormone (Tokarz et al., 2015). Therefore, cortisol acts as a mineralocorticoid as well as a glucocorticoid in fishes (Takahashi and Sakamoto, 2013). Whether another

mineralocorticoid exists in fishes remains an open question (McCormick et al., 2008; Sturm et al., 2005). Subsequent enzymatic conversion steps occur, primarily in the smooth endoplasmic reticulum but also in the mitochondria, with the final step to produce cortisol catalyzed by 11β-hydroxylase (Bremer and Miller, 2014; Tokarz et al., 2015). Cortisol passes through the interrenal cell membrane to be distributed throughout the body via the circulation and diffusion. Unlike in mammals, there does not appear to be a specific corticosteroid-binding globulin in fishes (Breuner and Orchinik, 2002; Hammond, 2016).

To upregulate production of cortisol when the HPI axis is activated by a stressor, circulating ACTH binds to the melanocortin 2 receptor (MC2R) on the interrenal cells (Aluru and Vijayan, 2008). The melanocortin 2 receptor accessory protein (MRAP) supports MC2R function by trafficking this receptor to the plasma membrane (Agulleiro et al., 2010; Dores et al., 2016). Although there are at least 2 paralogues of MRAP in teleosts, only MRAP1 has been shown to be required for teleost MC2R activation in a heterologous cell line (Dores and Garcia, 2015; Liang et al., 2015). This MC2R receptor system is G-protein coupled, such that ligand binding results in the production of intracellular cAMP by adenylate cyclase, which increases protein kinase A (PKA) activity to bring about phosphorylation and increased transcription of key players in steroidogenesis (Aluru and Vijayan, 2008; Lacroix and Hontela, 2001; Sewer and Waterman, 2003). Acute stimulation of rainbow trout head kidney tissue with ACTH *in vitro* results in increases in *star*, *p450scc*, and *mc2r* transcripts, and increased cortisol production (Aluru and Vijayan, 2008). Although the promoters of steroidogenic genes are less functionally characterized in fishes than in mammals, cAMP response elements (CRE) are found in many of the promoters of mammalian steroidogenic genes (Ruggiero and Lalli, 2016). Binding sites for steroidogenic factor 1 (SF-1) also are found in the promoter of most steroidogenic genes; SF-1 is

an orphan nuclear receptor (NR5A1) important in adrenal development as well as gene expression in steroidogenic cells (Ruggiero and Lalli, 2016; Val et al., 2003). Some work characterizing SF-1 has been carried out in zebrafish, *Danio rerio* (Kuo et al., 2005) and the salmonid arctic char (*Salvelinus alpinus*, Von Hofsten et al., 2003), but little is known in teleosts about the role of this transcription factor during the stress response. Chapter 3 of the present thesis addresses the impact of chronic social stress on the steroidogenic pathway, under both basal and stimulated conditions. This distinction is important because whereas chronic social stress results in sustained elevation of cortisol over several days, the response of these chronically stressed fish to an additional acute stressor is blunted (Jeffrey et al., 2014). The mechanism by which this blunting occurs appears localized, at least in part, to the head kidney, but little is known about the underlying mechanisms. Circulating cortisol exerts its effects in target tissues throughout the body via the corticosteroid receptors.

1.2.3 Corticosteroid receptors

Cortisol signalling in fishes occurs through GR and MR, both of which are cytosolic nuclear receptors which translocate to the nucleus upon receptor binding, where they then act as transcription factors to alter transcription of target genes (Faught et al., 2016). The teleost-specific whole genome duplication resulted in two paralogues of GR, GR1 and GR2 (Bury et al., 2003). Binding studies *in vitro* of the rainbow trout GR paralogues suggest GR2 has a greater affinity for cortisol than GR1, but functional differences between these two have not been well established in fishes (Bury et al., 2003). In mammals, the primary ligand for MR is aldosterone. Cortisol binds to MR in mammals with a greater affinity than aldosterone, which is why in certain tissues MR is co-expressed with the cortisol-metabolizing enzyme 11β-hydroxysteroid

dehydrogenase type 2 (11βHSD2) to attain aldosterone selectivity (Chapman et al., 2013). Fishes lack aldosterone, and at least some mineralocorticoid actions in fishes are mediated through cortisol and GR (Gilmour, 2005; Takahashi and Sakamoto, 2013). GR is also implicated in growth, metabolism, immune function, and stress (Vijayan et al., 2010). The functional consequences of GR activation in fishes are better characterized than MR, but recent studies support a potential role for MR in stress and metabolism (Faught and Vijayan, 2018; Faught and Vijayan, 2020; Sakamoto et al., 2016).

Cortisol has a wide array of physiological functions that are mediated through these receptors, including regulation of metabolism (mainly in the liver, muscle, and adipose tissue) to shift and replenish energy stores to cope with the demands of stress, as well as osmoregulation in the gill (Mommsen et al., 1999; Sadoul and Vijayan, 2016; Takei and Hwang, 2016). Some of these endpoints have been characterized during chronic social stress in juvenile salmonids (reviewed by Gilmour et al., 2005), as has target tissue receptor abundance (Jeffrey et al., 2012). The present thesis focuses on the mechanisms of regulation of the HPI axis itself, so the cortisol receptors are measured in the HPI axis tissues in Chapter 2 to gain insight into their role in negative feedback during chronic social stress.

1.2.4 Negative feedback

The HPI axis, like most endocrine axes, is regulated by negative feedback; that is, cortisol levels are detected by HPI axis tissues, and activity is adjusted accordingly (Bernier et al., 2009; Keller-Wood, 2015). Negative feedback plays a key role in returning cortisol to unstressed (basal) levels following stressor-mediated elevation. In mammals, this negative

feedback is mediated mainly at the level of the brain and pituitary, mostly by GR but also MR (Keller-Wood, 2015). The mammalian homologue of the POA is the paraventricular nucleus (PVN), and this area is targeted by negative feedback in mammals, as are the corticotropes in the pituitary (Keller-Wood, 2015). The mechanisms involved in negative feedback at a cellular level include transcriptional repression of *crf* and *pomc*; however cortisol can also exert negative feedback effects upstream of the PVN, and even nongenomically (Hill and Tasker, 2012; Keller-Wood, 2015). Negative feedback mechanisms are less well characterized in fishes than in mammals, but there is evidence to support a role for negative feedback in modulating HPI axis function in fishes. Both GR and MR are present in the brain, pituitary and head kidney of rainbow trout (Bury et al., 2003; Teitsma et al., 1999; Teles et al., 2013). Receptor knockdown or knockout disrupts stress axis functioning suggesting a role in negative feedback, although receptor abundance in all tissues is impacted so the mechanism is difficult to tease apart (Alderman et al., 2012; Faught and Vijayan, 2018). In addition, cortisol-mediated negative feedback has been functionally demonstrated at each HPI axis level. Cortisol implanted into the POA inhibited cortisol elevation due to a stressor in goldfish, *Carassius auratus* (Fryer and Peter, 1977). Adding cortisol to goldfish pituitary cells *in vitro* reduced their ACTH secretion (Fryer et al., 1984). Even at the level of the head kidney, there is evidence for ultra-short loop negative feedback by cortisol in *in vitro* preparations from coho salmon (*Oncorhynchus kisutch*) (Bradford et al., 1992). In Chapter 2 of the present thesis, negative feedback is assessed during chronic social stress to gain insight into how negative feedback operates in a context where elevated cortisol is sustained for several days.

1.2.5 Cortisol catabolism and 11βHSD2

One aspect of the stress response that has received less attention is the clearance of cortisol. Given that plasma cortisol levels reflect the net effect of cortisol production by the head kidney and cortisol clearance from the blood, the dearth of studies assessing cortisol kinetics in teleosts is surprising (but see Donaldson and Fagerlund, 1972; Nichols et al., 1985; Owen and Idler, 1972; Redding et al., 1984; Vijayan and Leatherland, 1990; Vijayan and Moon, 1994; Wilson et al., 1998). The first step in the catabolism of cortisol is its conversion to cortisone catalyzed by 11βHSD2 (Tokarz et al., 2013). In addition to inactivating cortisol, 11βHSD2 catalyses the synthesis of 11-ketotestosterone (11-KT), the primary androgen in teleosts (Tokarz et al., 2015). In mammals, 11βHSD1 catalyses the conversion of cortisone to cortisol which helps to amplify the cortisol signal; this reaction can comprise about 20-40% of cortisol production in humans (Basu et al., 2004; Chapman et al., 2013). However, teleost fishes lack *11βhsd1* (Tsachaki et al., 2017). The absence from fishes of both aldosterone (and therefore the role of 11βHSD2 in conferring aldosterone specificity at MR) and *11βhsd1* (making the deactivation of cortisol by 11βHSD2 irreversible), together with the presence of 11-KT as the primary androgen (involving 11βHSD2 in the reproductive system) suggest that although the functional activity of 11βHSD2 is conserved between fishes and mammals, its physiological roles may diverge. Knowledge of teleost 11βHSD2 remains limited, but in zebrafish, *11βhsd2* is expressed in many tissues, contains putative glucocorticoid response elements (GREs) in its promoter, and increases in response to cortisol exposure (Alderman and Vijayan, 2012; Best and Vijayan, 2017; Tokarz et al., 2013; Tsachaki et al., 2017). Additionally, whole-body inhibition of 11βHSD2 activity increased *crf* and *mr* transcript abundances in the POA (Alderman and Vijayan, 2012), suggesting a role for 11βHSD2 in the modulation of HPI axis negative feedback.

Overall, 11βHSD2 is the initial step in cortisol clearance, but it may also act to regulate cortisol availability at a cellular and/or receptor level.

The typical path of cortisol catabolism in vertebrates is through the hepato-biliary route (Aerts, 2018). The fate of radiolabelled cortisol in rainbow trout is predominantly the bile of the gall bladder, indicated by the accumulation of radioactive catabolites (Truscott, 1979; Wilson et al., 1998). Cortisol catabolites can also be eliminated through the gill and urine (Idler and Truscott, 1972). Based on the products identified in the bile, cortisol and cortisone are converted by 5β-reductase, then 3α-hydroxysteroid dehydrogenase, and 20β-hydroxysteroid dehydrogenase to 5β-dihydroxy-, tetrahydro-, and 20β-cortol- metabolites, respectively, with glucuronidation and sulphation occurring to increase solubility (Pottinger et al., 1992; Truscott, 1979). Recently, it was found that cortisone can be converted to 20β-hydroxycortisone by 20βHSD2, and 20β-hydroxycortisone is a metabolite that appears to be readily excreted into the holding water, avoiding the hepato-biliary route (Tokarz et al., 2013). Although little is known at present about the regulation of cortisol catabolism and excretion, this field of study is becoming increasingly relevant as measurement of cortisol in tissues like the scales is being validated as a non-lethal marker of chronic stress (Aerts et al., 2015; Laberge et al., 2019). The impact of chronic social stress on the tissue distribution and clearance of a cortisol bolus was assessed in Chapter 2.

1.3 Chronic stress

Acute stressors have received substantially more research attention in terms of the HPI axis and cortisol dynamics because they provide a rapid and robust activation of the HPI axis, resulting in a (somewhat) predictable rise and fall in cortisol level, although the cortisol profile

depends somewhat on the stressor severity and duration (Barton, 2002; Schreck and Tort, 2016). Although the rise in cortisol is attributable to HPI axis activation, the fall in cortisol is achieved through a combination of negative feedback, and clearance (Mommsen et al., 1999). An exact temporal distinction between chronic and acute stress is difficult to define as it is based on context (Schreck and Tort, 2016), but for the purposes of this thesis it is defined as lasting more than a few hours. In this framework, HPI axis activity during chronic stressors is less predictable because the prolonged nature of the response leads to a regulatory "tug of war" between stress axis activation and its shutdown by negative feedback. Chronic stressor responses are quite varied and context dependent. Many common chronic stressor exposures that result in cortisol elevation mimic aquaculture stressors, and can consist of either repeated acute stressors (Gilchriest et al., 2000; Madaro et al., 2015; Samaras et al., 2018) or high stocking density (Wunderink et al., 2011). However, there are also examples of chronic stress where plasma cortisol levels are no longer elevated but fish are responding to the stressor based on other endpoints, such as an attenuated response to an acute stressor (Madison et al., 2013; Vijayan and Leatherland, 1990). In these cases, the prolonged activation of the stress response is thought to lose its adaptive value, leading to inhibition of growth, reproduction and immune function (Wendelaar Bonga, 1997). Environmental contaminants can also be chronically stressful, and can interfere with steroidogenesis directly (Hontela and Vijayan, 2008). Paired juvenile rainbow trout provide a useful model to investigate chronic stress because of their well-characterized stress physiology, and their robust behaviour in forming social hierarchies (Gilmour et al., 2005).

1.4 Social hierarchies in fishes

Individuals living within groups often form social hierarchies, and it is well established that social behaviour and stress physiology are related (Johnsson et al., 2006; Sørensen et al., 2013). Hierarchies are formed often because of competition over limited resources such as territory, food, or mates, or to reduce the cost of prolonged aggressive interactions (Sloman and Armstrong, 2002). The glucocorticoid profile of several fish species has been assessed among individuals in various social groups. Some species of cichlid are highly social, meaning that they live in structured, cooperative groups and interact frequently. For instance, groups of *Neolamprologus pulcher* consist of a dominant breeding pair that tend to have lower cortisol levels, and several subordinate helpers that tend to have higher cortisol levels (Culbert et al., 2018). Other cichlid species (*Astatotilapia burtoni, Cichlasoma dimerus, Australoheros facetus*) tend to show higher cortisol levels in subordinate or non-territorial males (Baduy et al., 2017; Carpenter et al., 2014; Morandini et al., 2014). Zebrafish form hierarchies in pairs, with dominants having lower cortisol levels than their subordinate counterpart (Ivy et al., 2017; Tea et al., 2019). Elevation of cortisol in response to social subordination has also been observed in European eel (*Anguilla anguilla*), gulf toadfish (*Opsanus beta*), and sea bass (*Dicentrarchus labrax*) (Carbonara et al., 2019; Peters et al., 1980; Sloman et al., 2005). In socially mediated sequential hermaphrodites like the false clown anemonefish (*Amphiprion ocellaris*), changes in cortisol levels with dominance status may play a role in the associated sex change (Iwata and Suzuki, 2020; Iwata et al., 2019). Salmonids held in pairs and small groups typically form hierarchies within hours, yielding dominant and subordinate individuals (Johnsson et al., 2006; Øverli et al., 1999a). Over the course of days to weeks, cortisol levels remain high in subordinates while dominants typically have lower cortisol titres (Culbert and Gilmour, 2016;

DiBattista et al., 2006; Gilmour et al., 2017; Höglund et al., 2002; Laidley and Leatherland, 1988; Øverli et al., 1999a; Pottinger and Carrick, 2001; Sloman et al., 2001; Sloman et al., 2002a; Sørensen et al., 2011).

Salmonid hierarchies and territoriality occur in the wild (Jenkins, 1969) as well as under a variety of semi-natural and laboratory conditions. Social hierarchies in juvenile salmonids have received considerable research attention in a laboratory setting (Gilmour et al., 2005). Typical behaviours of dominant individuals include the acquisition of limited resources, and aggression. The limited resources in a lab setting typically include 'ownership' of the shared space or tank, and monopolization of food sources. Aggressive behaviours include nipping, chasing, and fighting (Ejike and Schreck, 1980; Noakes and Leatherland, 1977; Stringer and Hoar, 1955). As a result of these behaviours by dominant individuals, subordinate individuals tend to exhibit reduced feeding and locomotor activity (Winberg and Nilsson, 1993). Subordinates typically display reductions in growth rate beyond what is attributable to their lack of feeding (DiBattista et al., 2006).

Establishment of a hierarchy through agonistic interactions for dominance is acutely stressful for both individuals, with cortisol levels being elevated in both individuals five minutes after a winner and loser of a contest were identified (Øverli et al., 1999a). Three hours after hierarchy establishment, cortisol levels in the fish that became dominant had returned to unstressed levels similar to those of singly-held controls (Øverli et al., 1999a); plasma cortisol levels below ~10 ng mL^{-1} are considered typical of unstressed fish in salmonids (Gamperl et al., 1994). The pattern of the cortisol response in the fish that became dominant is consistent with that of other acute stressors such as netting, with cortisol increasing within minutes of stressor exposure, and coming back down within hours (Gamperl et al., 1994). In subordinate fish,

however, cortisol levels remain elevated 3 h and 24 h after hierarchy establishment (Øverli et al., 1999a). Indeed, subordinate individuals display significantly elevated plasma cortisol after 2, 3, 4, 5, 6, or 7 d of social interaction, demonstrating the chronic nature of this stressor (Culbert and Gilmour, 2016; Jeffrey et al., 2014; Sloman et al., 2001; Sloman et al., 2002a). Subordinate fish also display an attenuated response to an additional acute stressor (Jeffrey et al., 2014) which is often observed during chronic stressor exposures. While this is hypothesized to be due to changes at the receptor level in the head kidney (Mommsen et al., 1999), the mechanism by which this occurs in fish is not well understood, and is addressed in chapter 3. Interestingly, the elevated cortisol levels of subordinates rapidly return to baseline (within 2 days) after the pair is separated, although some of the behavioural inhibition persists at this time point (Culbert and Gilmour, 2016). Throughout the present thesis, several stress-axis related endpoints were assessed after 1 and/or 2 days of recovery from social stress to examine the mechanisms underlying both the maintenance of elevated cortisol for several days, and its rapid post-pairing decline.

1.5 Epigenetics and social stress

Fish physiology, like mammalian physiology, increasingly is being studied through the lens of epigenetic mechanisms (Best et al., 2018). Epigenetic changes are those that "heritably regulate the spatio-temporal genome expression that underlies the emergence of physiological phenotypes" (Best et al., 2018). The key mechanisms typically considered to comprise epigenetics include the modification of histones, methylation, and microRNA. Histones can be modified by reversible acetylation, methylation, or phosphorylation of specific amino acids (Allis and Jenuwein, 2016). These chemical modifications impact the interaction of positively

charged histones to negatively charged genomic DNA, which can alter chromatin state and access to DNA for gene transcription (Allis and Jenuwein, 2016). Chapter 4 of the present thesis explores the possible roles of microRNA and methylation in the context of chronic social stress, specifically relating to gene expression of *crf*. MicroRNA (miRNA) is a family of small (~20-25 nucleotides) RNA molecules that do not encode proteins (i.e. they are non-coding, or ncRNA) and are involved in post-transcriptional regulation of mRNA (He and Hannon, 2004; Juanchich et al., 2016). They were first discovered in 1993 in *Caenorhabditis elegans* (Lee et al., 1993) and have since been implicated in many biological processes, including in fishes (reviewed by Best et al., 2018; Bizuayehu and Babiak, 2014). Biogenesis of miRNA is reviewed in detail elsewhere (He and Hannon, 2004; Winter et al., 2009) but briefly, primary miRNA (pri-miRNA) is the transcription product of miRNA genes, and is processed by a complex containing the endonuclease Drosha. This processing results in pre-miRNA, which exhibits a hairpin structure and is exported from the nucleus by exportin-5, after which it is processed by the endoribonuclease Dicer to form the mature miRNA. MicroRNA are mostly numerically named (i.e. *miR-210*) and the 'arm' of the hairpin structure from which the mature miRNA derives dictates the -5p or -3p suffix (Ha and Kim, 2014). The mature miRNA is loaded into the RNA-induced silencing complex (RISC), which binds to the 3' untranslated region (UTR) of the target transcript to deadenylate it and/or inhibit its translation, leading to degradation (Huntzinger and Izaurralde, 2011; Sheu-Gruttadauria and MacRae, 2017). Complementarity of the miRNA to the 3'UTR is mostly determined by the seed sequence, i.e. the nucleotides at positions 2-7 of the miRNA (Mennigen and Zhang, 2016). MicroRNA are highly conserved among animals (Wheeler et al., 2009); however, the mRNA target sequences are less conserved. That is, miRNAs can be identified in the target species (e.g. rainbow trout) by examining miRNA in

other species. However, whether those miRNAs will retain the same targets or effects in different species is unclear. The recent availability of genomic and transcriptomic information for rainbow trout has helped get around this problem by providing information necessary for *in silico* prediction of miRNA-target binding (Mennigen and Zhang, 2016). Using such approaches has revealed miRNA involved in mediating effects of chronic social stress on lipid metabolism (Kostyniuk et al., 2018), and miRNA involved in responses to acute stressors (Cadonic et al., 2020). Chapter 4 aimed to similarly explore miRNA-mediated regulation of HPI axis function at the level of the POA.

Methylation of DNA is an epigenetic mechanism that can also alter (typically repress) target gene transcription, by direct or indirect interaction with transcription factor binding in the target gene's promoter (Ambrosi et al., 2017). Genomic DNA can be methylated at cytosines, often but not exclusively when they are followed by a guanine, denoted as CpG (de Mendoza et al., 2021). CpG islands are clusters of CpG loci, usually ~1000 base pairs (bp) long, and depleted in the rest of the genome relative to promoter regions, where they are associated with transcriptional regulation (Han and Zhao, 2008; Jones, 2012). DNA methyltransferase (DNMT) enzymes mediate methylation, with DNMT1 responsible for maintenance methylation during DNA replication while DNMT3A and 3B catalyze *de novo* methylation (Ambrosi et al., 2017; Baubec et al., 2015). Methylation has been implicated in the regulation of several physiological processes, including temperature responses and metabolism (reviewed in Best et al., 2018). To date, few studies in teleosts have identified methylation differences as potential regulators of stress responses or social behaviour (but see Khor et al., 2016; Lenkov et al., 2015; McGhee and Bell, 2014; Zou et al., 2021). However, key studies in mammals revealed a role for methylation in the response to chronic social defeat stress in mice, with mice that displayed social avoidance

post-defeat having less methylation present in the *crf* promoter, and increased *crf* transcript abundance than mice that did not avoid social interactions post-defeat (Elliott et al., 2010). This finding suggests that methylation may be involved in regulating responses to chronic behavioural stressors, a possibility that was tested in our chronic social stress model in Chapter 4.

1.6 Goals of the thesis

The objective of the present thesis was to probe the mechanisms underlying regulation of the HPI axis during chronic social stress to explain how elevated plasma cortisol levels are sustained in subordinate rainbow trout. In Chapter 2, negative feedback and clearance of cortisol were assessed by measuring cortisol receptor abundance in the HPI axis tissues, and the clearance and tissue uptake of cortisol. Chapter 3 assessed the contribution of the head kidney to the altered HPI axis function in subordinate fish. A combination of *in vivo*, *in vitro*, molecular, and cellular approaches was deployed to elucidate how subordinate fish can simultaneously exhibit elevated basal cortisol levels but attenuation of acute cortisol production in response to an additional stressor. Finally, Chapter 4 explored novel modes of *crf* regulation in the POA at a molecular level, specifically attempting to implicate miRNA and/or methylation in this process. Collectively, the experiments reported in the present thesis aimed to reveal novel information on the mechanisms that do, and do not, contribute to the regulation of the HPI axis during chronic social stress.

Chapter 2: Negative feedback function in the hypothalamic-pituitary-interrenal axis of rainbow trout (*Oncorhynchus mykiss*) subjected to chronic social stress

Analysis of GR protein abundance was performed by Dr. E. Faught in collaboration with Dr. M. M. Vijayan (University of Calgary, AB, CA).

2.1 Introduction

The glucocorticoid stress response is both critical for coping with a wide range of stressors and conserved across vertebrates. In fishes, the main glucocorticoid, cortisol, is produced by the HPI axis which has been well studied in teleosts, particularly rainbow trout (see Bernier et al., 2009; Faught et al., 2016; Vijayan et al., 2010, for review). The timing of a stressor is critical in determining how the HPI axis functions, with acute stressors evoking a response that lasts minutes to hours, whereas the response to a chronic stressor is measured in days to weeks (Boonstra, 2013). Chronic stress can arise from social interactions among conspecifics. Juvenile rainbow trout placed in pairs in a tank interact agonistically, and the outcome of this interaction determines their behavioural phenotype, either dominant or subordinate (Gilmour et al., 2005). Dominant fish are more aggressive, securing access to limited resources such as food and territory. Cortisol levels are elevated in these fish during hierarchy formation, but return to baseline within a few hours (Øverli et al., 1999a). Subordinate fish typically are less active, do not feed, and importantly, exhibit elevated cortisol levels (Gilmour et al., 2005). This elevation of cortisol persists for at least seven days in subordinates held in pairs (Sloman et al., 2001), and is accompanied by attenuation of the cortisol response to an acute stressor (Jeffrey et al., 2014). However, baseline cortisol levels and HPI axis reactivity in subordinates are restored just two days after being separated from their dominant counterpart (Culbert and Gilmour, 2016). Social subordination in rainbow trout therefore is a useful model for assessing the effects of chronic stress on HPI axis regulation, as well as how persistent these effects are following alleviation of stress.

Prolonged elevation of cortisol levels during chronic stress occurs despite the mechanisms available to lower circulating cortisol concentrations. For example, cortisol acts

through negative feedback to decrease HPI axis activity and hence circulating cortisol levels. In fishes, cortisol-mediated negative feedback has been functionally demonstrated at all levels of the HPI axis (Bernier et al., 2009). Cortisol implants into the nucleus preopticus (NPO) inhibited the rise in cortisol in response to acute stress in goldfish (Fryer and Peter, 1977), supporting a role for negative feedback activity at the level of corticotropin releasing factor (CRF) signalling from the preoptic area of the brain to the corticotropes of the anterior pituitary. At the level of the pituitary, CRF stimulates the release of adrenocorticotropic hormone (ACTH) into circulation. Addition of cortisol to the buffer superfusing goldfish pituitary cells reduced ACTH secretion (Fryer et al., 1984). Binding of ACTH to melanocortin-2 receptors (MC2R) on the interrenal cells, which are located in clusters throughout the head kidney, stimulates cortisol synthesis (Aluru and Vijayan, 2008). *In vitro* head kidney preparations from coho salmon support a role for ultra-short loop negative feedback by cortisol at the level of the interrenal cells (Bradford et al., 1992). Both the glucocorticoid (GR) and mineralocorticoid (MR) receptors that mediate the effects of cortisol on target tissues are expressed in the brain and head kidney (Bury et al., 2003; Teitsma et al., 1999; Teles et al., 2013), but little is known about the functional role of these receptors in cortisol-mediated negative feedback. Whole-body functional GR knockdown using the GR antagonist RU-486 in trout, or GR and MR knockout in zebrafish, disrupted aspects of stress axis functioning, suggesting a role for these receptors in the HPI axis itself (Alderman et al., 2012; Faught and Vijayan, 2018).

Cortisol is also metabolized and cleared from the fish, through mainly the hepatobiliary pathway, but also the kidney and gill (Idler and Truscott, 1972; Truscott, 1979). The first step in this pathway is the conversion of cortisol to cortisone by the enzyme 11βHSD2 (Tsachaki et al., 2017). Further reductases and dehydrogenases convert cortisone into more soluble forms for

excretion (Tokarz et al., 2013; Truscott, 1979). Recently, differences have come to light regarding the regulation of cortisol in mammals (or tetrapods) versus fishes. A key distinction is the apparent absence from fishes of the enzyme 11βHSD1 that catalyzes the regeneration of cortisol from cortisone (Baker, 2010; Tsachaki et al., 2017). The activities of 11βHSD1 and 11βHSD2 can amplify and silence, respectively, the physiological effects of glucocorticoids at a tissue or cellular level (Chapman et al., 2013). Without 11βHSD1, the dominant mechanisms that dictate cortisol levels in fishes are HPI axis activation, negative feedback, and clearance. Negative feedback control alongside hormone catabolism and clearance effectively lower circulating cortisol levels following an acute stressor, but how the balance between cortisol production and catabolism/clearance is altered during chronic stress to result in persistent elevation of circulating cortisol levels is less clear. A clearer understanding of the balance between cortisol production and reduction will provide insight into how cortisol levels are controlled during chronic stress.

The goal of the current study was to shed light on how cortisol levels remain elevated for several days during chronic social stress, despite the mechanisms in place to bring them down. We hypothesized that high cortisol levels in chronically stressed subordinate rainbow trout are sustained through reduced capacity for cortisol-mediated negative feedback and reduced cortisol clearance. To test this hypothesis, juvenile rainbow trout paired for four days (4 d) were injected with a cortisol load to assess their ability to remove cortisol from the circulation via negative feedback and/or clearance. In a separate experiment, radiolabelled cortisol was used to assess tissue uptake, a key factor in hormone clearance (Mommsen et al., 1999). At the tissue level, we assessed transcript abundances of key components of the HPI axis (*crf, pomca1, a2, b,* and two proteins involved in the rate-limiting step of steroidogenesis, *star,* and *p450scc*) to examine

stress axis activation. Simultaneously, we assessed negative feedback capacity by measuring transcript abundances of *gr1, gr2, mr,* and *11βhsd2*, and protein abundances of GR and 11βHSD2 in HPI axis tissues. To understand changes in clearance capacity, *11βhsd2* was also assessed in the liver, which is considered the primary excretion route for cortisol. The HPI axis was evaluated also during recovery from chronic stress by measuring endpoints in 4 d pairs that were separated by an opaque divider to allow for one or two days of recovery from social stress (4+1 d, 4+2 d groups). In line with the hypothesis above, we predicted that subordinate fish would exhibit some combination of impaired cortisol clearance and uptake, dysregulated negative feedback systems, and increased HPI axis activity.

2.2 Materials and methods

2.2.1 Experimental Animals

Juvenile rainbow trout (78.9 ± 1.3 g, N = 194) were obtained from Linwood Acres Trout Farm (Campbellcroft, Ontario) and held at the University of Ottawa in 1275 L fibreglass tanks in 13ºC, dechloraminated city of Ottawa tap water ("system" water) with a mild current, and under a 12L:12D photoperiod. Fish were scatter fed 0.5% body mass daily with Zeigler Silver pellets. These conditions served to minimize hierarchy formation in holding tanks. All protocols were approved by an institutional animal care committee (protocol BL-2118), and were in accordance with Canadian Council on Animal Care guidelines for the use of animals in research and teaching.

2.2.2. Experimental Protocols

The formation of social hierarchies was followed after 4 d of interaction by one of three protocols, to assess effects of chronic social stress on clearance of exogenous cortisol, tissue uptake of ^{3}H-cortisol, or transcript and protein abundance of HPI axis components.

2.2.2.1 Formation of social hierarchies

Social hierarchies were created using established protocols (Culbert and Gilmour, 2016; Gilmour et al., 2012; Gilmour et al., 2017; Jeffrey et al., 2014). Briefly, fish were lightly anaesthetized (0.05 g L^{-1} benzocaine; Sigma-Aldrich, Oakville, ON, CA) to measure mass and fork length, and to score fin damage. The fish within a pair were size matched according to fork length (differences averaged 0.3 ± 0.03 cm or 1.7 ± 0.2% of fork length) and mass (differences averaged 4.1 ± 0.3 g or 5.4 ± 0.4% of body mass; *N*=86 pairs). The fish within a pair were transferred to 40 L tanks supplied with flowing system water and were separated by a perforated, opaque divider for an overnight recovery period (day 0), following which the divider was removed to allow the fish to interact (day 1). Sham fish were handled in the same way but housed alone. Fish were fed 0.5% body weight per day, following the afternoon observation period, starting on observation day 2.

Behavioural observations were performed twice daily to assess social status by scoring fish on aggressive acts, position in the tank, and acquisition of a food pellet, with higher scores indicating more dominant behaviour. At the time of sample collection, fin damage accrued as a result of social interactions was scored. The mean scores across all observation periods for each of these measurements were analysed using a principal component analysis (PCA), to determine

an overall behaviour score (PC1) for each fish. The fish within a pair with the higher overall behaviour score was assigned dominant social status.

2.2.2.2 Experiment 1: Clearance of exogenous cortisol

This experiment assessed the ability of dominant and subordinate rainbow trout to clear an exogenous cortisol load. Fish (70.9 ± 2.2 g, N = 62) interacted as described above, yielding average behaviour scores of 1.62 ± 0.11 and -1.36 ± 0.12, respectively, for dominant and subordinate fish (N = 34 pairs). On day five, fish were lightly anaesthetized and weighed, and an initial 200 µL blood sample was withdrawn from the caudal vasculature. Fish were then given an intraperitoneal (i.p.) injection of 25 µg per 100g fish of cortisol 21-hemisuccinate sodium salt (Sigma-Aldrich) in 100 µL of saline, or saline alone as a control. The dose was chosen from pilot trials in which it caused a physiologically-relevant acute elevation of circulating cortisol concentrations. Fish were returned to the experimental tank and monitored until they regained equilibrium. At 2 h post-injection, fish again were lightly anaesthetized for a second 200 µL blood draw. At 3 h post-injection, fish were euthanized by terminal anaesthesia (0.5 g L^{-1}) and a final blood sample was collected. Sample collection times were chosen based on pilot trials that monitored the time course of cortisol levels post-injection. All blood samples were collected using a 23G needle and syringe rinsed with heparinized (Sigma-Aldrich H3393) 0.9% saline solution. Blood was centrifuged at 13,500 *g* for 3 min, and plasma was transferred to a new tube, flash frozen in liquid nitrogen and stored at -80°C for later analysis of cortisol concentration.

2.2.2.3 Experiment 2: 3H-cortisol tissue uptake

This experiment evaluated whether tissue uptake patterns of cortisol differed between dominant and subordinate rainbow trout. Fish (89.7 ± 3.0 g, N = 12) interacted as described above, yielding average behaviour scores of 0.90 ± 0.12 and -1.14 ± 0.30, respectively, for dominant and subordinate fish (N = 6 pairs). On day five, fish were lightly anaesthetised and a 200 µL blood sample was withdrawn from the caudal vasculature for plasma cortisol analysis. Blood withdrawal was immediately followed by injection into the caudal vasculature of 2 µCi of ^{3}H-cortisol (94.6 µCi mmol^{-1}; NET396250UC, Perkin-Elmer, Woodbridge, ON, CA) in 100 µL of saline (Wilson et al., 1998). After 2 h, fish were euthanized by anaesthetic overdose and a blood sample (1 mL) was collected from the caudal vasculature. Plasma was used for the measurement of total cortisol (see section 2.3.1) and radioactivity (see below).

Tissues (liver, gallbladder, gill, white muscle, posterior kidney) were dissected out, weighed, and digested in 5x volume of 1 N nitric acid in a 65ºC shaking water bath for 42 h. Radioactivity (corresponding to ^{3}H-cortisol and its metabolites) was measured in the supernatant of tissue digests and in plasma by scintillation counting (Tri-Carb Liquid Scintillation Analyzer, Perkin-Elmer) with quench correction. For each sample, 10 mL of EcoLume scintillation cocktail (MP Biomedicals, Solon, OH, USA) was added to 400 µL of supernatant or plasma. Samples were vortexed and incubated overnight in the dark prior to counting.

To determine cortisol uptake by each tissue, the concentration in µCi g^{-1} tissue was corrected for specific activity of ^{3}H in the plasma (µCi mL^{-1} plasma / ng mL^{-1} total plasma cortisol), where total plasma cortisol was the mean of the cortisol values at the beginning and end of the 2 h experiment. To determine whether tissue uptake rates scaled linearly with plasma cortisol, linear regressions of uptake rates on plasma cortisol levels were performed. In tissues

where this relationship was significant, y-intercepts were compared between social statuses. If uptake rate did not scale with plasma cortisol, we compared tissue uptake rates (corrected for specific activity) directly.

2.2.2.4 Experiment 3: Transcript and protein abundances of genes involved in HPI axis activation and negative feedback

This experiment assessed changes in transcript and protein abundances of key effectors of HPI axis activation (CRF, POMC, StAR, P450scc) as well as potential modulators of negative feedback (GR1, GR2, MR and 11βHSD2) after 4 d of social interaction and in fish allowed to recover from social stress for one or two days. For transcript analysis, fish (79.7 ± 1.5 g, N = 67) were paired as described above, yielding average behaviour scores of 1.53 ± 0.16 and -1.57 ± 0.11, respectively, for dominant and subordinate fish (N = 27 pairs). For fish (84.6 ± 2.7 g, N = 57) used for protein analysis, behaviour scores averaged 1.40 ± 0.16 and -1.63 ± 0.11, respectively, for dominant and subordinate fish (N = 23 pairs). On the morning of day 5, fish were either euthanized for tissue sample collection (4 d group) or the opaque, perforated divider was reinserted to separate the members of the pair. Observations of position in the tank and food acquisition continued on a twice daily basis until fish were sampled on the morning of day six (4+1 d group) or seven (4+2 d group).

Fish were euthanized by terminal anaesthesia and blood (~ 1 mL) was collected from the caudal vasculature for later analysis of plasma cortisol concentration. For transcript and protein analyses, the preoptic area of the brain (POA; see Bernier et al., 2008), pituitary, head kidney,

and liver were dissected out, snap frozen in liquid nitrogen, and stored at -80°C until further processing.

2.2.3 Analytical methods

2.2.3.1 Measurement of plasma cortisol

Plasma cortisol levels were measured using a commercially available radioimmunoassay kit (MP Biomedicals) previously validated for use in rainbow trout (Gamperl et al., 1994). The detection limit for this kit is 0.17 pg dL^{-1} and the inter- and intra-assay variabilities averaged 10.1% and 7.7%, respectively.

2.2.3.2 Measurement of transcript abundance by real-time RT-PCR

Whole head kidneys and liver were ground to a powder on dry ice with a mortar and pestle. Approximately 50 mg of powdered tissue, or whole preoptic areas or pituitaries, were sonicated (Sonic Dismembrator Model 100; Thermo Fisher Scientific, Waltham, MA, USA) on ice in TRIzol reagent (Thermo Fisher Scientific) until homogeneity for the extraction of RNA according to the manufacturer's guidelines. RNA was suspended in nuclease-free water and quantified using a Nanodrop 2000c UV-vis Spectrophotometer (Thermo Fisher Scientific). Genomic DNA was removed and cDNA was synthesized from 1 µg total RNA using the QuantiTect Reverse Transcription Kit (Qiagen, Hilden, Germany) according to the manufacturer's instructions.

Real-time RT-PCR was performed using a Rotor-Gene Q real-time PCR machine and the Rotor-Gene SYBR Green PCR kit (Qiagen). Primers (Table 1) were identified from the literature or, in the case of *11βhsd2*, were designed using Primer-BLAST, and specificity was verified by amplicon sequencing. Teleosts often have multiple paralogues, and this situation is compounded in rainbow trout by the additional salmonid-specific whole genome duplication event (Berthelot et al., 2014). Currently, functional differences between paralogues for many HPI axis genes remain unclear. Therefore, we targeted single paralogues where additional paralogues are not well characterized or have not been found (*crf, p450scc, star, 11βhsd2, mr*), and measured multiple paralogues separately in qPCR analyses where appropriate (*pomca1, pomca2, pomcb; gr1, gr2*).

Reactions were prepared according to the manufacturer's guidelines but scaled to a reaction volume of 10 µL: 5 µL 2X SYBR mix, 1 µL primer pair mix (containing 10 µM of each primer), 3 µM nuclease-free water, and 1 µL cDNA template. The PCR cycling conditions were as per the manufacturer's guidelines, using an annealing temperature of 60°C, except for *ef1a* (56°C). A standard curve was run for each tissue and primer set to confirm reaction efficiency (Table 1). Quality controls included a pooled control sample, a no-RT sample (to check for genomic DNA contamination; cDNA synthesis reaction carried out without reverse transcriptase), and a no-template sample (cDNA replaced with water). Transcript abundances of reference genes (Table 1) were determined for every tissue, and stability of reference gene expression across groups was verified. Relative fold-change of the target transcript was normalized to the reference gene and expressed relative to the sham group using the method of Pfaffl (2001).

2.2.3.3 Measurement of protein abundance by SDS-PAGE and Western blotting

Whole POAs were sonicated on ice in 4x volume of radioimmunoprecipitation assay (RIPA) buffer (150 mM NaCl, 1% Triton X-100, 0.5% sodium deoxycholate, 0.1% SDS, 50 mM Tris-HCl, 1 mM EDTA) supplemented with protease inhibitors (Thermo Fisher Scientific). Protein concentration was determined by Pierce bicinchoninic acid protein assay (BCA, Thermo Fisher Scientific), and homogenates were diluted to 4 mg mL^{-1} in RIPA buffer containing protease inhibitors and again to a final concentration of 2 mg mL^{-1} with 2x Laemmli buffer (Sigma-Aldrich).

For Gr, SDS-PAGE and western blotting were performed as described previously using an antibody that detects both Gr1 and Gr2 (Faught and Vijayan, 2018). For 11βHSD2, 40 µg of POA samples or 160 µg of liver samples were run on a 10% TGX Stain-Free FastCast polyacrylamide gel (Bio-Rad, Mississauga, ON, CA). Each gel also included a ladder (BLUeye Prestained, FroggaBio, Toronto, ON, CA) and a pooled control sample. Gels were run at 200 V for 1 h, then UV-exposed for 1 minute to activate total protein staining in the gel, followed by imaging (ChemiDoc XRS+, Bio-Rad). Proteins in the gel were transferred to 0.2 µm nitrocellulose membranes, using a Trans-Blot SD Semi-Dry Transfer Cell (Bio-Rad). The membrane was imaged to confirm transfer and for measurement of total protein in each lane for later normalization.

Membranes were blocked for 1 h at room temperature with shaking using a 5% skim milk solution (in Tris-buffered saline with 0.05% Tween-20, TBST), then incubated with diluted (in 2% skim milk in TBST) primary antibody (chicken anti-trout 11βHSD2; 1:10000 for POA and 1:5000 for liver) for 17 h at 4ºC with shaking. Custom antibodies (Genetel, Madison, WI, USA) were raised against two peptides corresponding to different regions of the 11βHSD2 protein:

RALRKENNNNNNINNNVEKIKK (C-terminal aa376-379) and SSYKTGQSGNQEYWENQYK (aa264-282). Hens were immunized with a mixture of both peptides, and IgY was collected from eggs, then affinity purified. The antibody was validated by identification of a band of the correct size, and the disappearance of this band by pre-absorption of the primary antibody with the peptide mixture prior to incubation (Fig. S2.2). Following 3 x 5 min washes in TBST, membranes were incubated with a 1:5000 dilution (in 2% skim milk in TBST) of the secondary antibody, goat anti-chicken horseradish peroxidase (HRP), for 1 h at room temperature. After 3 x 15 min washes in TBST, membranes were incubated with 1 mL Luminata Classico HRP substrate (MilliporeSigma, Burlington, MA, USA), and imaged using chemiluminescence (ChemiDoc XRS+, Bio-Rad). Relative protein abundance normalized to total protein was measured using ImageLab 6.0 according to Taylor et al. (2014).

2.2.4 Statistical Analysis

Data are expressed as mean values ± standard error of the mean (SEM). All statistical analyses were performed using Sigmaplot v13.0 (Systat Software, Inc., San Jose, CA, USA). For cortisol clearance, data were analyzed by two-way analysis of variance (ANOVA) using status and treatment as factors. For cortisol uptake, Student's *t*-tests were performed within each tissue to examine the effect of status, and linear regressions of tissue uptake on circulating cortisol followed by one-way ANCOVA were carried out. All other data (cortisol concentrations, transcript abundances, protein levels) were analysed for effects of social status by one-way ANOVA. Where data did not meet assumptions of normality and equal variance, they were transformed to meet these assumptions, or an equivalent non-parametric test was used. A significance level (α) of 0.05 was used.

2.3 Results

2.3.1 Clearance of an exogenous cortisol load

To assess the capacity for cortisol clearance from the circulation, dominant and subordinate fish were injected with cortisol or saline (as a control) (Fig. 2.1). Cortisol levels of subordinates prior to injection were higher than those of dominants (Fig. 2.1a). Saline-injected fish maintained stable cortisol levels across the 3 h sampling period. Neither the increase in plasma cortisol 2 h after injection (Fig. 2.1b; two-way ANOVA on ranks, $P_{status} = 0.873$, $P_{treatment} < 0.001$, $P_{int} = 0.721$), nor its decline during the following 1 h period (Fig. 2.1c; two-way ANOVA, $P_{status} = 0.278$, $P_{treatment} < 0.001$, $P_{int} = 0.575$) were significantly affected by social status.

2.3.2 Tissue uptake of ^{3}H-cortisol

Across the tissues examined, ^{3}H-cortisol uptake was highest in the gallbladder, followed by liver and posterior kidney (Fig. 2.2). Subordinate fish (plasma [cortisol] = 158.0 ± 15.7 ng mL^{-1}, $N = 6$) exhibited significantly higher ^{3}H-cortisol uptake than dominant fish (plasma [cortisol] = 6.64 ± 3.70 ng mL^{-1}, $N = 6$) in all tissues (Fig. 2.2; Student's *t*-tests, $P = 0.035, \leq$ 0.001, 0.001, 0.002, 0.001 for gallbladder to muscle, respectively). Tissue uptake of ^{3}H-cortisol scaled linearly with plasma cortisol in all tissues except gallbladder (Table 2.2). In all tissues except gallbladder, the slopes of the regression lines were not significantly different between dominant and subordinates (one-way ANCOVA, $P = 0.073$, 0.419, 0.159, 0.419 for liver, kidney, gill, and muscle, respectively). Comparison of y-intercepts between dominant and subordinate

fish revealed significantly higher tissue uptake of ^{3}H-cortisol in subordinate fish at a given cortisol concentration (one-way ANCOVA, $P = 0.002$, 0.004, 0.012, 0.003 for liver, kidney, gill, and muscle, respectively), suggesting greater tissue uptake and retention of cortisol in subordinate relative to dominant fish (Table 2.2).

2.3.3 Transcript and protein abundances of genes involved in negative feedback

Plasma cortisol levels in subordinate fish used for assessment of negative feedback function and HPI axis activity were significantly higher than those in dominant and sham fish after 4 d of social interaction (Fig. 2.3a; ANOVA, $P < 0.001$). One day after replacing the opaque divider to separate the fish in a pair (4+1 d group), plasma cortisol levels in recovering subordinate fish were about half that observed at 4 d, although still significantly higher than levels in dominant and sham fish (Fig. 2.3b; ANOVA, $P = 0.002$). Following 2 d of separation (4+2 d group), no significant differences were detected (Fig. 2.3c; ANOVA, $P = 0.263$).

The capacity for negative feedback was assessed by measuring transcript abundances and protein levels of 11βHSD2, GR1, GR2, and MR in HPI axis tissues. Relative to dominant and sham fish at 4 d of interaction, *11βhsd2* transcript abundance in subordinates tended to be elevated in the preoptic area (Fig. 2.4a; ANOVA, $P = 0.080$), and was significantly elevated in the pituitary (Fig. 2.4b; ANOVA, $P = 0.002$), but not the head kidney (Fig. 2.4g; ANOVA, $P = 0.770$). The significant elevation was maintained in the pituitary of recovering subordinate fish 1 d after separation from the dominant (Fig. 2.4e; ANOVA, $P = 0.010$), but was no longer apparent 2 d after separation (Fig. 2.4f; ANOVA, $P = 0.126$). Despite the trend observed in transcript

levels, protein abundance of 11βHSD2 in the POA was not altered by 4 d of social interaction (Fig. 2.4j; ANOVA, $P = 0.666$).

Transcript abundances for corticosteroid receptors (Figs. 2.5-2.7) were unaffected by social stress or recovery from social stress with the exception of *gr2* in head kidney, where transcript abundance was significantly lower in recovering subordinates than in dominants 1 d after replacement of the divider (Fig. 2.7e; ANOVA, $P = 0.036$). Interestingly, significantly lower GR protein abundance was detected in the POA of recovering subordinates 2 d after replacement of the divider (Fig. 2.5l; ANOVA, $P = 0.003$), despite the absence of differences in transcript abundances (Fig. 2.5c,f).

2.3.4 Transcript abundances of genes involved in HPI axis activity

Social interaction did not affect transcript levels of *crf* in the POA (Fig. 2.8a; ANOVA, $P = 0.354$). However, after 1 d of recovery, *crf* transcript abundance was significantly higher in recovering subordinates than in their dominant counterparts (Fig. 2.8b; ANOVA on ranks, $P = 0.032$), a difference that was no longer apparent at 2 d of recovery (Fig. 2.8c; ANOVA, $P = 0.801$). Transcript abundances of the three paralogues of *pomc* (*a1*, *a2*, *b*) did not differ with social status at any time point (Fig. 2.9).

In the head kidney, transcript abundances of *star* (Fig. 2.10a; ANOVA, $P = 0.014$) and *p450scc* (Fig. 2.10d; ANOVA, $P = 0.020$) were significantly elevated in subordinates after 4 d of interaction. No significant differences were observed for either gene after 1 d of recovery (Figs. 2.10b,e; ANOVA, $P = 0.115$ and 0.088, respectively). However, after 2 d of recovery, both

steroidogenic transcripts were significantly lower in subordinate fish compared to dominant fish (Fig. 2.10c,d; ANOVA, P = 0.029, and 0.047, respectively).

2.3.5 Hepatic transcript and protein abundance of 11βHSD2

Given the expected role of 11βHSD2 in cortisol excretion, transcript and protein abundances of 11βHSD2 were measured in liver. Neither transcript nor protein abundance of 11βHSD2 protein in the liver after 4 d of social interaction was affected by social status (Fig. 2.11; ANOVA, P = 0.745, and 0.750, respectively).

2.4 Figures

Figure 2.1 Plasma cortisol levels of dominant (Dom) and subordinate (Sub) rainbow trout (*Oncorhynchus mykiss*) measured after 4 d of social interaction (time = 0 h), as well as 2 h or 3 h following administration of an exogenous cortisol load or saline control (a). Panels b and c present the magnitude of the cortisol rise (from 0 to 2 h) and decline (from 2 to 3 h) following cortisol administration, respectively. Data are presented as means ± SEM (N = 12-18). In panels b and c, pairs of bars that share a letter are not significantly different from one another (b; 2-way ANOVA on ranks, $P_{status} = 0.873$, $P_{treatment} < 0.001$, $P_{int} = 0.721$ and c; 2-way ANOVA, $P_{status} = 0.278$, $P_{treatment} < 0.001$, $P_{int} = 0.575$).

Figure 2.1

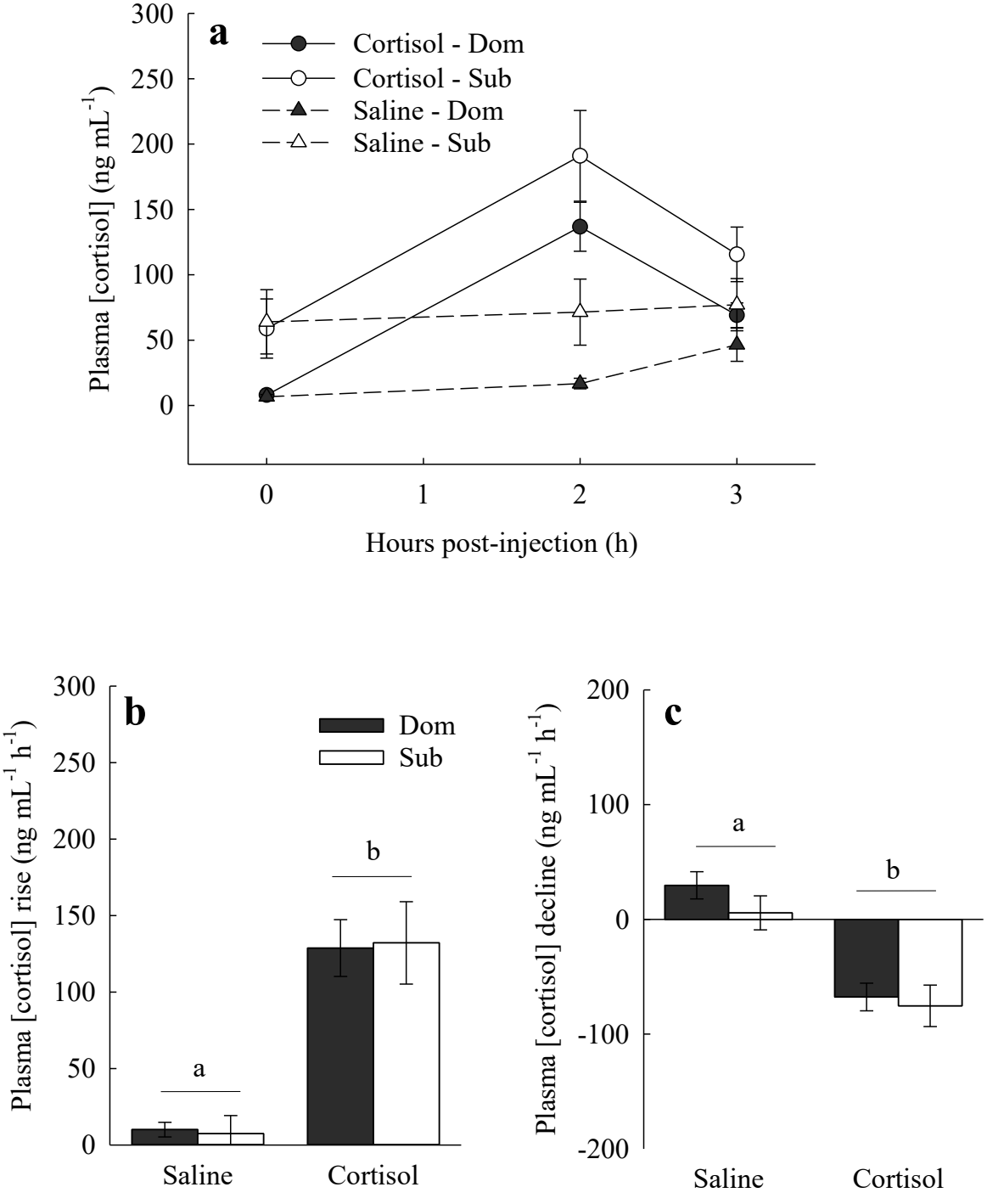
a
Cortisol - Dom
Cortisol - Sub
Saline - Dom
Saline - Sub
Plasma [cortisol] (ng mL-1)
300
250
200
150
100
50
0
0
1
2
3
Hours post-injection (h)
b
Dom
Sub
Plasma [cortisol] rise (ng mL-1 h-1)
300
250
200
150
100
50
0
a
b
Saline
Cortisol
c
Plasma [cortisol] decline (ng mL-1 h-1)
200
100
0
-100
-200
a
b
Saline
Cortisol

Figure 2.2

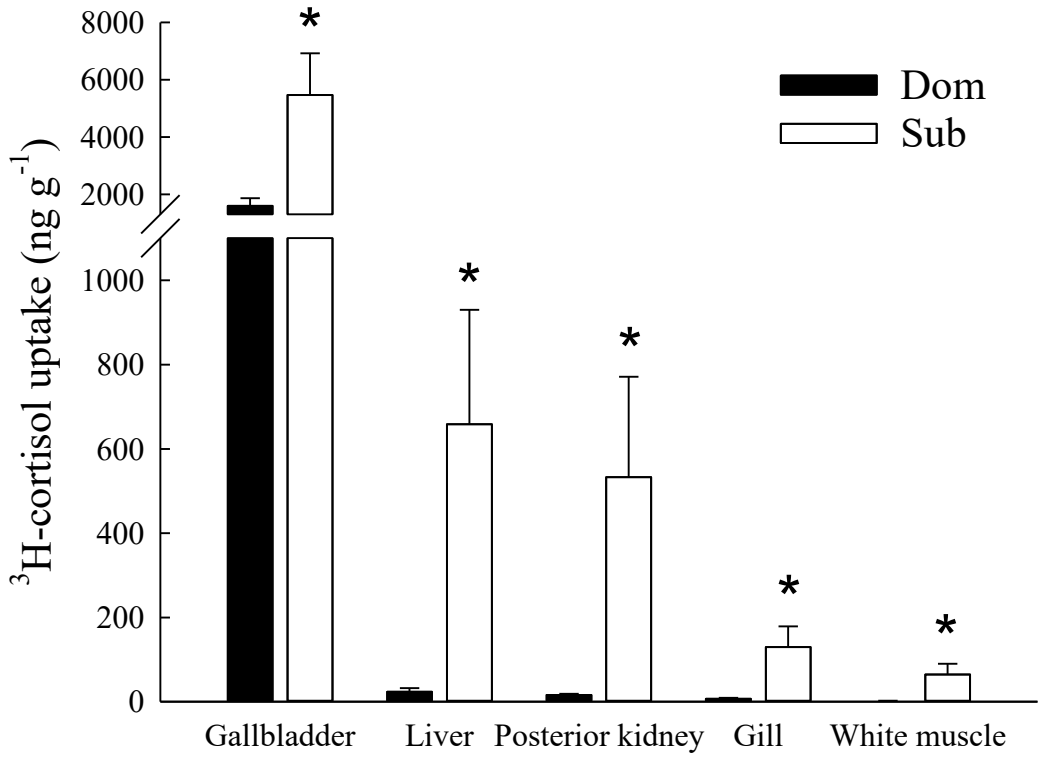

Figure 2.2 Uptake of ^{3}H-cortisol into tissues of dominant (Dom) and subordinate (Sub) rainbow trout (*Oncorhynchus mykiss*) after 4 d of social interaction. Uptake rates were determined from tissues collected 2 h after administration of ^{3}H-cortisol. Values are expressed as ng of cortisol taken up per g tissue, corrected for plasma ^{3}H-cortisol specific activity. Data are presented as means ± SEM (N = 6). An asterisk represents a significant difference within a tissue between dominant and subordinate trout (Student's t-tests, P = 0.035, ≤ 0.001, 0.001, 0.002, 0.001 for gallbladder to muscle, respectively).

Figure 2.3

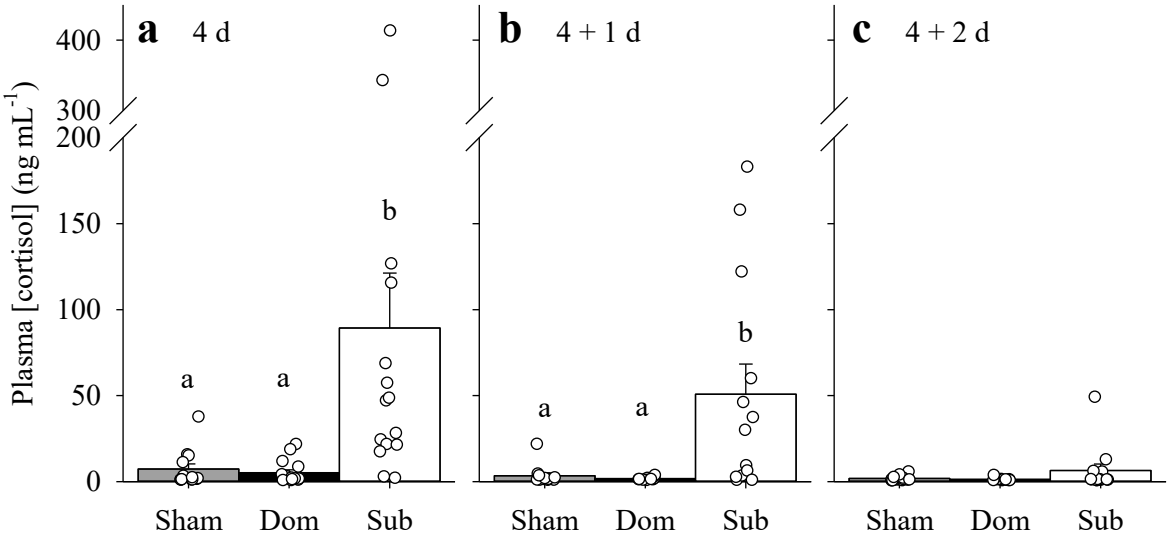

Figure 2.3 Plasma cortisol concentrations in dominant (Dom), subordinate (Sub) and sham-treated rainbow trout (*Oncorhynchus mykiss*) after 4 d of social interaction (a), or 4 d of social interaction followed by 1 (b) or 2 d (c) of recovery by replacement of the opaque divider to separate the members of a pair. Data are presented as means ± SEM (N = 12-16), with values for individuals shown as data points. Bars that share a letter are not significantly different from one another (ANOVA, P = <0.001, 0.002 and 0.263 for panels a to c, respectively).

Figure 2.4 Transcript levels of *11βhsd2* in the preoptic area (POA; a-c), pituitary (Pit; d-f), and head kidney (HK; g-i) of dominant (Dom), subordinate (Sub) and sham-treated rainbow trout (*Oncorhynchus mykiss*) after 4 d of social interaction (a, d, g), or 4 d of social interaction followed by 1 (b, e, h) or 2 d (c, f , i) of recovery by replacement of the opaque divider to separate the members of a pair. Transcript abundance was normalized to the geometric mean of reference genes *ef1α* and *β-actin* and expressed relative to the value for sham-treated fish. Panels j to l present POA 11βHSD2 protein abundances. Protein abundance was normalized to total protein and expressed relative to a pooled control sample. Data are presented as means ± SEM (N = 5-8), with values for individuals shown as data points. Bars that share a letter are not significantly different from one another (ANOVA, P = 0.080 for a, 0.311 for b, 0.526 for c, 0.002 for d, 0.010 for e, 0.126 for f, 0.770 for g, 0.266 for h, 0.138 for i, 0.666 for j, 0.870 for k, 0.780 for l).

Figure 2.4

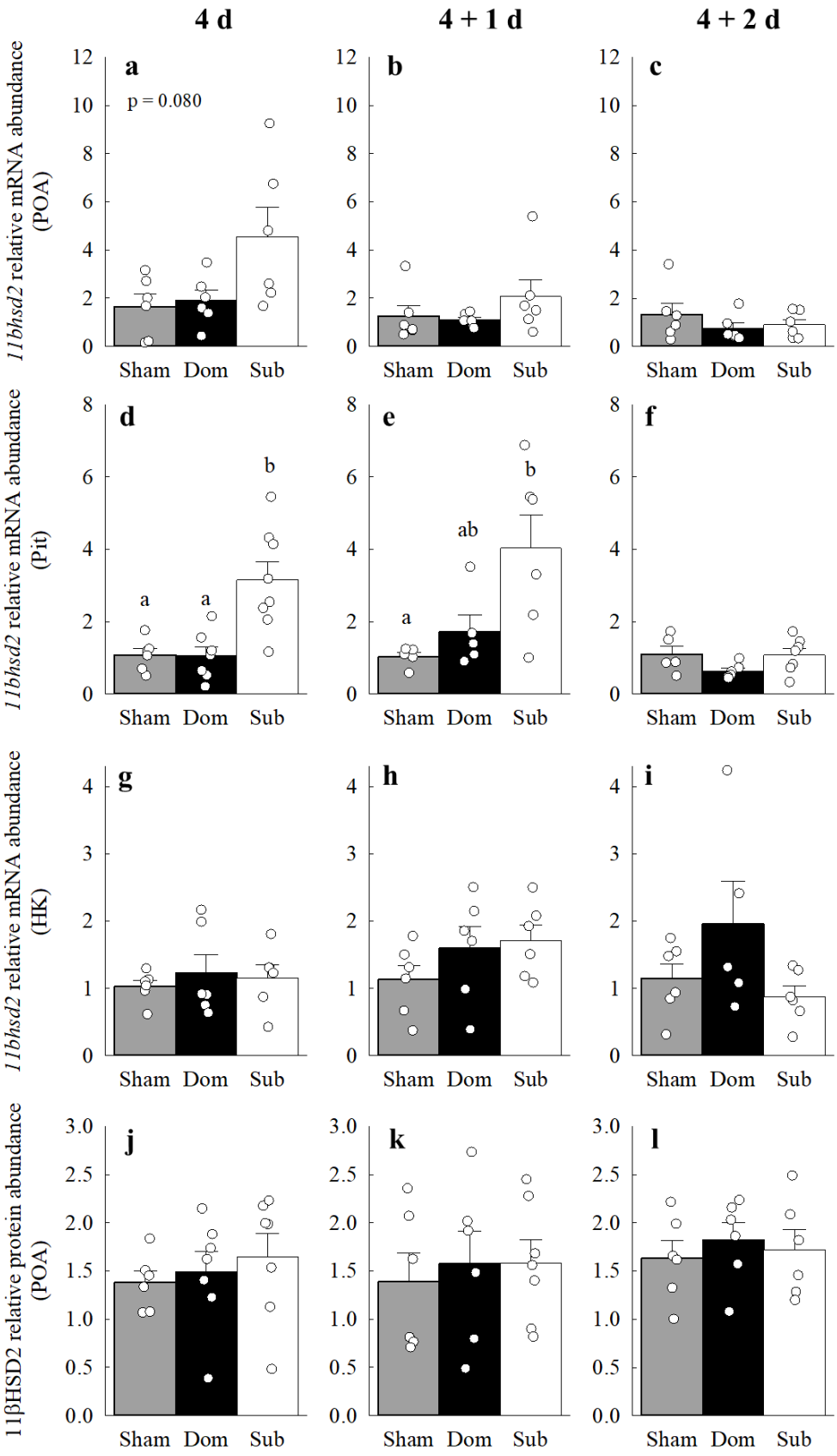
4 d
4 + 1 d
4 + 2 d
a
b
c
p = 0.080
d
e
f
g
h
i
j
k
l
11bhsd2 relative mRNA abundance (POA)
11bhsd2 relative mRNA abundance (Pit)
11bhsd2 relative mRNA abundance (HK)
11βHSD2 relative protein abundance (POA)
Sham
Dom
Sub

Figure 2.5 Transcript levels of the corticosteroid receptors *gr1* (a-c), *gr2* (d-f), and *mr* (g-i) in the preoptic area (POA) of dominant (Dom), subordinate (Sub), and sham-treated rainbow trout (*Oncorhynchus mykiss*) after 4 d of social interaction (a, d, g), or 4 d of social interaction followed by 1 (b, e, h) or 2 d (c, f , i) of recovery by replacement of the opaque divider to separate the members of a pair. Transcript abundance was normalized to the geometric mean of reference genes *ef1α* and *β-actin* and expressed relative to the value for sham-treated fish. Panels j to l present POA GR protein abundances. Protein abundance was normalized to total protein and expressed relative to a pooled control sample. Data are presented as means ± SEM (N = 6-7), with values for individuals shown as data points. Bars that share a letter are not significantly different from one another (ANOVA, P = 0.346 for a, 0.915 for b, 0.131 for c, 0.625 for d, 0.805 for e, 0.235 for f, 0.861 for g, 0.709 for h, 0.244 for i, 0.141 for j, 0.170 for k, 0.003 for l).

Figure 2.5

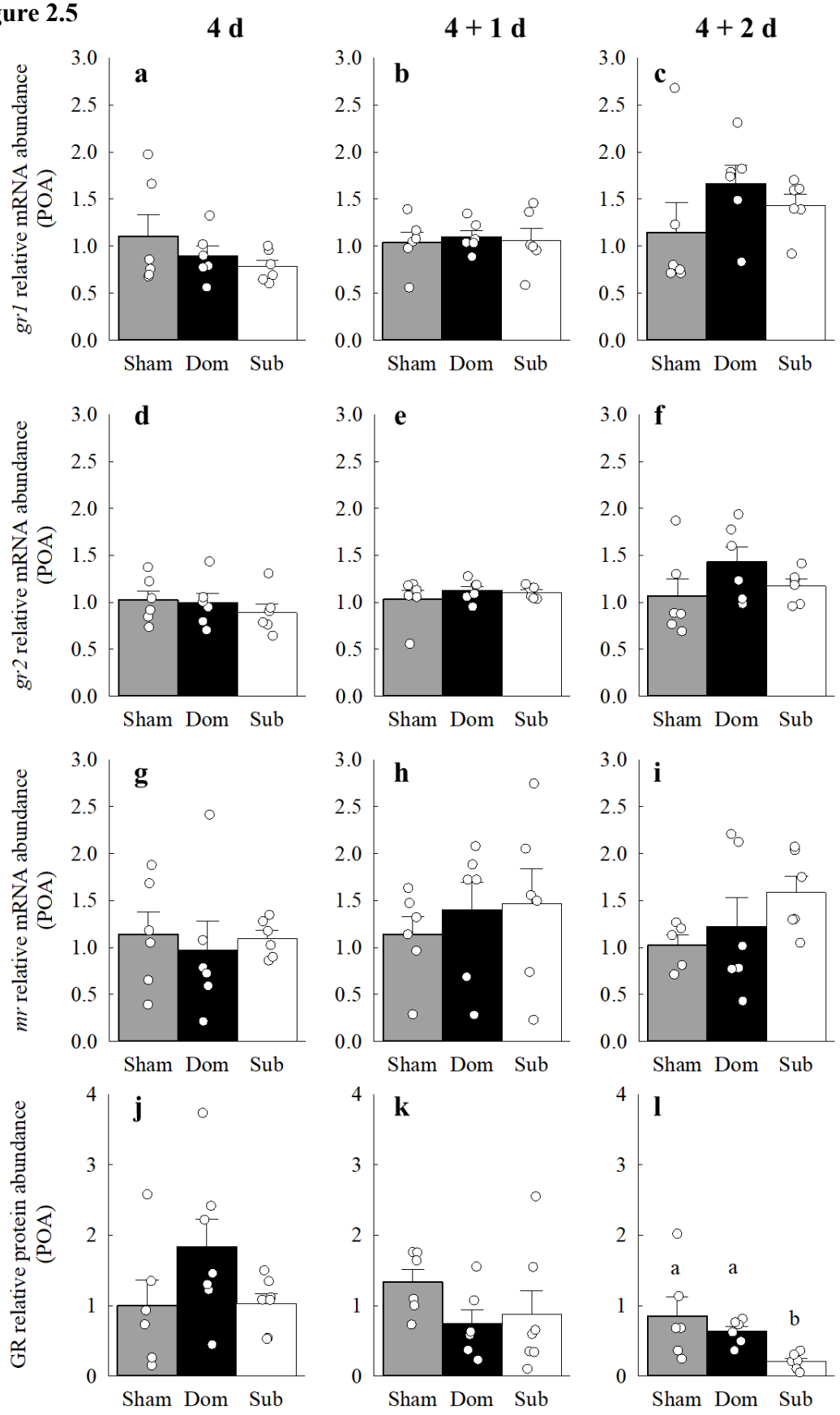
4 d
4 + 1 d
4 + 2 d
gr1 relative mRNA abundance (POA)
gr2 relative mRNA abundance (POA)
mr relative mRNA abundance (POA)
GR relative protein abundance (POA)
a
b
c
d
e
f
g
h
i
j
k
l
Sham
Dom
Sub
a
a
b

Figure 2.6 Transcript levels of the corticosteroid receptors *gr1* (a-c), *gr2* (d-f), and *mr* (g-i) in the pituitary (Pit) of dominant (Dom), subordinate (Sub), and sham-treated rainbow trout (*Oncorhynchus mykiss*) after 4 d of social interaction (a, d, g), or 4 d of social interaction followed by 1 (b, e, h) or 2 d (c, f , i) of recovery by replacement of the opaque divider to separate the members of a pair. Transcript abundance was normalized to the geometric mean of reference genes *ef1α* and *β-actin* and expressed relative to the value for sham-treated fish. Data are presented as means ± SEM (N = 5-8), with values for individuals shown as data points. Bars that share a letter are not significantly different from one another (ANOVA, P = 0.907 for a, 0.495 for b, 0.333 for c, 0.341 for d, 0.557 for e, 0.276 for f, 0.627 for g, 0.063 for h, 0.461 for i).

Figure 2.6

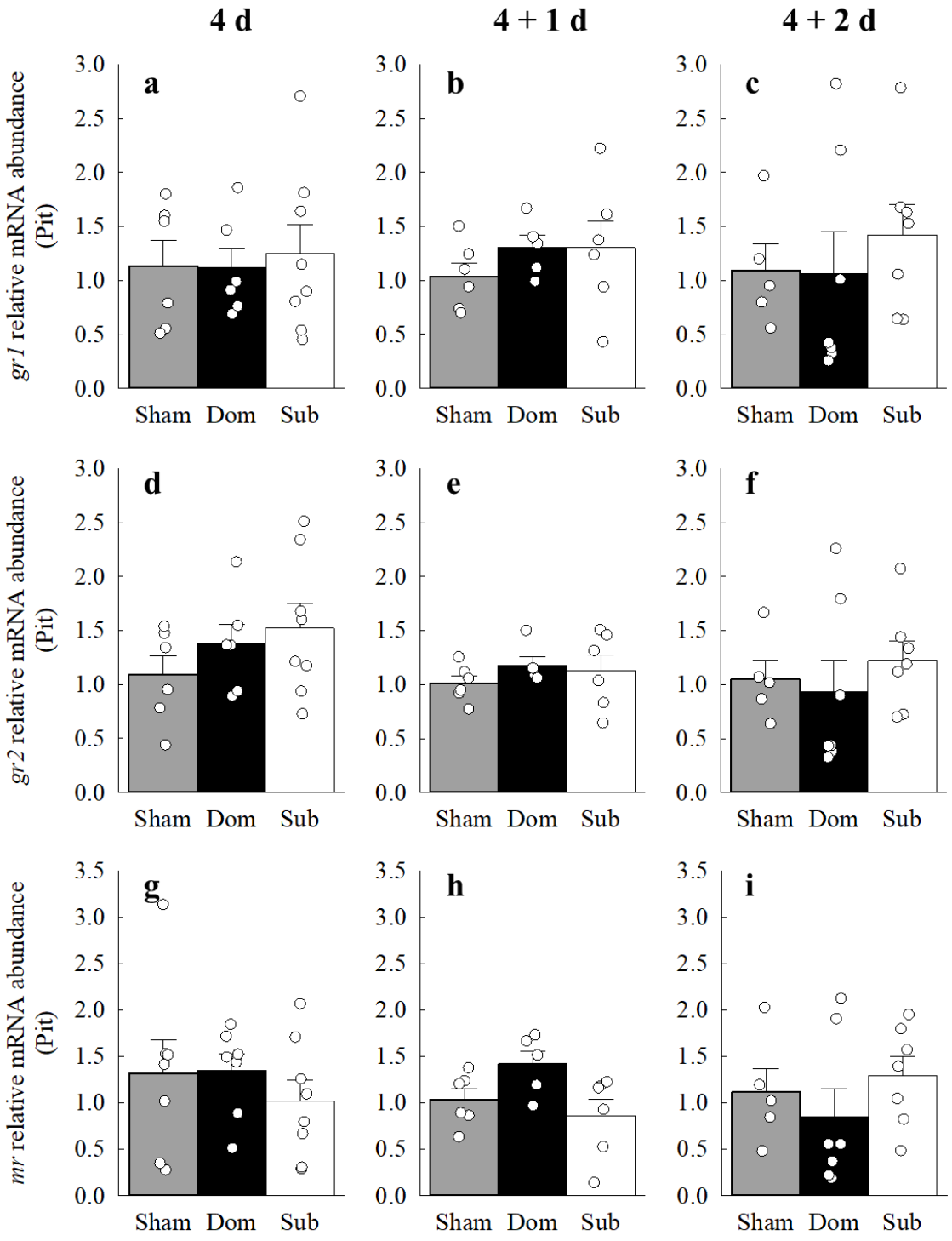
4 d
4 + 1 d
4 + 2 d
a
b
c
d
e
f
g
h
i
gr1 relative mRNA abundance (Pit)
gr2 relative mRNA abundance (Pit)
mr relative mRNA abundance (Pit)
Sham
Dom
Sub
0.0
0.5
1.0
1.5
2.0
2.5
3.0
3.5

Figure 2.7

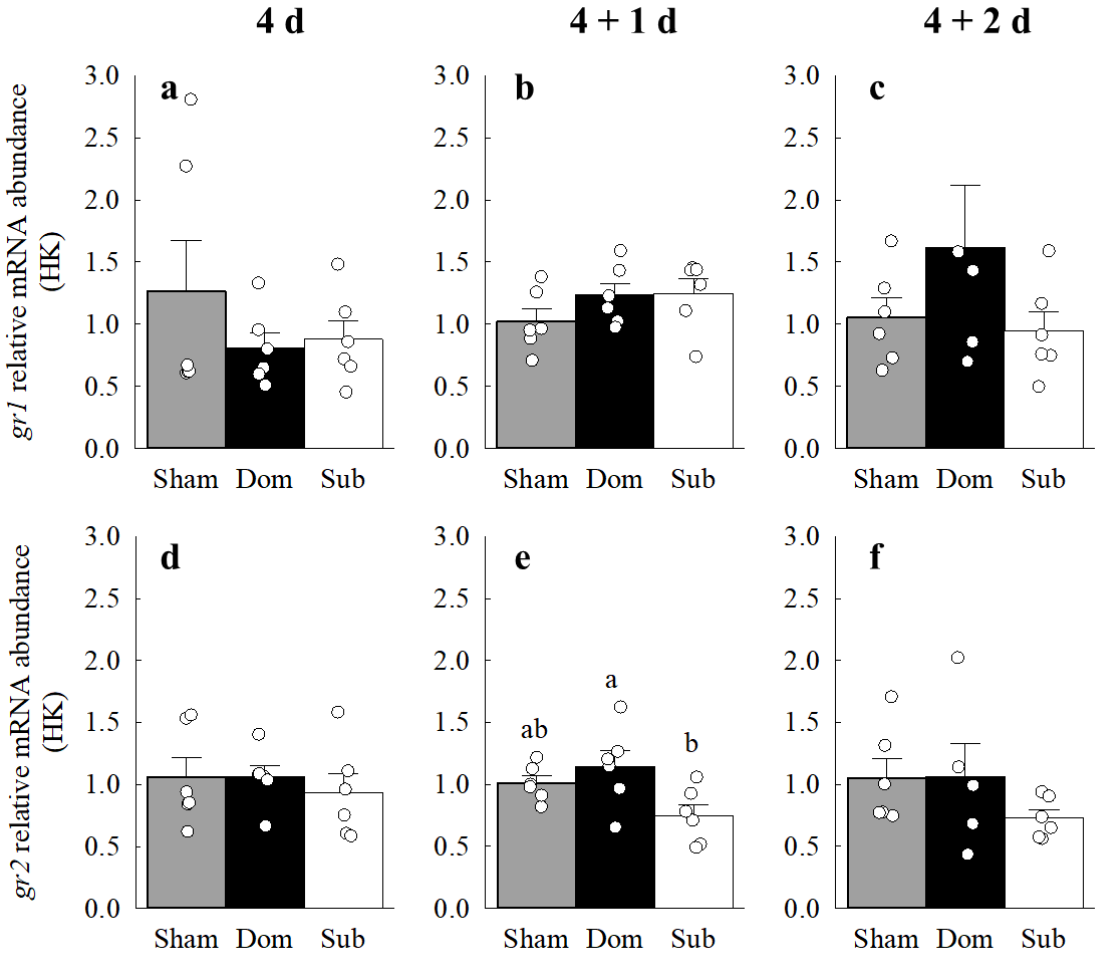

Figure 2.7 Transcript levels of the corticosteroid receptors *gr1* (a-c), and *gr2* (d-f) in the head kidney (HK) of dominant (Dom), subordinate (Sub), and sham-treated rainbow trout (*Oncorhynchus mykiss*) after 4 d of social interaction (a, d), or 4 d of social interaction followed by 1 (b, e) or 2 d (c, f) of recovery by replacement of the opaque divider to separate the members of a pair. Transcript abundance was normalized to the geometric mean of reference genes *ef1α* and *β-actin* and expressed relative to the value for sham-treated fish. Data are presented as means ± SEM (N = 5-6), with values for individuals shown as data points. Bars that share a letter are not significantly different from one another (ANOVA, P = 0.660 for a, 0.279 for b, 0.320 for c, 0.773 for d, 0.036 for e, 0.325 for f).

Figure 2.8

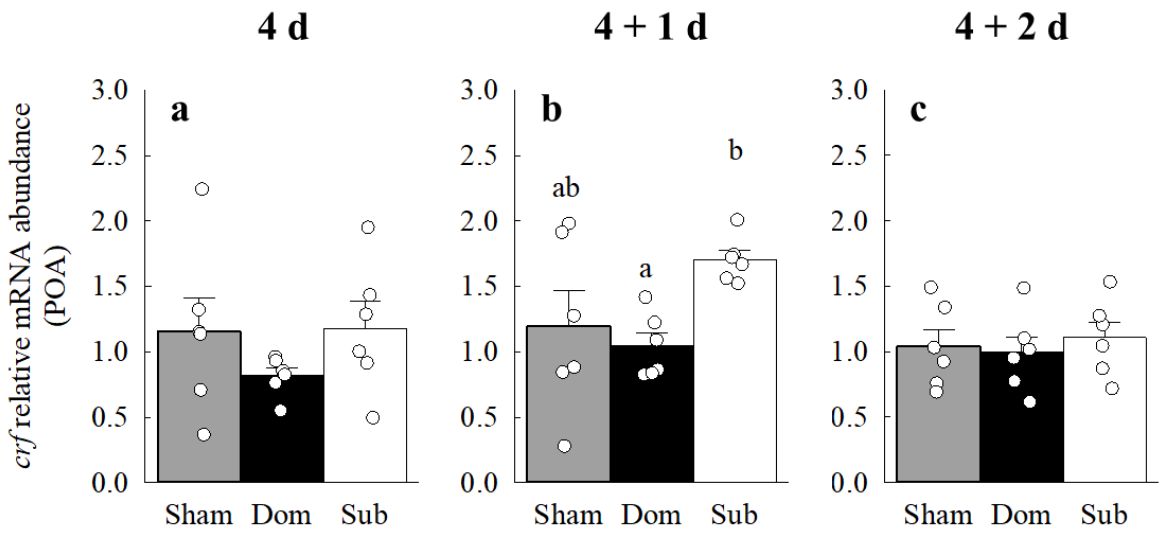

Figure 2.8 Transcript levels of corticotropin releasing factor (*crf*) in the preoptic area (POA) of dominant (Dom), subordinate (Sub), and sham-treated rainbow trout (*Oncorhynchus mykiss*) after 4 d of social interaction (a), or 4 d of social interaction followed by 1 (b) or 2 d (c) of recovery by replacement of the opaque divider to separate the members of a pair. Transcript abundance was normalized to the geometric mean of reference genes *ef1α* and *β-actin* and expressed relative to the value for sham-treated fish. Data are presented as means ± SEM (N = 6) with values for individuals shown as data points. Bars that share a letter are not significantly different from one another (ANOVA, P = 0.354, 0.032, 0.081 for panels a to c, respectively).

Figure 2.9 Transcript levels of the pro-opiomelanocortin paralogues *pomca1* (a-c), *pomca2* (d-f), and *pomcb* (g-i) in the pituitary of dominant (Dom), subordinate (Sub), and sham-treated rainbow trout (*Oncorhynchus mykiss*) after 4 d of social interaction (a, d, g), or 4 d of social interaction followed by 1 (b, e, h) or 2 d (c, f , i) of recovery by replacement of the opaque divider to separate the members of a pair. Transcript abundance was normalized to the geometric mean of reference genes *ef1α* and *β-actin* and expressed relative to the value for sham-treated fish. Data are presented as means ± SEM (N = 5-8), with values for individuals shown as data points. Bars that share a letter are not significantly different from one another (ANOVA, P = 0.369 for a, 0.055 for b, 0.303 for c, 0.554 for d, 0.181 for e, 0.071 for f, 0.478 for g, 0.420 for h,0.222 for i).

Figure 2.9

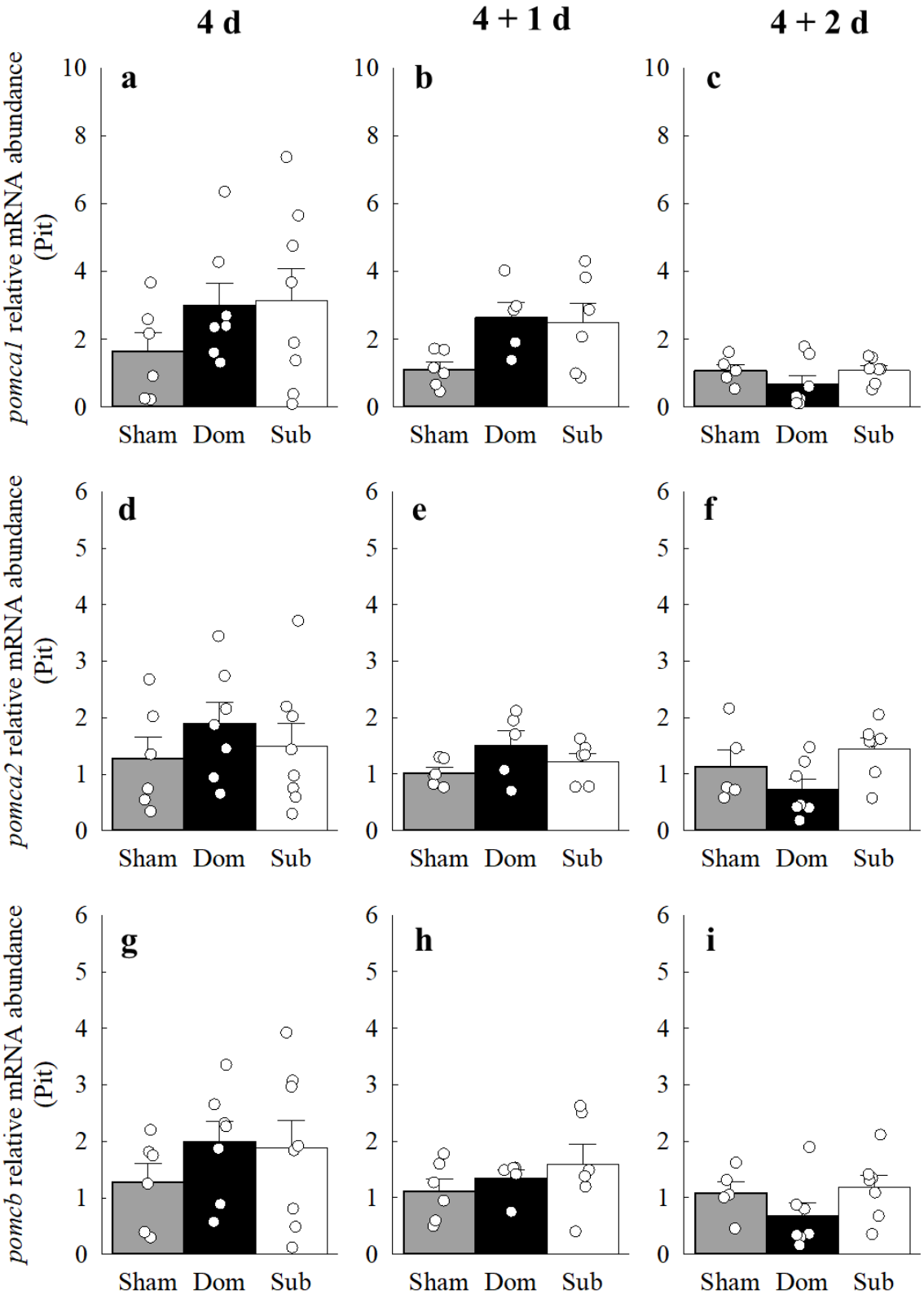
4 d
4 + 1 d
4 + 2 d
a
b
c
d
e
f
g
h
i
pomca1 relative mRNA abundance (Pit)
pomca2 relative mRNA abundance (Pit)
pomcb relative mRNA abundance (Pit)
Sham
Dom
Sub

Figure 2.10

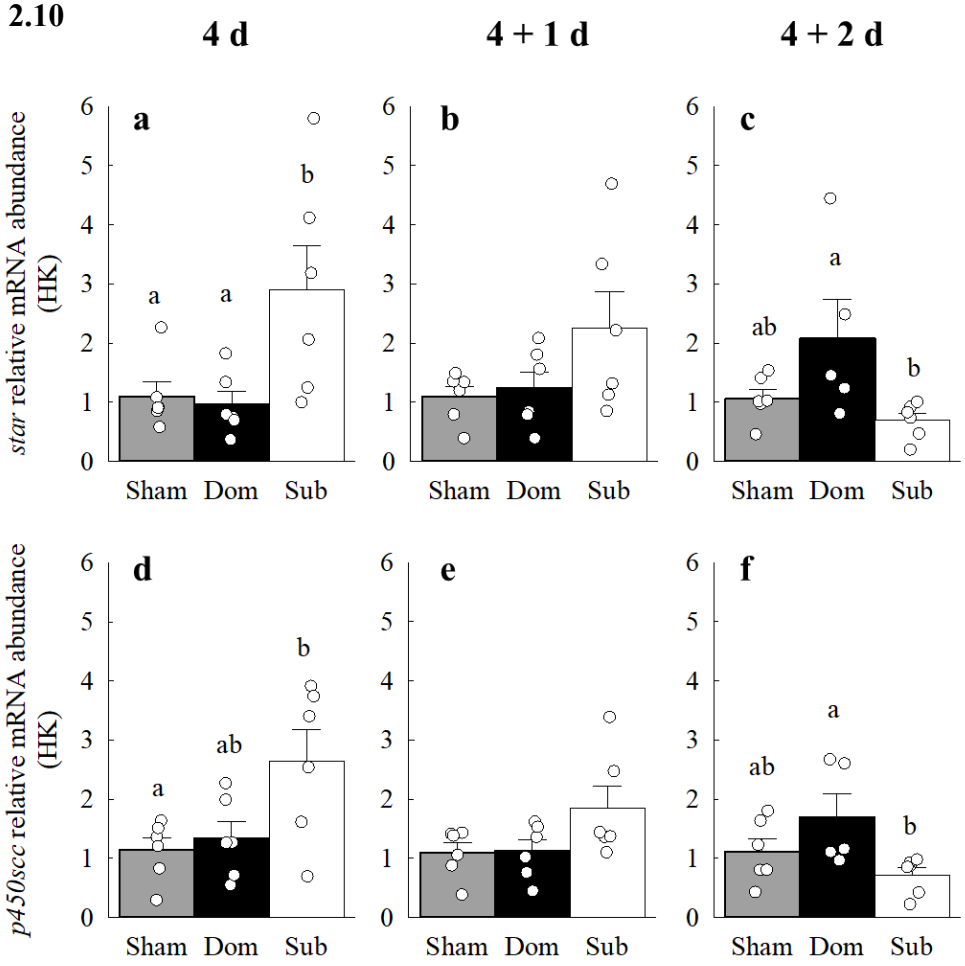

Figure 2.10 Transcript levels of steroidogenic acute regulatory protein, *star* (a-c), and cholesterol side-chain cleavage enzyme, *p450scc* (d-f), in the head kidney of dominant (Dom), subordinate (Sub), and sham-treated rainbow trout (*Oncorhynchus mykiss*) after 4 d of social interaction (a, d), or 4 d of social interaction followed by 1 (b, e) or 2 d (c, f) of recovery by replacement of the opaque divider to separate the members of a pair. Transcript abundance was normalized to the geometric mean of reference genes *ef1α* and *β-actin* and expressed relative to the value for sham-treated fish. Data are presented as means ± SEM (N = 5-6), with values for individuals shown as data points. Bars that share a letter are not significantly different from one another (ANOVA, P = 0.014 for a, 0.115 for b, 0.029 for c, 0.030 for d, 0.088 for e, 0.047 for f).

Figure 2.11

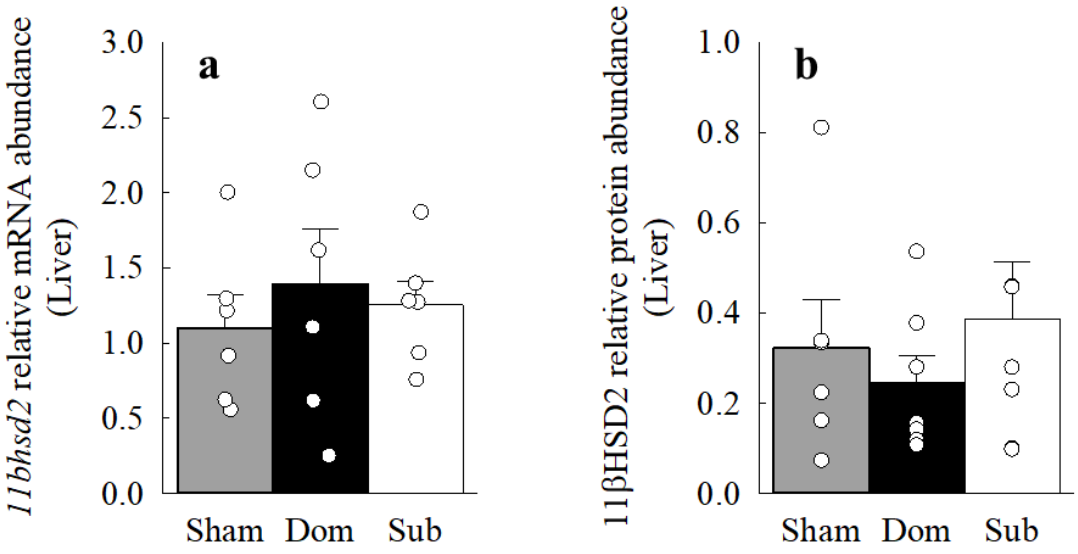

Figure 2.11 Transcript levels of *11βhsd2* in the liver (a) of dominant (Dom), subordinate (Sub) and sham-treated rainbow trout (*Oncorhynchus mykiss*) after 4 d of social interaction Transcript abundance was normalized to the reference gene *β-actin* and expressed relative to the value for sham-treated fish. Panel b presents liver 11βHSD2 protein abundances. Protein abundance was normalized to total protein and expressed relative to a pooled control sample. Data are presented as means ± SEM (N = 6-7), with values for individuals shown as data points. Bars that share a letter are not significantly different from one another (ANOVA, P = 0.745, 0.750 for panels a and b, respectively).

2.5 Tables

Table 2.1 Gene-specific primers used for real-time RT-PCR.

Gene	Primer sequence (5' to 3')	Amplicon size (bp)	Efficiency (%)	Accession number	Source
gr1	F: TTCCAAGTCCACCACATCAA R: GGAGAGCTCCATCTGAGTCG	115	102	NM_001124730.1	Ings et al., 2011
gr2	F: GGGGTGATCAAACAGGAGAA R: CTCACCCCACAGATGGAGAT	140	108	NM_001124482.1	Ings et al., 2011
mr	F: GGCAGCGTTTGAGGAGATGA R: CATGGCGTCCAGTAGCTTGG	127	104	AF209873.1	Teles et al., 2013
11βhsd2	F: AGGGCAAGGCTGTCTTCATC R: CCTCCCCACACAGATCCAAC	117	106	NM_001124218.1	-
crf	F: ACAACGACTCAACTGAAGATCTCG R: AGGAAATTGAGCTTCATGTCAGG	54	102	AF296672.1	Bernier et al., 2008
pomca1	F: TGGAAGGGGGAGAGGGAGAG R: CGTCCCAGCTCTTCATGAAC	162	101	AB462418	Valen et al., 2011
pomca2	F: CTGGAGGCTGGGACTGCGGA R: CGTCCCAGCTCTTCATGAAC	157	94	AB462419	Valen et al., 2011
pomcb	F: GACTAAGGTAGTCCCCAGAACCCTCAC R: GACAGCGGTTGGGCTACCCCAGCGG	103	99	DQ508935	Valen et al., 2011
p450scc	F: GCTTCATCCAGTTGCAGTCA R: CAGGTCTGGGGAACACATCT	140	103	S57305.1	Aluru and Vijayan, 2008
star	F: TGGGGAAGGTGTTTAAGCTG R: AGGGTTCCAGTCTCCCATCT	101	103	AB047032.2	Aluru and Vijayan, 2008
β-actin	F: AGAGCTACGAGCTGCCTGAC R: GTGTTGGCGTACAGGTCCTT	179	100	NM_001124235.1	Moltesen et al., 2016
ef1α	F: CATTGACAAGAGAACCATTGA R: CCTTCAGCTTGTCCAGCAC	95	108	NM_001124339.1	Birceanu et al., 2015

For primer sets used in multiple tissues, efficiencies were determined for each tissue individually, and listed here is the mean efficiency across tissues.

Table 2.2 Linear regressions of tissue ^{3}H-cortisol uptake ('uptake', ng g^{-1}) on plasma cortisol concentration ('[cortisol]', ng mL^{-1}).

Tissue	Status	Regression Equation	R_{adj}^2	*P*-value	ANCOVA $P_{intercept}$
Liver	Dom	uptake = 2.16[cortisol] + 9.78	0.935	0.001	0.002
	Sub	uptake = 3.05[cortisol] + 176.66	0.768	0.014	
Posterior kidney	Dom	uptake = 0.66[cortisol] + 11.63	0.671	0.029	0.004
	Sub	uptake = 2.60[cortisol] + 121.55	0.711	0.022	
Gill	Dom	uptake = 0.55[cortisol] + 3.34	0.942	<0.001	0.012
	Sub	uptake = 0.55[cortisol] + 42.50	0.752	0.016	
White muscle	Dom	uptake = 0.09[cortisol] + 1.71	0.694	0.025	0.003
	Sub	uptake = 0.29[cortisol] + 18.76	0.815	0.009	

Regressions for gallbladder were not significant (P = 0.616 and P = 0.504 for dominants and subordinates, respectively) and therefore are not included in the table. N = 6 pairs for each tissue.

2.6 Discussion

The present study aimed to determine how cortisol levels remain elevated for several days during chronic social stress, despite the mechanisms in place to bring them down. We predicted that subordinate trout would exhibit some combination of impaired cortisol clearance, dysregulated negative feedback, and/or increased HPI axis activity to account for the prolonged elevation of cortisol. Our findings suggest that the capacity to metabolize and excrete cortisol is maintained in subordinate trout, as is the capacity for negative feedback control of the HPI axis. Subordinate fish exhibited increased transcript abundance of *p450scc* and *star*, proteins involved in the rate-limiting steps in cortisol biosynthesis (Aluru and Vijayan, 2006; Arukwe, 2008; Geslin and Auperin, 2004; Stocco, 2000), suggesting an increase in steroidogenic capacity that is consistent with the hypothesis that increased HPI axis activity contributes to the persistent elevation of cortisol during chronic social stress.

Use of a cortisol challenge to assess negative feedback and clearance capacity at the whole-animal level revealed no differences in rates of cortisol decline between dominant and subordinate fish. That subordinates can readily reduce their cortisol levels was also evidenced by their rapid return to unstressed plasma cortisol levels when separated from their dominant counterpart. Approximately half of the subordinate fish (6 of 13) reduced cortisol to <10 ng mL^{-1} within 24 h of separation, while most subordinates had cortisol levels typical of unstressed fish after 2 d. These data confirm the rapid recovery of cortisol levels in subordinates reported by (Culbert and Gilmour, 2016), and show that at least in some fish, recovery is even more rapid than previously reported. To tease apart the individual contributions of cortisol clearance and negative feedback to the lowering of cortisol levels at the whole-animal level, each was investigated.

We assessed tissue uptake, which contributes to the ability to clear cortisol (Mommsen et al., 1999), using ^{3}H-cortisol. As in previous studies that have used this approach, the importance of hepatobiliary cortisol clearance was evident from the high rates of uptake in the liver and bile (Donaldson and Fagerlund, 1972; Redding et al., 1984; Truscott, 1979; Vijayan and Leatherland, 1990; Wilson et al., 1998). Gallbladder and liver uptake of ^{3}H-cortisol were elevated in subordinate fish experiencing chronic social stress. Similar accumulation in the hepatobiliary pathway has been observed with other chronic stressors such as high stocking density (Vijayan and Leatherland, 1990) and confinement (Pottinger et al., 1992; Redding et al., 1984). Although we assessed uptake only at 4 d of social stress, it is likely that corticosteroid accumulation begins within hours of stressor onset. For example, Pottinger et al. (1992) reported that biliary accumulation of corticosteroids was detected 2 h into confinement stress, and continued to rise over 4 d as plasma cortisol levels were sustained around 60 ng mL^{-1}. Despite enhanced tissue uptake and elevated cortisol levels in subordinates, neither transcript nor protein abundance of 11βHSD2, the initial step in cortisol catabolism, were elevated in the liver of subordinate fish. This result was somewhat surprising because *11βhsd2* gene expression appears to be regulated by cortisol in fishes. Putative glucocorticoid response elements (GREs) were found upstream of the *11βhsd2* gene in zebrafish (Alderman and Vijayan 2012), and 24 h of cortisol exposure in zebrafish larvae elevated *11βhsd2* mRNA abundance, a response abolished by the GR antagonist RU-486 (Best and Vijayan, 2017; Tokarz et al., 2013; Tsachaki et al., 2017). Notably, however, glucocorticoid regulation of 11βHSD2 in mammals is both age- and tissue-specific (Chapman et al. 2013), and the same may be true in fishes. Further study of clearance mechanisms, particularly potential limitations during chronic stress, is warranted.

In mammals, brain expression of both GR and 11βHSD1 modulates negative feedback control of hypothalamic-pituitary-adrenal (HPA) axis activity by cortisol (Chapman et al., 2013). Negative feedback is enhanced by 11βHSD1-produced local amplification of cortisol in the hypothalamus and pituitary (Carter et al., 2009; Johnstone et al., 2000). Fishes lack *11βhsd1*, but express *11βhsd2* in HPI axis tissues (Alderman and Vijayan, 2012; Fuzzen et al., 2010; Kusakabe et al., 2003; Nematollahi et al., 2009). Moreover, brain and head kidney *11βhsd2* transcript abundance and activity were altered by exposure to an acute stressor (Alderman and Vijayan, 2012; Fuzzen et al., 2010; Nematollahi et al., 2009), suggesting a role for 11βHSD2 in modulating negative feedback through local control of cortisol signalling in HPI axis tissues. Chronic social subordination elevated transcript abundance of *11βhsd2* in the pituitary, which persisted 1 d after pair separation. A similar trend for *11βhsd2* elevation was observed in the preoptic area, but was not statistically significant. No significant effects were observed in the head kidney, although steroidogenic cells comprise only about 1:8000 of total HK cells (Hontela et al., 2008), making it difficult to detect changes that are specific to these rare cells (Fierro-Castro et al 2015). Upregulation of *11βhsd2* in the pituitary, but not the preoptic area or head kidney, was also found after 23 d of repeated acute stressors in Atlantic salmon (Madaro et al., 2015), suggesting that this pituitary response may be consistent among long-term stressors. Increased *11βhsd2* transcript abundance would be expected to reduce pituitary cortisol signalling and hence negative feedback control. However, in the context of elevated circulating cortisol levels (which may be responsible for the increased transcript abundance of *11βhsd2* in the pituitary), increased *11βhsd2* may serve to maintain the ability for negative feedback by matching the capacity for cortisol breakdown to circulating cortisol levels.

Evidence from GR knockout studies supports a role for GR in modulating negative feedback in the HPI axis, with zebrafish lacking functional GR exhibiting higher unstressed cortisol levels and an increased cortisol response to a stressor (Faught and Vijayan, 2019; Ziv et al., 2012). Similarly, basal and stressor-induced corticosterone levels were elevated in mice with partial knockdown of GR (Harris et al., 2012). However, the elevated cortisol levels of trout experiencing chronic social stress were not explained by reduced GR expression – transcript and protein (where measured) abundances of GRs were quite stable at all levels of the HPI axis after 4 d of social interaction. These data are consistent with the tight regulation of GRs observed in other tissues during chronic social stress, including gill and white muscle (Jeffrey et al., 2012). The exception is the liver, where *gr2* mRNA and Gr protein were downregulated in subordinate trout (Jeffrey et al., 2012), likely as a protective mechanism against the metabolic consequences of chronically elevated glucocorticoids (Gilmour et al., 2012; Kostyniuk et al., 2018; Kostyniuk et al., 2019a). Similarly, fairly stable expression of corticosteroid receptors has been reported in other studies that have examined HPI axis tissues during a chronic stress scenario. For example, Teles et al. (2013) used cortisol implants to mimic a chronic stressor and found no impact on receptor transcript abundances in whole brain and head kidney of trout after five days. Minor impacts on receptor transcript abundances in trout were detected in response to a chronic confinement stressor, particularly in the pituitary (Kiilerich et al., 2018). Madaro et al. (2015) subjected Atlantic salmon to unpredictable chronic stress for 23 days, which downregulated *gr1* and *gr2* mRNA in the POA, and upregulated *gr1*, *gr2*, and *mr* mRNA in the pituitary, suggesting that longer duration and/or repeated acute (with recovery in between) rather than continuous stressor exposure, may be more effective in altering receptor expression. Collectively, however, the evidence that chronic stress impacts negative feedback regulation of HPI axis activity

through modulation of GR is weak, in contrast to the situation in mammals where chronic social subordination generally results in downregulation of central GR alongside elevated glucocorticoids (reviewed by McKittrick et al., 2009).

Examination of the targets of negative feedback is an alternative approach to assess negative feedback activity. Although some of these endpoints were measured previously (Jeffrey et al., 2012; Jeffrey et al., 2014), they were assessed again here for direct comparison to transcript abundances of corticosteroid receptors and *11βhsd2* in HPI axis tissues. Transcript abundance of HPI axis genes would be expected to increase in response to the stress of social interaction, with activation of negative feedback subsequently decreasing transcript levels. Separation of the pair and release of this feedback may result in a transient rebound in transcription. This pattern is evident with *crf*, where the significant elevation of *crf* mRNA observed in subordinate trout after 8 h, 1 d (Bernier et al., 2008), and 3 d (Doyon et al., 2003) disappears by 4 d (current study) and 5 d (Jeffrey et al., 2012). After 1 d of separation, a significant elevation of *crf* mRNA was detected in recovering subordinates. This elevation may reflect alleviation of GR-mediated transcriptional repression of *crf* as cortisol levels fall during recovery. Similarly, *pomca* and *pomcb* mRNA were elevated in the pituitary of subordinate trout after 1 d of interaction (Winberg and Lepage, 1998). The current study showed that this elevation has disappeared by 4 d, and at 5 d of interaction, plasma ACTH was lower in subordinates (Jeffrey et al., 2012; Jeffrey et al., 2014). Collectively, this pattern suggests negative feedback activity. Paralogue-specific *pomc* effects in salmonids have yet to be identified, but where more than one paralogue has been measured, they typically respond similarly (Gilchriest et al., 2000; Madaro et al., 2015; Madison et al., 2013; Winberg and Lepage, 1998). Unlike *crf*, *pomc* transcript abundance did not increase during recovery, perhaps because negative feedback was

tempered in the pituitary by the impact on local cortisol catabolism of the significant elevation of *11βhsd2* mRNA levels at both 4 d of social interaction and 1 d of recovery.

In the head kidney of subordinates, transcript abundances of both *p450scc* and *star* were elevated, suggesting increased capacity for cortisol biosynthesis, in line with the elevated cortisol levels in these fish. Elevated *star* and *p450scc* mRNA also have been measured following other types of chronic stressors (or substitutes) in fishes, including 5 and 15 d of crowding (Castillo et al., 2008; Fierro-Castro et al., 2015) and 5 d of ACTH treatment (McQuillan et al., 2011). Transcription of *star* and *p450scc* is stimulated by ACTH (Aluru and Vijayan, 2008), but in a chronic stress scenario, prolonged stimulation of the stress axis can cause hypertrophy and hyperplasia of steroidogenic cells. For example, chronically stressed rats exhibit adrenal hypertrophy and hyperplasia accompanied by an increase in the corticosterone response to ACTH (Ulrich-Lai et al., 2006). Previous studies in fish have linked low social rank with larger head kidney (*Lepomis gibbosus,* Erickson, 1967) or interrenal nuclei (*O. kisutch*, Ejike and Schreck, 1980; *O. mykiss*, Noakes and Leatherland, 1977). However, these coarse metrics don't always reflect cortisol production (Scott and Rennie, 1980) so finer measurement of interrenal cell abundance and morphology may further elucidate the impacts of chronic social stress on the head kidney (addressed in chapter 3).

In summary, the findings of the current study suggest that both negative feedback and cortisol catabolism and clearance are functional during chronic social stress, and dysregulation of these processes does not account for the prolonged elevation of circulating cortisol levels in subordinate fish. However, elevated *p450scc* and *star* mRNA abundance in the head kidney of subordinate fish suggests that an increased capacity for corticosteroid biosynthesis contributes to high cortisol in these fish, a possibility that warrants further investigation.

2.7 Supplementary information

Immunohistochemical localization of GR1 in head kidney tissue

Given that the head kidney is heterogenous and steroidogenic cells are rare, confirmation of Gr presence in in steroidogenic cells would support transcript abundance in the head kidney as an indicator of negative feedback capacity. Therefore, immunohistochemistry was used to determine whether Gr colocalized with steroidogenic cells (using P450scc as a marker) and/or chromaffin cells (using tyrosine hydroxylase as a marker).

A juvenile rainbow trout (203 g) was used for immunohistochemical localization of glucocorticoid receptor 1 (Gr1), tyrosine hydroxylase (Th), and P450scc in the head kidney. Following terminal anaesthesia (0.5 g L^{-1} benzocaine), the head kidney was perfused via the posterior cardinal vein with 40 mL heparinized (2 IU mL^{-1}) 0.9% saline. The head kidney, including surrounding tissue to maintain its structure, was dissected out and fixed in 4% paraformaldehyde (PFA) overnight at 4ºC. Following washing in phosphate-buffered saline (PBS), surrounding tissue was trimmed away and the head kidney was cryoprotected in 30% sucrose (in PBS) for 17 h at 4ºC. The tissue was embedded and frozen in Shandon Cryomatrix (Thermo Fisher Scientific), and 12 µM sections were generated (Leica CM3050 S cryostat) and collected on slides (Superfrost Plus, Thermo Fisher Scientific).

Antigen retrieval was performed by incubating slides for 30 min at 65ºC in sodium citrate buffer (10 mM, 0.5% Tween-20). Sections were washed 3x in PBST (PBS + 0.2% Triton X-100) and permeabilized by incubating in PBST for 30 min. Sections were then incubated in primary antibodies diluted 1:1000 in PBST for 17 h at 4ºC. A commercially available antibody was used

for tyrosine hydroxylase (Th; mouse host, 22941, Immunostar, Hudson, WI, USA), the P450scc antibody (rabbit host) was a kind gift from Dr. Graham Young (University of Washington, USA; Kobayashi et al., 1998), and the Gr1 antibody (guinea pig host) was a kind gift from Dr. Olivier Kah (Université de Rennes, France; Tujague et al., 1998). Following 3x PBST washes, sections were incubated in secondary antibodies as follows: Th, goat anti-mouse Alexa Fluor 594; P450scc, goat anti-rabbit 488; Gr1, goat anti-guinea pig Alexa Fluor 568 (respectively, A11032, A11034, A11075, Thermo Fisher Scientific), all diluted 1:400 in PBST and incubated in the dark for 3 h at room temperature. A final three washes with PBST were followed by mounting in Vectashield Antifade Mounting Medium with DAPI (Vector Laboratories, Burlingame, CA, USA) and imaging (Olympus FV1000 confocal microscope, Olympus, Toronto, ON, CA.).

Figure S2.1. Representative images of the head kidney of a juvenile rainbow trout (*Oncorhynchus mykiss*) showing immunofluorescent localization of P450scc (green) as a marker for steroidogenic cells, tyrosine hydroxylase (TH, red) as a marker for chromaffin cells, and GR1 (red), with DAPI (blue) as a nucleus marker. Panels A and B, which is a higher magnification image of the area in A marked by the white box, show the arrangement of chromaffin (red) and steroidogenic (green) cells. Panels C and D show co-localization of GR1 (red) to steroidogenic (green) cells. Although GR1 was widely expressed in head kidney tissue, more intense immunofluorescence was apparent in steroidogenic cells. Panel E is a negative control in which the primary antibodies for P450scc and GR1 were omitted; no fluorescence was apparent.

Figure S2.1

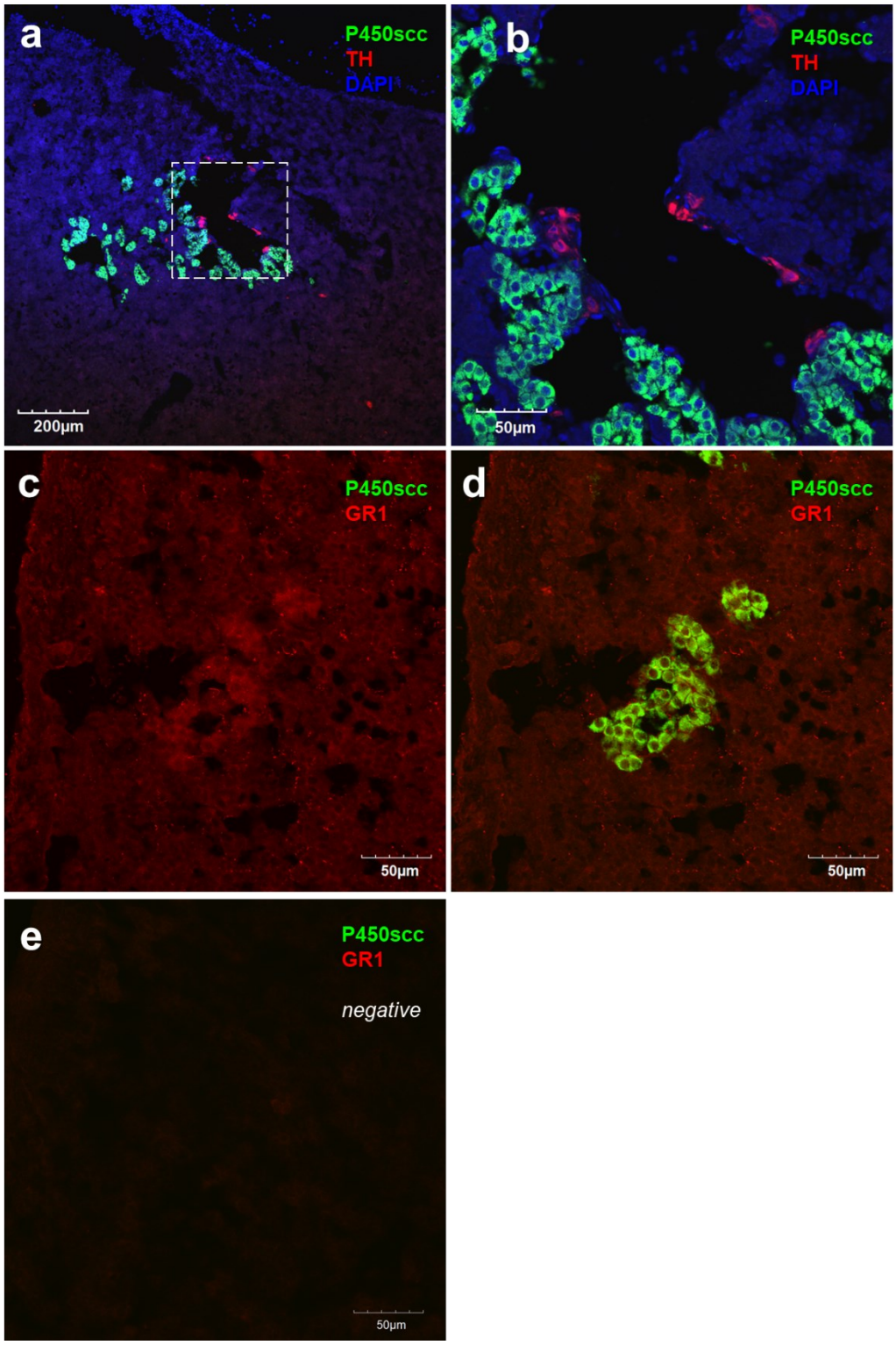
a
P450scc
TH
DAPI
200µm
b
P450scc
TH
DAPI
50µm
c
P450scc
GR1
50µm
d
P450scc
GR1
50µm
e
P450scc
GR1
negative
50µm

Figure S2.2

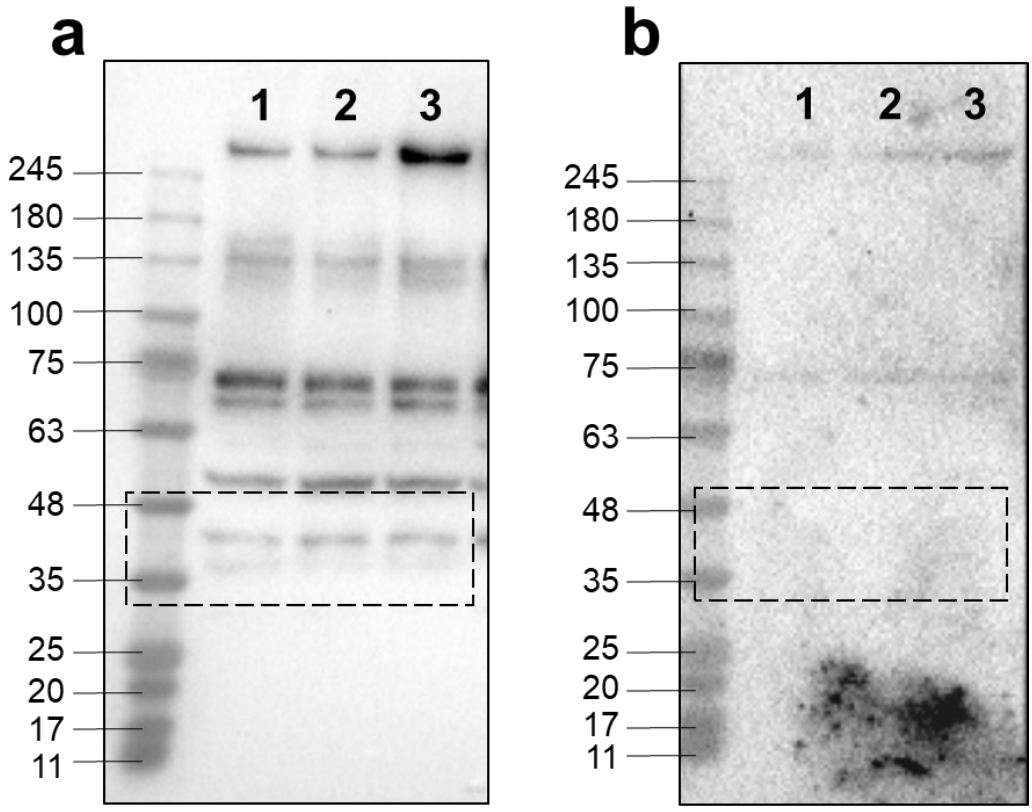

Figure S2.2 Validation of the 11βHSD2 antibody in rainbow trout (*Oncorhynchus mykiss*) showing 3 representative preoptic area samples (POA, 40 µg) incubated with 1:5000 (0.24 µg mL^{-1}) primary antibody (a) or with 1:5000 primary antibody pre-absorbed with a 10-fold higher (2.4 µg mL^{-1}) concentration of both immunizing peptides for 2 h at RT (b). The expected band region (43.8 kDa, Genbank accession NP_001117690.1) is indicated by the dashed box, and the presence of the band (a) is eliminated by preabsorption (b).

Chapter 3: Regulation of cortisol production in the head kidney of rainbow trout (*Oncorhynchus mykiss*) during chronic social stress

A part of the data in this chapter (Fig. 3.2a, b) also appears in Chapter 2 (Fig. 2.10a, d).

3.1 Introduction

Juvenile salmonid fish form pecking-order social hierarchies that can result in some individuals experiencing chronic stress (Bessa et al., 2021; Gilmour et al., 2005; Winberg et al., 2016). Rank within a hierarchy is determined by competitive ability, with dominants being more aggressive and claiming a greater share of resources such as territory and food (McCarthy et al., 1992; Metcalfe et al., 1989; Noakes and Leatherland, 1977). The behavioural differences that distinguish dominant and subordinate fish are accompanied by physiological differences. In particular, subordinate fish tend to have a physiological phenotype characteristic of chronic stress (Bessa et al., 2021; Gilmour et al., 2005; Winberg et al., 2016). A key feature of this phenotype is the sustained elevation of plasma cortisol concentrations (Culbert and Gilmour, 2016; DiBattista et al., 2006; Höglund et al., 2002; Jeffrey et al., 2012; Jeffrey et al., 2014; Sloman et al., 2001; Sloman et al., 2002a; Sørensen et al., 2011; Winberg and Lepage, 1998). The primary site of cortisol synthesis in teleosts is the head kidney, where the steroidogenic interrenal cells are located. It is well established that cortisol is produced in response to ACTH in fishes, but less is known about the signalling pathways that control the rate of steroidogenesis and how these pathways are modulated in different physiological contexts (Faught et al., 2016). For example, the sustained elevation of circulating cortisol in subordinate rainbow trout suggests increased cortisol production by interrenal cells. At the same time, however, the plasma cortisol response to acute stress is attenuated in subordinate trout, as is the head kidney cortisol response to ACTH *in vitro* (Jeffrey et al., 2014; Sloman et al., 2002a). The cellular mechanisms underlying the sustained elevation of cortisol production during chronic social stress and the apparently simultaneous limitations on acute cortisol production in response to a stressor warrant investigation.

Cortisol production in response to a stressor is under the control of the HPI axis in fishes. Upon perception of a stressor, the preoptic region of the brain releases CRF to the pituitary (Bernier et al., 2008). In response, the anterior pituitary produces ACTH which is released into the bloodstream (Bernier et al., 2009). ACTH signals steroidogenic cells in the head kidney to increase cortisol production via the melanocortin-2 receptor (MC2R), a G-protein coupled receptor (Aluru and Vijayan, 2008). Trafficking of MC2R to the plasma membrane is aided by two melanocortin receptor accessory proteins (MRAP), MRAP1 and MRAP2, with MRAP1 being required for receptor activation (Agulleiro et al., 2010; Dores et al., 2016). Binding of ACTH to MC2R increases adenylate cyclase activity, and the subsequent increase in cAMP stimulates protein kinase A (PKA) and cortisol synthesis (Lacroix and Hontela, 2001). PKA-mediated phosphorylation of transcription factors is key in transcriptional upregulation of steroidogenic genes in mammals (Ruggiero and Lalli, 2016). Although direct functional studies are limited in fishes, ACTH treatment of head kidney tissue increases mRNA levels of both steroidogenic acute regulatory (*star*) protein and p450 side-chain cleavage (*p450scc*) enzyme, collectively considered the rate-limiting steps in steroidogenesis (Aluru and Vijayan, 2008). A key player in the transcriptional regulation of many steroidogenic genes is the transcription factor steroidogenic factor 1 (SF-1), a nuclear receptor in the NR5A group (Chai et al., 2003; Hsu et al., 2003; Quek and Chan, 2009). The gene encoding this transcription factor is *ff1* (*Fushi tarazu factor-1*), and the zebrafish paralogues *ff1b* and *ff1d* are considered co-orthologues for mammalian *sf-1*, likely duplicated in the teleostean whole genome duplication (Kuo et al., 2005). During primer design, we found a salmonid-specific duplication of *ff1b*, and named them *ff1b1* and *ff1b2*. Much of the evidence for *ff1b* and *ff1d* function comes from zebrafish, including the requirement of *ff1b* for interrenal development and transcriptional control of *p450scc* (Chai et al.,

2003; Hsu et al., 2003; Quek and Chan, 2009). There is also evidence in a salmonid, Arctic char (*Salvelinus alpinus*), for SF-1 presence in steroidogenic tissues (Von Hofsten et al., 2003). Despite its relatively recent discovery, the role of SF-1 as a master regulator of basal and cAMP-induced steroidogenic gene expression in mammalian models is becoming clearer (Ruggiero and Lalli, 2016; Schimmer and White, 2010; Val et al., 2003). This transcription factor is only starting to receive attention in fishes.

The present study investigated regulation of cortisol production by the head kidney in fish experiencing chronic social stress. The cortisol profile of subordinate fish has two key characteristics that we aimed to elucidate; (1) sustained elevation of chronic cortisol production, and (2) attenuated acute cortisol production (Jeffrey et al., 2014; Sloman et al., 2002a). To address the mechanisms underlying sustained elevation in cortisol production by the subordinate head kidney, we assessed *in vitro* cortisol production by isolated head kidney tissue, transcript abundances of the steroidogenic genes *star*, *p450scc* and the *ff1* paralogues, and steroidogenic cell size and abundance. To determine why the head kidney from subordinates has lowered acute cortisol production, we used ACTH to stimulate acute cortisol production both *in vivo* and *in vitro*, and we examined the signalling pathway by measuring cortisol production in response to dibutyryl-cAMP (db-cAMP), transcript abundances of *mc2r*, *mrap1*, and *mrap2*, and cAMP levels and overall phosphorylation by PKA. Given that both aims involve the production of cortisol in different contexts, several of these endpoints provide insight into both chronic and acute cortisol production.

3.2 Materials and methods

3.2.1 Experimental animals

Juvenile rainbow trout, weighing 104.4 ± 3.0 g (mean ± SEM, $N = 96$; see Table S1 for all weight and length data) were obtained from Linwood Acres Trout Farm (Campbellcroft, Ontario) and held at the University of Ottawa in 1275 L fibreglass tanks supplied with flowing, aerated, 13ºC, dechloraminated city of Ottawa tap water ("system" water) with a mild current. Fish were scatter fed 0.5% body mass daily with Zeigler Silver pellets and held under a 12L:12D photoperiod. These conditions served to minimize hierarchy formation in holding tanks. All protocols were approved by an institutional animal care committee (protocol BL-2118), and were in accordance with Canadian Council on Animal Care guidelines for the use of animals in research and teaching.

3.2.2 Experimental protocols

Experiments were carried out on dominant and subordinate trout, achieved by allowing size-matched pairs of trout to establish a social hierarchy. Sham-treated fish were included in some experiments. To investigate mechanisms of basal cortisol production, head kidneys were used to determine basal cortisol production *in vitro*, measure transcript abundances of key steps in the steroidogenic pathway, and determine steroidogenic cell size and abundance via flow cytometry. To investigate mechanisms of stimulated (acute) cortisol production, fish were challenged *in vivo* with ACTH to assess the plasma cortisol response, and head kidney tissue was challenged *in vitro* with different doses of ACTH or db-cAMP. Additionally, head kidney

transcript abundance of the ACTH receptor system, cAMP levels, and abundance of proteins phosphorylated by PKA were measured.

Social hierarchies were created using established protocols (Culbert and Gilmour, 2016; Gilmour et al., 2012; Jeffrey et al., 2014). Briefly, juvenile rainbow trout from stock tanks were lighted anaesthetized (in 0.05 g L^{-1} benzocaine; Sigma-Aldrich, Oakville, ON, CA) to obtain their weight, length, and initial fin damage score. Weight and length were used to ensure that individuals allocated to a pair were size-matched (Table S1). Differences in length averaged 0.4 ± 0.0 cm (1.9 ± 0.2%; N = 45 pairs) and differences in weight averaged 5.4 ± 0.6 g (5.2 ± 0.6%; N = 45 pairs). Pairs were held in 40 L tanks supplied with flowing system water, with individuals initially separated by an opaque perforated divider (day 0). Fish were allowed to recover overnight, and the following day the divider was removed to allow fish to interact (day 1). Behavioural observations (5 min) were performed twice daily (morning and afternoon) on days 1 through 4. To assess willingness to acquire food, pairs were offered one pellet during each observation period starting on day 2. After the second behavioural observation of the day, fish were offered 0.5% body weight per day on days 2 through 4. Sham fish were handled identically to paired fish, but were held alone.

Aggressive acts, position in the tank, and acquisition of a food pellet were scored in each observation period, with higher values indicating more dominant behaviour. Fin damage was assessed at the time of sampling, and compared to the initial value to yield a score for fin damage accrued during social interaction. For each individual, the scores for each parameter were averaged across all observation periods. Mean scores for aggressive acts, position, acquisition of a food pellet and fin damage were analyzed using a principal component analysis (PCA) to yield

a behaviour score (the first principal component, PC1) for each fish, and the individual with the higher behaviour score within a pair was considered to be dominant.

On day 5, a subset of pairs was used to assess *in vivo* cortisol production in response to exogenous ACTH (see below). All other fish were euthanized by terminal anaesthesia (in 0.5 g L^{-1} benzocaine; Sigma-Aldrich). Blood (~1 mL) was withdrawn from the caudal vasculature using a 23G needle and syringe rinsed with heparinized (H3393, Sigma-Aldrich) 0.9% saline solution. Whole blood was centrifuged at 13,500 *g* for 3 min. The resulting plasma was transferred to a new tube, flash frozen, and stored at -80°C until measurement of cortisol concentrations. Head kidney tissue was dissected out and processed in one of three ways; flash frozen and stored at -80°C for quantification of transcript and protein abundances, transferred to L-15 medium to assess cortisol production *in vitro*, or processed into a cell suspension for flow cytometry (see Supplementary material).

3.2.3 In vivo *cortisol production in response to ACTH*

On day 5, fish were lightly anesthetized (in 0.05 g L^{-1} benzocaine; Sigma-Aldrich), and a small (100 µL) blood sample was withdrawn from the caudal vasculature with a heparinized 27G needle. Fish were then injected intraperitoneally with 22.5 µg kg^{-1} ACTH (1-24 fragment, A0298, Sigma-Aldrich) in 0.9% saline (2 µL g^{-1}) using a 27G needle. The ACTH dose and timing were chosen based on Pottinger and Carrick (2001). Saline vehicle injections were not used in the present study because in previous work using the same protocol, no significant rise in cortisol levels occurred following saline vehicle injection (Chapter 2). Fish were returned to their tank (without the divider in place), observed to ensure that they recovered quickly from the

anaesthetic, and terminally sampled 2 h later as described above. Plasma cortisol concentrations were measured in pre- and post-injection blood plasma to assess the cortisol response to ACTH.

3.2.4. Analytical approaches

3.2.4.1 Measurement of cortisol concentrations

A commercial radioimmunoassay kit (MP Biomedicals, Solon, OH, USA) was used to measure cortisol levels in plasma and media according to the manufacturer's instructions. This kit was validated for use with rainbow trout (Gamperl et al., 1994). The detection limit for the kit is 0.17 pg dL^{-1} and the inter- and intra-assay variabilities (expressed as the coefficient of variation) averaged 7.2% and 3.3%, respectively.

3.2.4.2 Measurement of transcript abundances by semi-quantitative RT-PCR

Head kidney tissue stored at -80°C was ground to a fine powder on dry ice. Total RNA was extracted from an aliquot (~50 mg) of powdered tissue by sonicating in Trizol reagent on ice (Sonic Dismembrator Model 100; Thermo Fisher Scientific, Waltham, MA, USA), and extracting as per the manufacturer's instructions (Trizol Reagent, Life Technologies, Carlsbad, CA, USA). RNA was resuspended in 30 µL nuclease-free water and quantified using a Nanodrop 2000c UV-vis Spectrophotometer (Thermo Fisher Scientific). The Quantitect cDNA synthesis kit (Qiagen, Toronto, ON, CA) was used to remove genomic DNA and synthesize cDNA from 1 µg of total RNA, according to the manufacturer's instructions. A "no-RT" control with water in place of reverse transcriptase was used to verify absence of genomic DNA (gDNA).

Transcript abundance was measured by semi-quantitative real-time RT-PCR using a Rotor-Gene Q PCR cycler and the Rotor-Gene SYBR green qPCR kit (Qiagen), according to the manufacturer's instructions. In each reaction, which was scaled down to 10 μL, 1 μL of cDNA was used as template except for *β-actin* where 1 μL of a 50x dilution was used. Every run included "noRT" and no template controls. A final primer concentration of 1 μM was used for all genes (Table 1). Cycling conditions were those specified by the manufacturer for the Rotor-Gene SYBR Green PCR Kit, with a combined annealing/extension temperature of 60°C except for *ff1b2*, where 56°C was used. The primers for ff1 paralogues were designed using Primer-BLAST and their specificity was verified by sequencing the amplified products. Primer efficiency was determined by serial dilution of a pooled cDNA sample and was between 90-110% for all primer sets (Table 1). Melt curves confirmed amplification of a single product in all cases. The reference gene *β-actin* was used for normalization, and stability across social status was verified by one-way ANOVA. Transcript abundance was analysed using the method of Pfaffl (2001), and expressed as fold-change relative to the sham group.

3.2.4.3 Measurement of PKA-induced phosphorylation by SDS-PAGE and western blotting

Head kidney tissue stored at -80°C was ground to a fine powder on dry ice and homogenized in RIPA buffer (150 mM NaCl, 1% triton X-100, 0.5% sodium deoxycholate, 0.1% SDS, 50 mM Tris-HCl, 1 mM EDTA) containing protease inhibitor mini tablets (88665, Thermo Fisher Scientific) and phosphatase inhibitors (100 mM NaF, 4 mM Na-pyrophosphate, 2 mM Na-orthovanadate). Homogenates were diluted 100-fold in RIPA buffer to assay protein concentrations by the bicinchoninic acid assay (Pierce, Thermo Fisher Scientific) using bovine serum albumin (BSA, Sigma-Aldrich) as a protein standard. Prior to western blotting,

homogenates were diluted with RIPA and 2x Laemmli buffer (Thermo Fisher Scientific) to an appropriate protein concentration, determined from the linear range of a dilution curve.

Diluted protein homogenates were heated to 100°C for 3 min and run on a 10% TGX Stain-Free gel (Bio-Rad Laboratories, Mississauga, ON, CA) with a protein size marker (BLUeye Prestained Protein Ladder, FroggaBio, Concord, ON, CA) at 200 V for 55 min. The gel and a polyvinylidene fluoride (PVDF) membrane were soaked in transfer buffer (25 mM Tris, 192 mM glycine, 20% methanol) for 15 min, following which proteins were transferred from the gel to the blot using a semi-dry transfer unit (Trans-Blot SD, Bio-Rad) at 15 V for 1 h. Total protein staining (UV) was imaged on the blot for later normalization (Bio-Rad ChemiDoc XRS+). The blot was blocked with 5% skim milk (Bioshop, Burlington, ON, CA) in Tris-buffered saline with Tween (TBST, 150 mM NaCl, 20 mM Tris, 0.05% Tween) for 1 h at room temperature (RT) with shaking. Blots were incubated overnight with primary antibody (Phospho-PKA Substrate Rabbit mAb #9624S, Cell Signaling Technology, Beverly, MA, USA) in 2% skim milk in TBST at a concentration of 1:10,000 with shaking at 4°C. Blots were washed 3 x 5 min in TBST with shaking, and then incubated with anti-rabbit horseradish peroxidase (HRP) secondary antibody (1:5000) for 1 h at RT. Blots were washed again 3 x 15 m, and then Luminata Classico HRP substrate (EMD Millipore, Thermo Fisher Scientific) was added (5 mL per blot) prior to chemiluminescent imaging (Bio-Rad ChemiDoc XRS+). Total lane staining was quantified and normalized to total protein using ImageLab 6.0 (Bio-Rad) according to Taylor and Posch (2014).

3.2.4.4 *In vitro* cortisol production

The general approach for *in vitro* head kidney preparations was based on the protocols of Aluru and Vijayan (2006) and Jeffrey et al. (2014). Head kidney tissue was dissected out, rinsed in cold Leibovitz's L-15 medium (Gibco, Thermo Fisher Scientific) and weighed. The tissue was transferred to a glass petri dish on ice with 100 mL L-15 medium per gram tissue, minced to 1 mm^3 pieces, and incubated at 13ºC with shaking for 3 h. Following the 3 h rest period, tissue pieces were allocated evenly among wells in a 48-well microplate (Corning Costar, Corning, NY, USA). Exact weights were determined at the end of the experiment for normalization and were typically ~ 25 mg per well. Treatments (ACTH, A6303 or db-cAMP, D0627; Sigma-Aldrich) were added to the appropriate wells in duplicate to achieve concentrations of $1x10^{-5}$ to 1 IU mL^{-1} ACTH (in 10-fold steps), and 1 or 4 mM db-cAMP. These concentrations were chosen based previous studies (Aluru and Vijayan, 2006; Bélair-Bambrick, 2016; Jeffrey et al., 2014; Patiño et al., 1986) and pilot trials. Tissue was incubated at 13ºC with shaking for 4 h, an incubation time chosen based on the results of Aluru and Vijayan (2006) and pilot trials that indicated linear cortisol production. The contents of each well were centrifuged for 2 min at 13,000 *g*. The resulting supernatant was frozen in lN_2 and stored at -80°C until measurement of cortisol concentrations (as described above), and the remaining tissue was weighed to normalize cortisol production to tissue weight.

3.2.5 Statistical analysis

Values are presented as means ± 1 standard error of the mean (SEM). Statistical analyses were performed using Sigmaplot v13.0 (Systat Software, Inc., San Jose, CA, USA). Student's *t*-

tests were performed to detect significant differences between dominant and subordinate fish, whereas one-way analysis of variance (ANOVA) followed by Tukey post-hoc tests was used where sham fish were included in the analysis. Where treatment or time were included as additional factors, two-way ANOVAs with Tukey post-hoc tests were used. Where necessary, data were transformed to meet the assumptions of normality and equal variance for parametric tests. If data could not be transformed to meet the assumptions, then an equivalent nonparametric test was used. The significance level (α) was 0.05.

3.3 Results

3.3.1 Plasma cortisol and behaviour within social hierarchies

Trout held in pairs for 4 d established social hierarchies as evidenced by strongly divergent behaviour scores (Table 3.2). Plasma cortisol concentrations after 4 d of social interaction were significantly higher in subordinate trout relative to dominant and/or sham fish for all experiments (Table 3.2).

3.3.2 Mechanisms underlying the sustained elevation of cortisol in subordinate trout

In vitro basal cortisol production (i.e. in the absence of stimulation by ACTH) was significantly higher for head kidney tissue from subordinate fish than dominant fish (Fig. 3.1a; Mann-Whitney U Test, $P = 0.026$). Additionally, a significant relationship between basal cortisol production and plasma cortisol values was detected in subordinates (Fig. 3.1b; linear regression, $R^2 = 0.742$, $P < 0.001$). This relationship was not significant in dominant fish ($P = 0.505$).

To examine potential factors underlying the difference in basal cortisol production between dominant and subordinate fish, abundances of transcripts associated with steroidogenesis were measured in head kidney tissue. Transcript abundances of *star* and *p450scc*, proteins involved in key rate-limiting steps in steroidogenesis, were significantly affected by chronic social stress (Fig. 3.2a,b; ANOVA, $P = 0.023$ and 0.039, respectively). For *star*, transcript abundance was significantly higher in subordinates than dominants ($P = 0.028$) but not shams. For *p450scc*, a significant difference was detected between subordinate and sham fish ($P = 0.044$).

Transcript abundances of three trout paralogues, *ff1b1*, *ff1b2*, and *ff1d*, of the transcription factor SF-1 were differentially affected by chronic social stress (Fig. 3.2c-e). Significant effects of social status were detected for transcript abundances of *ff1b2* (ANOVA, $P = 0.045$) and *ff1d* ($P < 0.001$), but not *ff1b1* ($P = 0.658$). Post-hoc analysis was unable to identify the source of the significant difference for *ff1b2*, although comparisons with subordinates yielded $P = 0.062$ and 0.084 for shams and dominants, respectively. The *ff1d* paralogue of SF-1 was most impacted by chronic social stress, with the transcript abundance in subordinates being at least an order of magnitude greater than those in sham and dominants.

Because differences in interrenal cell abundance could contribute to differences in transcript abundances, flow cytometry was used to assess interrenal cells. No significant effect of social status on interrenal cell number or size was detected (see Supplementary material).

3.3.3 Stimulation of cortisol production in vivo *and* in vitro

An ACTH challenge was used to compare the acute plasma cortisol response in dominant versus subordinate trout. Plasma cortisol levels increased significantly in both groups following intraperitoneal injection of ACTH (Fig. 3.3a; 2-way repeated measures ANOVA, $P = 0.038$ for the interaction of social status and time post-injection). Although subordinates had significantly higher cortisol levels prior to injection ($P = 0.007$), their cortisol levels did not rise as sharply as those of dominants in response to ACTH, resulting in similar cortisol levels 2 h post-injection. Direct comparison of the net cortisol response to ACTH confirmed the significantly attenuated plasma cortisol response of subordinate relative to dominant fish (Fig. 3.3b; Student's *t*-test, $P = 0.038$).

To examine the mechanisms underlying attenuation of the cortisol response to ACTH *in vivo* in subordinate trout, cortisol production was measured *in vitro* in head kidney preparations from dominant versus subordinate trout. Cortisol production in response to stimulation (Fig. 3.4a) was corrected for basal cortisol production (Fig. 3.1a). Basal cortisol production was more than an order of magnitude lower than stimulated production and correction did not impact response patterns. Head kidney tissue from subordinate fish exhibited lower cortisol production in response to stimulation with 0.1 IU mL^{-1} ACTH than did tissue from dominant fish (Mann-Whitney U test, $P = 0.005$). To further probe the basis of this difference, dose-response curves were created using concentrations of ACTH ranging from 10^{-5} to 1 IU mL^{-1} (Fig. 3.4b). The maximal response of subordinate fish was significantly lower than that of dominant fish (Fig. 3.4c; Student's *t*-test, $P = 0.033$), a pattern consistent with the response to ACTH in Fig. 4a. The ACTH concentration at which half maximal cortisol production was reached (EC50) averaged 0.112 ± 0.045 IU mL^{-1} (N=8) and did not differ significantly between dominant and subordinate

fish (Mann-Whitney U test, $P = 0.121$). To eliminate potential contributions of MC2R signalling to differences in cortisol production, the cell permeable cAMP analogue db-cAMP was used. The cortisol response to db-cAMP was dose-dependent overall, being higher at 4 mM than 1 mM, and the response to db-cAMP regardless of dose was significantly lower in subordinate fish (Fig. 3.4a; two-way ANOVA, $P_{dose} = 0.001$, $P_{status} = 0.003$, $P_{dose\ x\ status} = 0.548$).

Transcript abundances of the ACTH receptor system were measured in the head kidney of sham, dominant, and subordinate rainbow trout (Fig. 3.5) to determine whether the ACTH receptor system was altered by 4 d of chronic social stress. No differences were detected in mRNA relative levels of the melanocortin-2 receptor (*mc2r*) itself (Fig. 3.5a; ANOVA, $P = 0.336$). However, transcript abundances of both of the accessory proteins *mrap1* and *mrap2* were significantly higher in subordinates than in sham fish (Figs. 3.5b,c; ANOVA, $P = 0.010$ and 0.011, respectively).

Functional consequences of these differences in transcript abundance were assessed by measuring cAMP concentrations and phosphorylation of head kidney proteins by PKA. Head kidney tissue cAMP concentration following incubation with blank or 0.1 IU mL^{-1} ACTH for 20 min did not differ between dominant and subordinate fish (data not shown). However, the relative abundance of head kidney proteins phosphorylated by PKA was significantly higher in tissue collected from subordinate than sham fish (Fig. 3.6; ANOVA, $P = 0.018$).

3.4 Figures

Figure 3.1

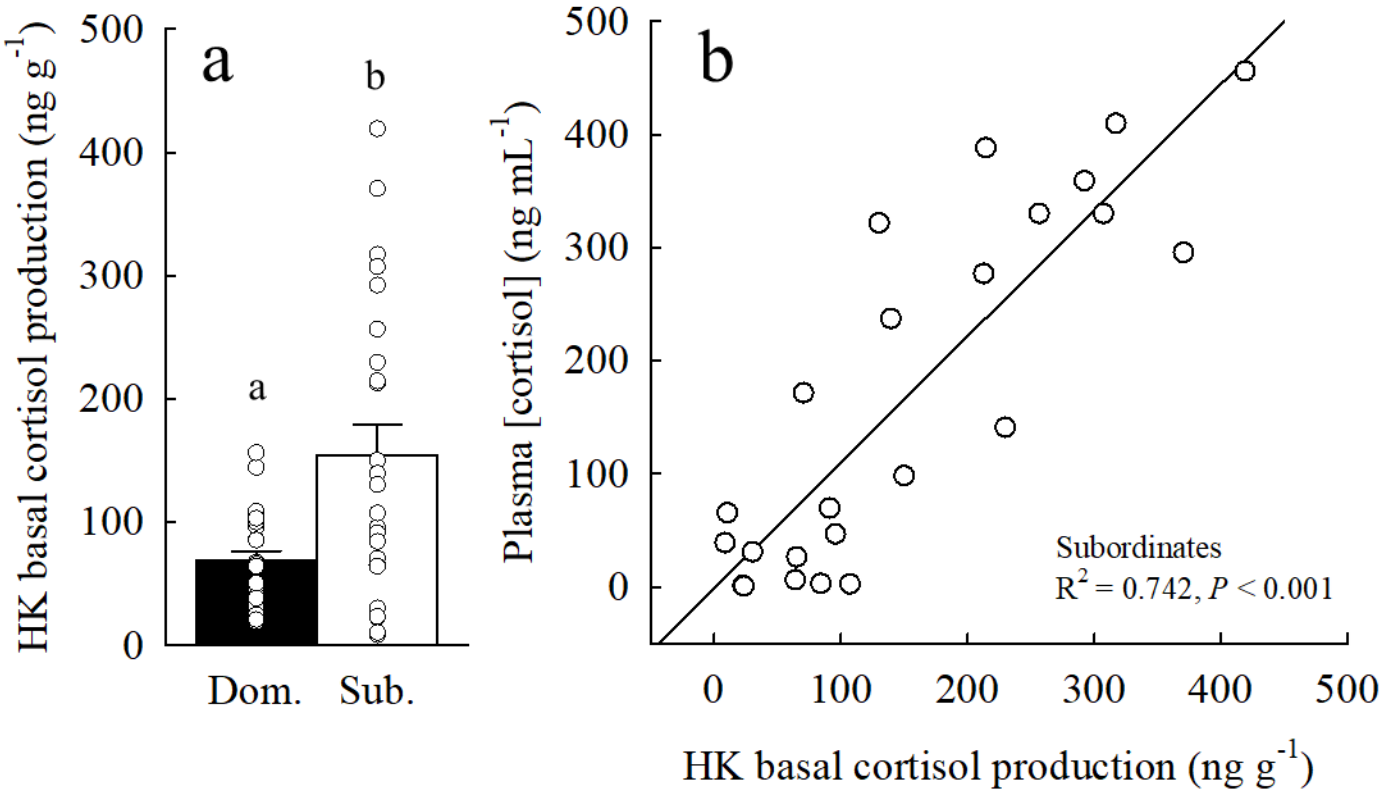

Figure 3.1 Cortisol production *in vitro* by unstimulated head kidney (HK) tissue from dominant and subordinate rainbow trout, *Oncorhynchus mykiss* (a). Different letters indicate a significant difference (Mann-Whitney U Test, $P = 0.026$). Data are means ± SEM with individual values shown as white symbols, and $N = 24$ pairs. A significant relationship between head kidney cortisol production *in vitro* and circulating plasma cortisol concentrations *in vivo* was detected in subordinate fish by linear regression analysis (b). The corresponding relationship in dominant fish was not significant (data not shown).

Figure 3.2 Transcript abundances of key components of the steroidogenic pathway (a,b) and regulatory factors (c-e) in the head kidney of sham, dominant (Dom), and subordinate (Sub) rainbow trout (*Oncorhynchus mykiss*). All values are normalized to *β-actin* as a reference gene, and expressed as fold-change relative to the sham group. Data are expressed as means ± SEM with individual values shown using white symbols ($N = 6$ in all cases). Bars that share a letter are not significantly different from one another (ANOVA, $P = 0.023$, 0.039, 0.658, 0.045, <0.001, for panels a to e, respectively).

Figure 3.2

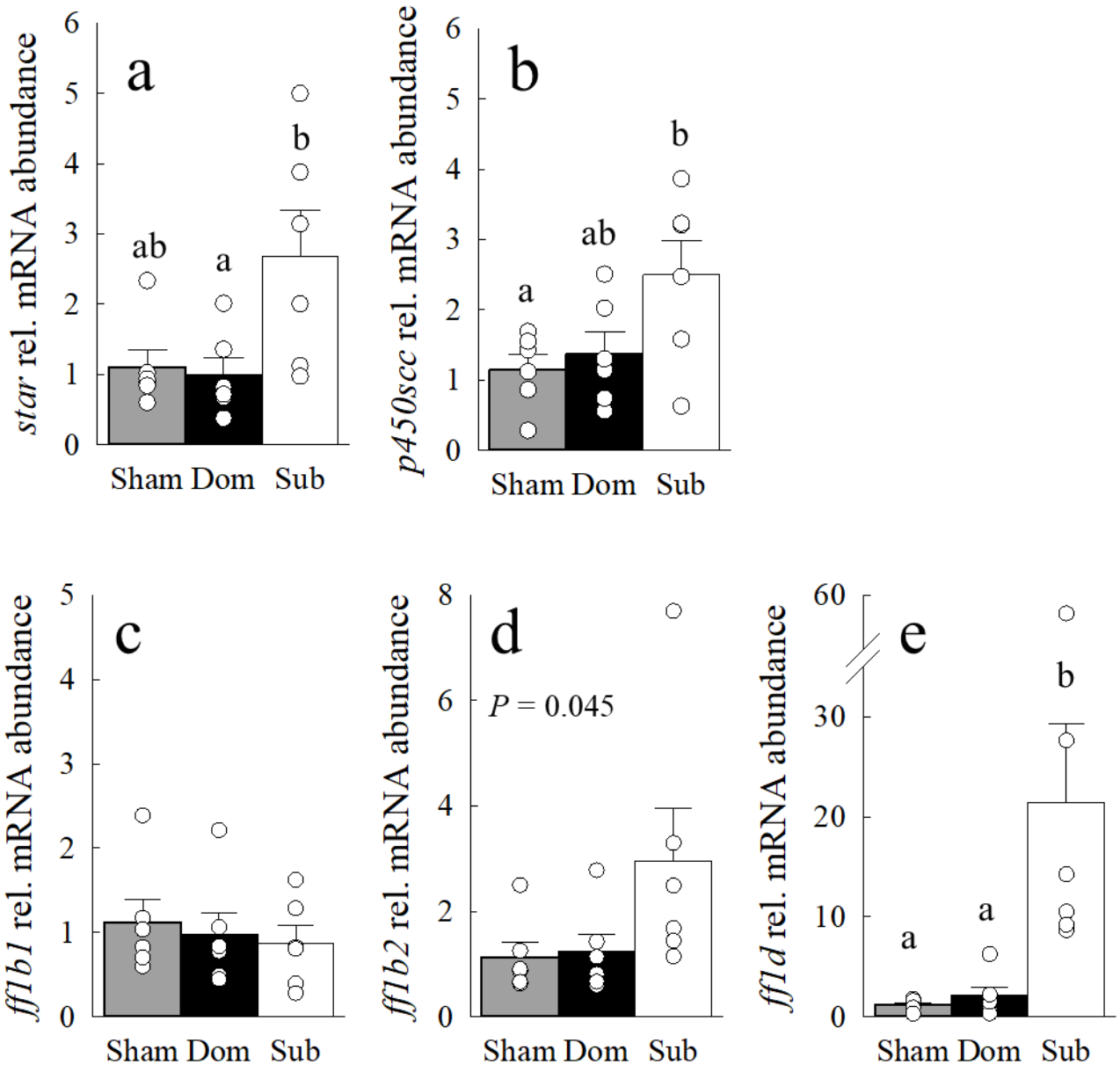
a
star rel. mRNA abundance
ab
a
b
Sham Dom Sub
b
p450scc rel. mRNA abundance
a
ab
b
Sham Dom Sub
c
ff1b1 rel. mRNA abundance
Sham Dom Sub
d
P = 0.045
ff1b2 rel. mRNA abundance
Sham Dom Sub
e
ff1d rel. mRNA abundance
a
a
b
Sham Dom Sub

Figure 3.3

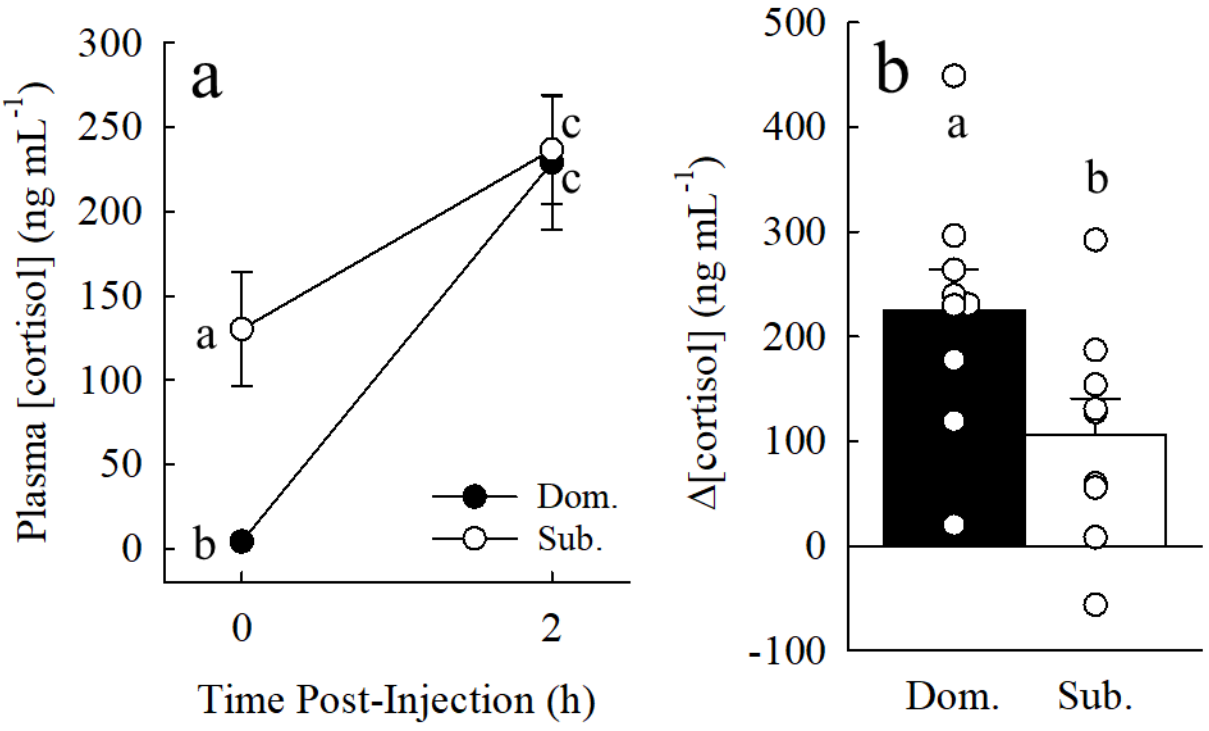

Figure 3.3 Plasma [cortisol] response to ACTH injection in dominant (Dom) and subordinate (Sub) rainbow trout (*Oncorhynchus mykiss*) as a function of time (a), and as the net increase relative to pre-injection levels (b). In (a), a significant interaction between the factors of social status and time post-injection was detected (2-way RM ANOVA, $P = 0.038$); points that share a letter are not significantly different from one another. In (b), different letters indicate a significant difference (Student's *t*-test, $P = 0.038$). Data are shown as means ± SEM ($N = 9$ pairs) with individual values shown as white symbols in (b).

Figure 3.4 Cortisol production *in vitro* by head kidney tissue from dominant (Dom) and subordinate (Sub) rainbow trout (*Oncorhynchus mykiss*) in response to ACTH or dibutyryl-cAMP (db-cAMP). In (a) and (b), basal (unstimulated) cortisol production for each preparation was subtracted from the corresponding stimulated cortisol production. Panel b presents a representative summary of the dose-response curves for ACTH, with all values shown as means. The curves represent sigmoidal dose-response regressions performed on all values for dominant or subordinate fish ($y = min + (max-min)/(1+10^{logEC50-x})$). Regression analyses carried out on values for individual fish yielded their maximal responses (shown in c) and EC50 values (no difference, see text for details). In (a), a significant effect of status was detected for ACTH (Mann-Whitney U test, $P = 0.005$), and for db-cAMP, significant main effects of dose and status were detected (two-way ANOVA, $P_{dose} = 0.001$, $P_{status} = 0.003$, $P_{dose\ x\ status} = 0.548$). In (c), a significant effect of status was detected (Student's *t*-test, $P = 0.033$). Data are presented as means ± SEM with individual values shown as white symbols in (a) and (c). In (a), $N = 18$, 9, and 6 pairs for ACTH, 1 mM, and 4 mM db-cAMP, respectively. In (b) and (c), $N = 8$ pairs. Bars or pairs of bars that share a letter are not significantly different from one another, and an asterisk at the legend represents a significant main effect of status for db-cAMP.

Figure 3.4

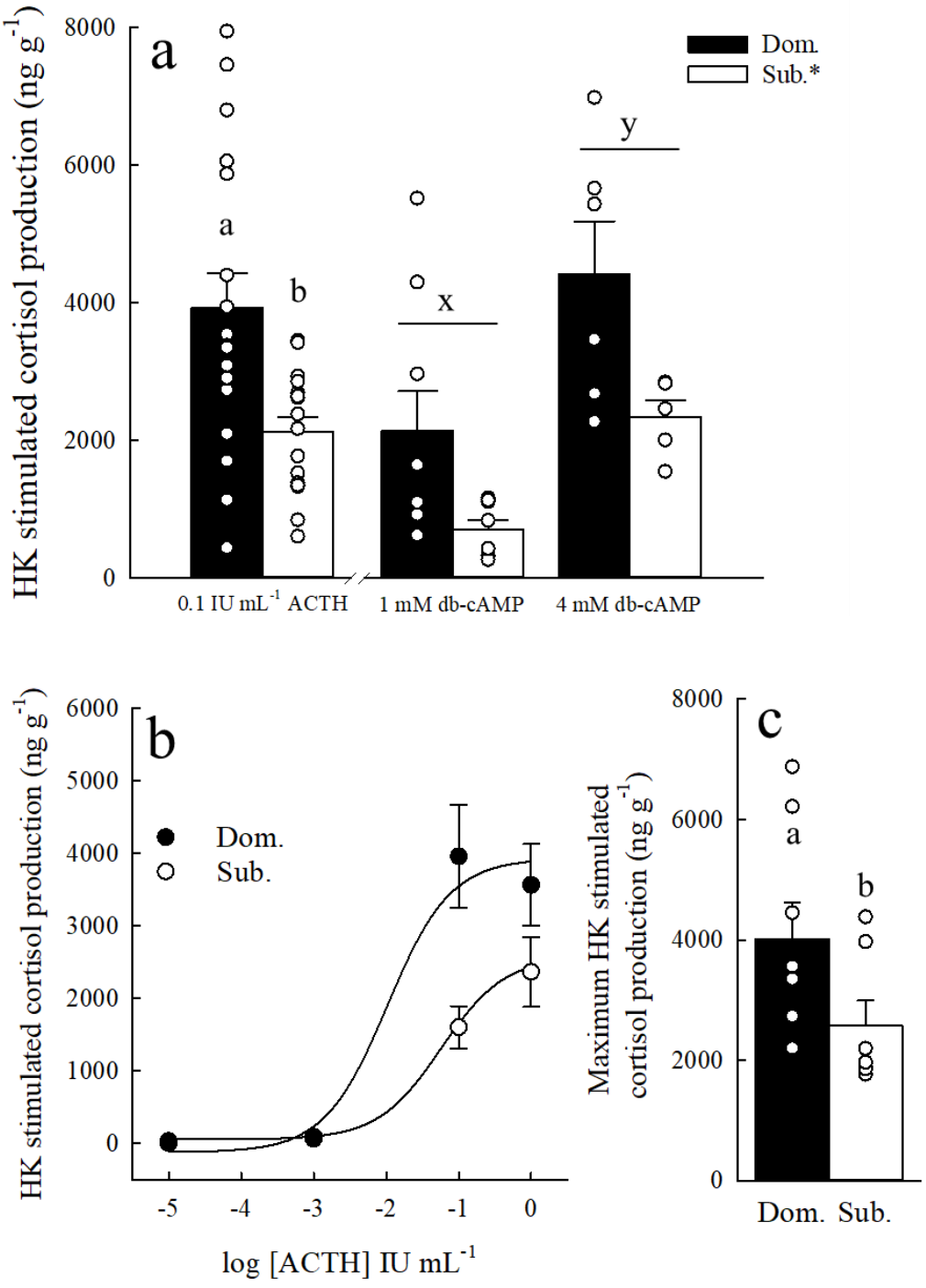
a
Dom.
Sub.*
HK stimulated cortisol production (ng g-1)
8000
6000
4000
2000
0
a
b
x
y
0.1 IU mL-1 ACTH
1 mM db-cAMP
4 mM db-cAMP
b
Dom.
Sub.
HK stimulated cortisol production (ng g-1)
6000
5000
4000
3000
2000
1000
0
-5
-4
-3
-2
-1
0
log [ACTH] IU mL-1
c
Maximum HK stimulated cortisol production (ng g-1)
8000
6000
4000
2000
0
a
b
Dom.
Sub.

Figure 3.5

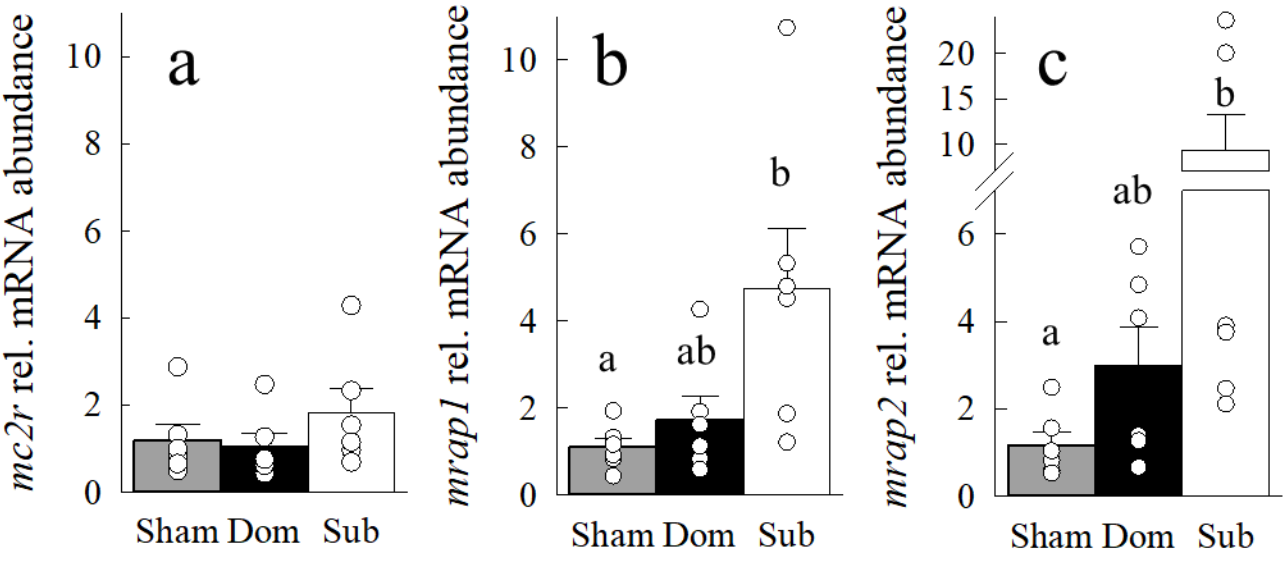

Figure 3.5 Transcript abundances of key components of the ACTH receptor system in the head kidney of sham, dominant (Dom), and subordinate (Sub) rainbow trout (*Oncorhynchus mykiss*). All values are normalized to *β-actin* as a reference gene, and expressed as fold-change relative to the sham group. Data are expressed as means ± SEM with individual values shown using white symbols ($N = 6$ in all cases). Bars that share a letter are not significantly different from one another (ANOVA, $P = 0.336, 0.010, 0.011$, for a to c, respectively).

Figure 3.6

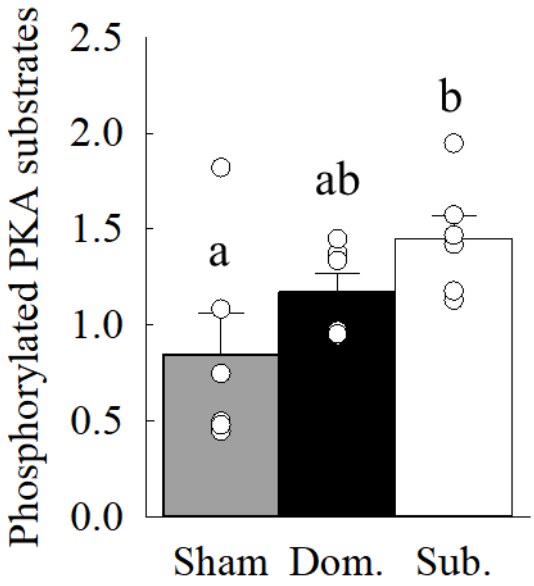

Figure 3.6 Relative abundance of proteins phosphorylated by protein kinase A (PKA) in the head kidney of sham, dominant (Dom), and subordinate (Sub) rainbow trout (*Oncorhynchus mykiss*). Values are normalized to lane total protein and expressed as fold-change relative to a pooled control sample. Data are expressed as means ± SEM with individual values shown using white symbols ($N = 6$). Bars that share a letter are not significantly different from one another (ANOVA, $P = 0.018$).

3.5 Tables

Table 3.1 Gene-specific primers for real-time RT-PCR.

Gene	Primer sequence (5' to 3')	Amplicon size (bp)	Efficiency (%)	Accession number	Source
mrap1	F: GACGAGCGCAAACTGAAA R: CTGACTGAACGGGACATGAA	116	109	NM_001246347.1	(Sandhu et al., 2019)
mrap2	F: CGGACCCGGACTACAAGTGGA R: GGCCCACCCAGAAGCCTATCA	111	105	NM_001246353.1	(Sandhu et al., 2019)
mc2r	F: GAGAACCTGTTGGTGGTGGT R: GAGGGAGGAGATGGTGTTGA	105	94	NM_001124680.1	(Aluru and Vijayan, 2008)
ff1b1	F: ACGTCTGGCCTACCTCATAG R: TTTCAAAGGGACGCCTTGT	64	93	NM_001124537.1	-
ff1b2	F: TGGTAGGCGTAATGGACTACA R: TGTCCTCTTGAAGAAGCCCTTA	131	93	XM_021605623.1	-
ff1d	F: CTACAGACCCTACAGGCGGA R: CAGTAGCTTCACATCGGGGT	81	108	XM_014143565.1	-
p450scc	F: GCTTCATCCAGTTGCAGTCA R: CAGGTCTGGGGAACACATCT	140	103	S57305.1	(Aluru and Vijayan, 2008)
star	F: TGGGGAAGGTGTTTAAGCTG R: AGGGTTCCAGTCTCCCATCT	101	103	AB047032.2	(Aluru and Vijayan, 2008)
β-actin	F: AGAGCTACGAGCTGCCTGAC R: GTGTTGGCGTACAGGTCCTT	179	100	NM_001124235.1	(Moltesen et al., 2016)

mrap, melanocortin 2 receptor accessory protein; *mc2r*, melanocortin 2 receptor; *ff1,* fushi tarazu factor 1; *p450scc*, cytochrome p450 side chain cleavage enzyme; *star*, steroidogenic acute regulatory protein.

Table 3.2 Plasma cortisol concentrations (ng mL^{-1}) and behaviour scores for fish in all experiments.

		Plasma [cortisol] (ng mL^{-1})				Behaviour score	
	N	**SHAM**	**DOM**	**SUB**	**P-value**	**DOM**	**SUB**
ACTH challenge	9	n/a	4.1±2.3[a]	130.1±33.6[b]	< 0.001	1.41±0.28	-1.52±0.22
***In vitro* head kidney preparations**	24	n/a	6.0±2.8[a]	171.1±32.1[b]	< 0.001	1.38±0.17	-1.37±0.14
Real-time RT-PCR / western blotting	6	4.14±2.35[a]	2.4±0.5[a]	170.5±67.9[b]	< 0.001	2.00±0.13	-1.89±0.19
Flow cytometry	6	n/a	7.8±4.6	293.5±55.3	< 0.001	1.53±0.44	-1.70±0.08
Overall		4.14±2.35[a] (6)	5.0±1.8[a] (45)	161.5±23.2[b] (45)	< 0.001	1.49±0.12	-1.51±0.09

For cortisol, different superscript letters indicate significant differences (ACTH challenge, t-test on log-transformed data; *in vitro* head kidney preparations, Mann-Whitney U test; Real-time RT-PCR / western blotting, ANOVA on log-transformed data; overall, ANOVA on ranks). Data are presented as means ± SEM. *N* values apply to each group in the experiment or are provided in parentheses following the mean value.

3.6 Discussion

The current study assessed cortisol production in the head kidney to elucidate why subordinate rainbow trout exhibit chronic elevation of plasma cortisol and, at the same time, attenuation of acute cortisol responses. Overall, the data suggest that increased abundance of steroidogenic machinery helps to sustain elevated basal rates of cortisol production by the head kidney. The attenuation of acutely stimulated cortisol production appears to arise downstream of cAMP signalling and occurs despite a potential for enhanced receptor signalling in the steroidogenic cells of subordinate fish. However, both contexts focus on cortisol production and therefore the implication of these findings are intertwined.

Measures of head kidney steroidogenesis in the absence of acute stimulation in the current study aligned with the elevation of plasma cortisol in subordinate fish. Head kidney tissue isolated from subordinate fish produced significantly more cortisol *in vitro* than did tissue from dominant fish under basal condition, i.e. in the absence of acute stimulation. Similar elevation of basal cortisol production was observed for head kidney tissue of rainbow trout confined for 48 hours (Balm and Pottinger, 1995), and of coho salmon reared at high density (Patiño et al., 1986), both considered to be chronic stressors. The plasma cortisol concentrations of subordinate fish correlate significantly to their basal *in vitro* cortisol production, suggesting a direct link between basal cortisol production *in vitro* and the resultant plasma cortisol concentrations. Why this correlation was not observed in dominant fish remains unclear. To determine mechanisms underlying the high basal rate of cortisol production in subordinates, we examined key steps in the steroidogenic pathway.

Elevated transcript abundances of both *star* and *p450scc* in head kidney tissue from subordinate trout suggest that these proteins, which are involved in the rate-limiting steps in

steroidogenesis (Aluru and Vijayan, 2006; Arukwe, 2008; Geslin and Auperin, 2004; Stocco, 2000), likely contribute to sustaining higher rates of cortisol production in subordinates. The underlying mechanisms that contribute to these observed increases in transcript abundance are not always clear in teleosts. In mammals, increases in ACTH and cAMP caused by stress axis activation are known to upregulate transcription of *p450scc* and *star* (Ruggiero and Lalli, 2016; Sewer and Waterman, 2003). Similarly, ACTH stimulation of rainbow trout head kidney tissue *in vitro* increased *star* and *p450scc* mRNA levels (Aluru and Vijayan, 2006; Aluru and Vijayan, 2008). In rainbow trout chronically stressed by confinement, Balm and Pottinger (1995) found that *in vitro* cortisol production corresponded to plasma ACTH levels. The presence of residual ACTH was deemed to be unlikely, so the authors hypothesized that higher basal cortisol production reflected chronic ACTH exposure. Although a similar effect may occur in subordinate trout, circulating ACTH levels during chronic social stress in salmonids have been reported as elevated, unchanged, and lower than those in controls (Höglund et al., 2000; Jeffrey et al., 2012; Jeffrey et al., 2014). Therefore, even though ACTH signalling is the main pathway by which *star* and *p450scc* are upregulated during stress, we hesitate to attribute elevated transcript abundances of these genes to chronic ACTH elevation in subordinate trout. An alternative or additional signalling pathway that can influence transcription of steroidogenic genes is provided by SF-1.

SF-1 is a nuclear receptor that is known to upregulate *p450scc* in zebrafish (Chai et al., 2003; Hu et al., 2001; Quek and Chan, 2009), and all steroidogenic genes including *star* and *p450scc* in mammalian models (Val et al., 2003). Mice heterozygous for SF-1 (i.e. SF-1+/-) mounted attenuated corticosterone responses to stressors, although interestingly, their *p450scc* and *star* levels were unchanged and upregulated, respectively (Bland et al., 2000). The latter

effects were attributed to the involvement of additional regulatory mechanisms controlling these genes. It is important to note that development of the adrenal occurred with reduced SF-1 in these mice and was therefore abnormal, so organ abnormalities and compensatory mechanisms likely contributed to the phenotype that was observed. Based on sequence and functional studies in selected teleosts (Kuo et al., 2005), in combination with updated salmonid sequence information, SF-1 appears to have three gene paralogues in rainbow trout, *ff1b1*, *ff1b2*, and *ff1d*. In socially stressed rainbow trout, two of the three exhibited elevated transcript abundances (*ff1b2* and *ff1d*), with *ff1d* being profoundly upregulated. Thus, transcriptional regulation in subordinate fish appears to be geared towards increasing steroidogenesis, even upstream of *star* and *p450scc* gene expression. It is not yet known what regulates SF-1 activity, but there is evidence that changes in the lipid environment can alter SF-1 activity (Urs et al., 2007).

Beyond its role in regulating steroidogenesis, SF-1 is also involved in the proliferation of steroidogenic cells in mammals (Beuschlein et al., 2002). Chronic stress can alter the size and abundance of steroidogenic cells, although whether SF-1 plays a role in mediating these effects does not appear to have been studied. For example, chronic variable stress for 14 days in rats led to increased size and abundance of cells in a zone-specific fashion within the adrenal gland (Ulrich-Lai et al., 2006). In fishes, various stressors have been associated with reports of interrenal hypertrophy and hyperplasia (Gallo and Civinini, 2003). Specifically pertaining to social stress, coho salmon (*Oncorhynchus kisutch*) exhibited increased interrenal cell nuclear diameter after two weeks of subordinate social status (Ejike and Schreck, 1980). Among trios of swordtail, dominants exhibited the lowest interrenal cell nuclear diameters after 10 days (Scott and Currie, 1980), and when held in groups of four for four weeks, the least aggressive pumpkinseed sunfish had the greatest quantity of interrenal tissue (Erickson, 1967). In the

current study, flow cytometry was used to quantitatively assess interrenal cell size and abundance, but did not reveal any differences between dominant and subordinate trout. Trout in the present study interacted for four days, which may not have been sufficient time for effects on cell size or abundance to appear; the studies cited above used longer interaction periods. Regardless, these data confirm that neither increases in interrenal cell size nor increases in interrenal cell abundance contributed to the elevated cortisol levels or transcript abundances detected in subordinate trout.

Although basal cortisol levels of subordinate fish are chronically elevated, exposure of these fish to an acute stressor revealed an attenuated cortisol response (Jeffrey et al., 2014; Øverli et al., 1999b). Indeed, blunting of the cortisol response to an acute stressor is a common observation in fish experiencing chronic stress caused by a variety of factors (Barcellos et al., 1999a; Barton et al., 1987; Madaro et al., 2015; Samaras et al., 2018; Samaras et al., 2021; Wunderink et al., 2011). Whether this attenuation of the acute cortisol response is a regulatory safeguard against cortisol exceeding a given set-point or allostatic overload/exhaustion is not clear, and may well vary by stressor. Studies have rarely identified the mechanisms through which attenuation occurs, which was a focus of the present study. In comparison to assessing stress axis function through exposure to acute stressors, an ACTH challenge uncovers impacts at the head kidney level specifically. Using *in vivo* ACTH administration, we found that the cortisol response in subordinate fish was attenuated, indicating that blunting of the acute cortisol response in subordinate trout arises at least in part at the head kidney level. This finding is consistent with previous reports of attenuated cortisol production by *in situ* (Sloman et al., 2002) or isolated (Jeffrey et al., 2014) head kidney preparations from subordinate trout. Similarly, head

kidney tissue from subordinate trout produced less cortisol in response to ACTH stimulation *in vitro* in the present study than did preparations from dominant trout.

Chronic stressors beyond social stress also caused lowering of ACTH-stimulated cortisol production by *in vitro* head kidney preparations. For example, this effect was observed in brook charr (*Salvelinus fontinalis*) subjected to high stocking density (Vijayan and Leatherland, 1990), and in rainbow trout and gilthead sea bream (*Sparus aurata*) subjected to 48 h of confinement (Balm and Pottinger, 1995; Rotllant et al., 2000). A reduced capacity for cortisol production when circulating cortisol is high suggests a role for negative feedback in restricting cortisol production. Head kidney preparations can display reduced rates of cortisol secretion when cortisol becomes sufficiently high in the medium (Bradford et al., 1992), but this *in vitro* negative feedback was avoided in the current study by controlling incubation time. It is also worth pointing out that dominant fish had higher medium cortisol concentrations (and rates of cortisol production) than subordinate fish. Moreover, perfusion setups, which avoid cortisol buildup in the medium, detected attenuated cortisol production in chronically stressed fish (Balm and Pottinger, 1995; Sloman et al., 2002a), supporting an *in vivo* origin for the attenuation. Whether a negative feedback mechanism acts *in vivo* is less clear. Studies in two fish species compared ACTH-mediated cortisol production following exposure to a chronic stressor or exogenous cortisol administration. Attenuation occurred only with the chronic stressor, which is not consistent with negative feedback by cortisol (Balm and Pottinger, 1995; Rotllant et al., 2000). Furthermore, fish experiencing chronic stress can show attenuation of the acute stress response even when plasma cortisol is not higher than in control fish (Barcellos et al., 1999b; Madaro et al., 2015). Although we cannot rule out negative feedback as a contributor to

inhibition of the acute cortisol response, it is unlikely to be the only mechanism reducing the response of head kidney tissue to ACTH.

To reveal potential mechanisms at the level of steroidogenesis, we used dose-response curves to probe the dynamics of the ACTH response during chronic social stress. As when head kidney tissue was incubated with a single concentration of ACTH, the maximal response predicted from the dose response curve was lower in subordinate fish. However, no significant difference in EC50 was detected. This result suggests that the lower acute cortisol production observed in subordinate head kidney tissue was not caused by reduced sensitivity to ACTH. This is interesting given that desensitization or downregulation of the ACTH receptor has been hypothesized to underlie the diminished acute response seen in fish undergoing chronic stress (Mommsen et al., 1999). A lack of change in ACTH sensitivity is supported by the observation that transcript abundances of its receptor system were not lowered. Indeed, transcript abundances of *mrap1* and *mrap2* were higher in subordinates, suggesting the potential for an enhanced response to ACTH binding. The receptor for ACTH is a G-protein coupled receptor and brings about an increase in cAMP levels. Levels of cAMP were measured in head kidney tissue both basally and stimulated with ACTH, but did not differ, possibly owing to the difficulty of detecting the cAMP of the very rare interrenal cells in the head kidney tissue as a whole (Hontela et al., 2008). Levels of proteins phosphorylated by PKA in the head kidney tissue of subordinate fish were elevated relative to sham fish, which could support their elevated basal steroidogenesis.

Use of the permeable cAMP analogue db-cAMP allowed cortisol production downstream of cAMP to be examined independently of MC2R activation. When head kidney tissue was challenged with db-cAMP *in vitro*, preparations from subordinates produced less cortisol than those from dominants, indicating that steroidogenesis itself plays a role in attenuation of the

acute cortisol response in subordinate fish. This blunted steroidogenic response to db-cAMP occurs despite elevations in basal *star* and *p450scc* transcript abundance. Although the mechanisms underlying this blunted response remain to be determined, one possibility might include limited cholesterol availability (Kostyniuk et al., 2018).

In summary, we have uncovered key aspects of how chronic social stress impacts cortisol production by the head kidney both under basal conditions where it is increased, and when challenged with ACTH or cAMP, where it is attenuated. High plasma cortisol concentrations in subordinate fish reflect increased basal rates of cortisol production supported by increased transcript abundances of *star* and *p450scc*, key elements in steroidogenesis. Increased transcript abundances of two paralogues of *sf-1* during chronic social stress are particularly interesting as this master regulator of steroidogenesis may underlie upregulation of *star* and *p450scc* and possibly other steroidogenic enzymes. At the same time, ACTH challenges both *in vivo* and *in vitro* point to the head kidney as a major source of the attenuated cortisol response of subordinates to an additional acute stressor. Despite apparent increases in the basal steroidogenic capacity, challenging the head kidney with cAMP revealed limitations on the steroidogenic response to stimulation. Further studies are needed to uncover the mechanisms underlying this apparent contradiction.

3.7 Supplementary information

Table S3.1 Weight and length data for all rainbow trout (*Oncorhynchus mykiss*) and size differences within pairs.

					Size differences within pairs			
	N fish	**Weight (g)**	**Length (cm)**	**N pairs**	**ΔWeight (g)**	**ΔWeight (%)**	**ΔLength (cm)**	**ΔLength (%)**
ACTH challenge (pairs only)	18	85.6 ± 6.7	19.6 ± 0.5	9	3.3 ± 1.3	3.4 ± 1.1	0.4 ± 0.1	2.1 ± 0.6
In vitro head kidney preparations (pairs only)	48	117.7 ± 4.0	21.8 ± 0.2	24	5.9 ± 0.9	5.3 ± 0.9	0.4 ± 0.1	1.9 ± 0.2
Real-time RT-PCR / western blotting (pairs and shams)	18	81.6 ± 2.7	19.6 ± 0.2	6	5.3 ± 1.4	6.3 ± 1.5	0.5 ± 0.0	2.6 ± 0.0
Flow cytometry	12	113.8 ± 4.6	21.8 ± 0.3	6	7.0 ± 1.2	6.1 ± 1.0	0.3 ± 0.1	1.2 ± 0.3
Overall	96	104.4 ± 3.0	21.0 ± 0.2	45	5.4 ± 0.6	5.2 ± 0.6	0.4 ± 0.0	1.9 ± 0.2

Data are presented as means ± SEM.

Flow cytometry methods

Head kidney tissue was dissected out, rinsed in cold L-15 medium (Gibco, Thermo Fisher Scientific) and weighed. Tissue was transferred to a glass Petri dish on ice with 100 mL L-15 medium per gram tissue, and minced to 1 mm^3 pieces. The minced tissue was incubated in L-15 medium containing 2 mg mL^{-1} collagenase/dispase (Roche, Basel, Switzerland) with shaking for 1 h at room temperature (RT) with trituration every 15 min. The homogenates were passed through 100 µm and 40 µm cell strainers (Thermo Fisher Scientific), rinsed with 5 and 2 mL of L-15, respectively, and then centrifuged at 13°C for 5 min at 200 *g*. The pelleted cells were fixed by gentle resuspension in 2 mL of 4% PFA for 15 min at RT. Cells were centrifuged again at 13°C for 10 min at 500 *g*, washed twice in 5 mL ice-cold phosphate-buffered saline (PBS), and centrifuged at 13°C for 5 min at 500 *g*. During the second wash, a 10 µL aliquot was taken to determine cell concentration using a hemocytometer. The fixed, washed cells were resuspended in ice-cold 100% methanol and stored at -20°C until immunostaining.

For immunostaining, samples were divided into triplicates to include no-antibody and secondary-only controls for flow cytometry. Appropriate primary and secondary antibody concentrations were determined by pilot trials. A volume of the methanol suspension containing 10 million cells was washed with 5 mL of PBS containing 1% bovine serum albumin (PBS-BSA) and centrifuged at 13°C for 10 min at 1000 *g* (all spins used these conditions). The pelleted cells were resuspended in 1 mL of PBS-BSA containing 1:10,000 rabbit anti-trout P450scc antibody, a kind gift from Dr. Graham Young (University of Washington, USA; Kobayashi et al., 1998) or blank, and incubated with shaking for 30 min at RT. Following washing twice in 5 mL PBS-BSA, cells were resuspended in 1 mL of PBS-BSA containing Alexa Fluor 647 (1:2000) or blank, and incubated in the dark with shaking for 30 min at RT.

Cells were washed with PBS-BSA followed by PBS, resuspended in 2 mL PBS, and transferred to plastic 13x75 mm tubes for flow cytometry. Samples were run on a Gallios flow cytometer (Beckman Coulter, Mississauga, ON, CA), using the red laser (633 nm) and FL6 filter (670 nm) for Alexa Fluor 647, and the blue laser (488 nm) for forward and side scatter. Collected data were analysed using Kaluza software (Beckman Coulter, Mississauga, ON, CA), including doublet exclusion and creation of thresholds based on the background signal from secondary-only controls. The number of P450scc-positive cells was calculated as a proportion of all singlet events.

Figure S3.1

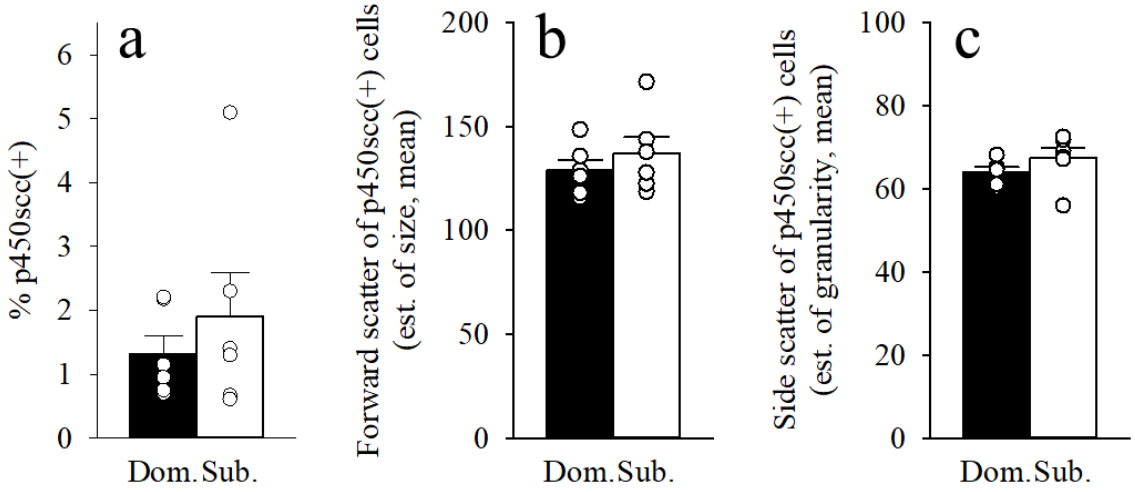

Figure S3.1. Flow cytometry data from head kidney (HK) cells from dominant (Dom.) and subordinate (Sub.) rainbow trout (*Oncorhynchus mykiss)*. The properties of singlet events (cells) positive for p450scc staining are shown, including the percentage of positive events out of all events (a), forward scatter (an estimate of cell size, panel b) and side scatter (an estimate of cell granularity, panel c). Data are expressed as means ± SEM with individual values shown using white symbols ($N = 6$ in all cases). (Student's *t*-test, $P = 0.628$, 0.402, 0.128, in a-c respectively).

Chapter 4: Alternative routes of stress axis regulation during chronic social stress in rainbow trout (*Oncorhynchus mykiss*): AVT, methylation and miRNA

Assessment of miRNA and methylation in this chapter was performed in collaboration with Dr. J. Mennigen (University of Ottawa, ON, CA). Dr. D. Zhang (Saint Louis University, MO, USA) provided assistance with *in silico* miRNA predictions.

4.1 Introduction

Juvenile rainbow trout form dominance hierarchies that result in subordinate individuals experiencing chronic social stress and prolonged elevation of plasma cortisol levels. Cortisol production is under the control of the hypothalamic-pituitary-interrenal (HPI) or stress axis. When a stressor is perceived, corticotropin releasing factor (CRF) is released from neurons in the preoptic area (POA) of the brain (Bernier et al., 2009) onto corticotropes in the *pars distalis* of the anterior pituitary (Gorissen and Flik, 2016). The corticotropes release adrenocorticotropic hormone (ACTH) into the circulation (Baker et al., 1996), and ACTH stimulates cortisol production by steroidogenic cells in the head kidney. Cortisol signalling elicits a suite of physiological responses intended to allow the animal to cope with the stressor (Vijayan et al., 2010; Wendelaar Bonga, 1997).

While marked elevations in circulating cortisol levels are observed during chronic social stress, parallel elevations in transcript abundance of *crf* in the POA are not always observed. Transcripts of *crf* have been assessed in dominant-subordinate pairs of rainbow trout after social interactions of various duration. Elevated transcript abundance of *crf* in the POA of subordinate fish was observed after 8 h, 1 d (Bernier et al., 2008), and 3 d of interaction (Doyon et al., 2003). However, after 5 d of interaction, *crf* transcript abundance in the POA of subordinates was not different from that of dominant fish, even though the subordinate fish continued to exhibit elevated circulating cortisol (Jeffrey et al., 2012; Jeffrey et al., 2014). Backström et al. (2021) reported elevated *crf* transcript abundance in subordinate trout after 5 d of social interaction, but these fish were held in groups of four, and whole brain rather than POA was used to assess *crf* mRNA abundance (Backström et al., 2021). Collectively, these findings suggest that *crf*

transcript abundance is initially elevated in response to chronic social stress but can decrease over time by an as yet unknown mechanism, while circulating cortisol remains elevated.

The effect of cortisol on *crf* transcription is equivocal. The mRNA expression of *crf* appears to be under negative feedback control in goldfish (*Carassius auratus*), because exogenous cortisol elevation reduced *crf* transcript abundance in the POA (Bernier et al., 1999). The reduction in mRNA abundance was prevented by co-administration of the glucocorticoid receptor (GR) antagonist RU-486, suggesting transcriptional regulation by GR (Bernier et al., 1999). However, cortisol administration increased *crf* abundance in rainbow trout (Jeffrey et al., 2012; Madison et al., 2015) and blockade of cortisol signalling with RU-486 decreased *crf* transcription in the trout POA (Alderman et al., 2012; Doyon et al., 2006). Characterization of the *crf* promoter, and particularly the status of glucocorticoid response elements (GRE), could provide insight into this discrepancy.

An additional potential regulator of the HPI axis during chronic social stress in rainbow trout is arginine vasotocin (AVT), which is homologous to arginine vasopressin (AVP) in mammals (Godwin and Thompson, 2012). AVT neurons are found in the POA and often co-localize with CRF neurons (Bernier et al., 2009; Godwin and Thompson, 2012). Although many of the AVT neurons project to the neurohypophysis, there is evidence that AVT-immunoreactive nerve fibers contact corticotropes (Bernier et al., 2009), AVT can stimulate ACTH production *in vitro* from the anterior pituitary of trout (Baker et al., 1996), and central administration of AVT *in vivo* in rainbow trout elevated plasma cortisol levels (Gesto et al., 2014). CRF was a stronger ACTH secretagogue than AVT, but the two peptides worked synergistically to increase ACTH release at all tested dose combinations (Baker et al., 1996). In addition, changes in transcript abundance of *avt* have been observed in response to stressors. For example, *avt* mRNA increased

in the parvocellular neurons of the rainbow trout POA with confinement stress, but not with exposure to repeated stressors for several days (Gilchriest et al., 2000). Dominant and subordinate zebrafish had different spatial distribution and abundance of *avt* in the POA after 5 d of interaction, with subordinates having higher abundance than dominant fish in the parvocellular neurons (Larson et al., 2006; Pavlidis et al., 2011). Thus, AVT warrants examination as a potential regulator of the stress axis during chronic stress in rainbow trout.

Methylation of the *crf* promoter is another potential mechanism through which stress axis activity may be modulated during chronic social stress. In rodents, social defeat stress is an experimental paradigm similar to subordination stress in trout, but typically shorter in duration (Beery and Kaufer, 2015; Elliott et al., 2010; Hostetler and Ryabinin, 2013). Mice exhibit variation in the response to social defeat stress that is associated with variation in *crf* mRNA abundance, as well as methylation of the *crf* promoter (Elliott et al., 2010). Epigenetic changes caused by stress have been studied mainly in rodents (reviewed by Stankiewicz et al., 2013), although increasingly in other taxa (Seebacher and Krause, 2019). One of the first important studies implicating DNA methylation in the stress response was the effect of maternal care on glucocorticoid receptor methylation and subsequent stress responses (Weaver et al., 2004). In addition to chronic social defeat mentioned above (Elliott et al., 2010), methylation of the *crf* promoter is modified in rodents by chronic variable mild stress (Sterrenburg et al., 2011), and maternal deprivation (Chen et al., 2012). Evidence exists for stress-related methylation changes in birds: social competition among free-living tree swallows was accompanied by changes in methylation patterns and transcript abundance in several corticosteroid-related genes in the hypothalamus (Bentz et al., 2021). Methylation is being increasingly investigated in teleosts and recently, methylation of the *crf* promoter has been assessed in olive flounder (*Paralichthys*

olivaceus) in the context of tissue differences, but not stress (Zou et al., 2021). Stress-related changes in methylation have been observed in teleosts. In the cichlid *Astatotilapia burtoni*, global methylation state was manipulated, which influenced outcomes of rank ascension (Lenkov et al., 2015). Paternal care quality in three-spined stickleback is associated with DNA methyltransferase 3a (*dnmt3a*) mRNA in the brain of offspring (McGhee and Bell, 2014). When zebrafish were exposed to the synthetic glucocorticoid dexamethasone for 24 h as larvae, they exhibited changes in gonadotropin-releasing hormone 3 (*gnrh3*) transcript abundance and promoter methylation as 120 d old adults (Khor et al., 2016). To our knowledge, no study to date has addressed the methylation status of any stress axis gene during chronic social stress in fishes. The methylation status of the *crf* promoter may play an important functional role during social interactions in trout, and is an avenue worth exploring.

Another potential route for regulation of *crf* during chronic social stress in rainbow trout is through microRNA (miRNA). These short RNA molecules do not encode a protein, but rather bind to the 3' untranslated region (UTR) of target mRNA transcripts to alter their stability and translation (Best et al., 2018). Specifically, the miRNA creates a silencing complex with Argonaute (AGO) protein and GW182, which facilitates miRNA binding to the 3'UTR, followed by translational repression and/or deadenylation of the target mRNA, and ultimately its degradation (Huntzinger and Izaurralde, 2011; Sheu-Gruttadauria and MacRae, 2017). Through RNA and genome sequencing, a robust miRNA repertoire is now available in trout, facilitating *in silico* prediction of miRNA that target the 3'UTR of particular transcripts (Berthelot et al., 2014; Juanchich et al., 2016; Mennigen and Zhang, 2016). To date, few studies have investigated miRNA in chronic social stress in fishes. An acute stressor altered abundance of four selected miRNA in liver, head kidney, and extracellular vesicles of rainbow trout (Cadonic et al., 2020).

Kostyniuk et al. (2018, 2019b) identified several differentially regulated miRNAs in the liver of dominant and subordinate rainbow trout. Numerous miRNA are modulated by stressors (Du et al., 2019), although few stand out specifically for involvement in the endocrine stress response.

The objective of the current study was to gain insight into mechanisms that allow for maintained elevation of plasma cortisol without concurrent elevation of *crf* transcript abundance in rainbow trout experiencing chronic social stress. We measured *crf* transcript abundance in the POA of rainbow trout, and explored three potential avenues of regulation. Given that AVT is also able to stimulate ACTH release from the pituitary in rainbow trout (Baker et al., 1996), we assessed its transcript abundance in the POA during chronic social stress. We also assessed abundances of three miRNAs predicted to target *crf* and *11βhsd2*, the latter chosen for its potential role in negative feedback regulation in the POA (Chapter 2). Finally, we quantified methylation status of the *crf* promoter by bisulphite sequencing as a putative route for control of *crf* levels during chronic stress. Together, these data provide insight into potential routes that regulate *crf* transcription and/or modify *crf* mRNA availability during chronic social stress. Altered *crf* availability could translate to altered CRF signalling to the pituitary, and impact downstream stress axis function.

4.2 Materials and methods

4.2.1 Experimental Animals

Juvenile rainbow trout, weighing 102.5 ± 3.8 g (mean ± SEM, N = 76) were obtained from Linwood Acres Trout Farm (Campbellcroft, Ontario) and held at the University of Ottawa in 1275 L fibreglass tanks supplied with flowing, aerated, 13ºC, dechloraminated city of Ottawa

tap water ("system" water) with a mild current. Fish were scatter fed 0.5% body mass daily with Zeigler Silver pellets and held under a 12L:12D photoperiod. These conditions served to minimize hierarchy formation in holding tanks. All protocols were approved by an institutional animal care committee (protocol BL-2118), and were in accordance with Canadian Council on Animal Care guidelines for the use of animals in research and teaching.

4.2.2 Experimental Protocols

Pairs of juvenile rainbow trout were allowed to establish social hierarchies for 1 or 4 days, after which fish were euthanized. The 1 d pairs were used to assess transcriptional changes in *crf*, *11βhsd2*, and their associated miRNAs at a point earlier in the interaction period to examine temporal changes in mRNA-miRNA relationships. Blood plasma was obtained to determine circulating levels of cortisol, and the POA was dissected out to extract total RNA (for miRNA and mRNA analysis) or genomic DNA (for methylation analysis). The POA for one set of fish was used exclusively for mRNA and miRNA analysis by real-time RT-PCR (qPCR). To allow analysis of the link between promoter methylation and transcript abundance, the POA for a second set of fish was split between genomic DNA isolation for promoter methylation analysis by bisulphite sequencing and RNA isolation for quantification of transcripts by qPCR.

Fish were set up to form social hierarchies according to previous protocols (Culbert and Gilmour, 2016; Gilmour et al., 2012; Gilmour et al., 2017; Jeffrey et al., 2014). Briefly, juvenile rainbow trout were lightly anaesthetized (0.05 g L^{-1} benzocaine; Sigma-Aldrich, Oakville, ON, CA) to measure mass and fork length, and to score fin damage. The fish within a pair were size matched according to fork length (differences averaged 0.4 ± 0.04 cm or 1.9 ± 0.2% of fork

length) and mass (differences averaged 5.0 ± 0.7 g or 5.0 ± 0.7% of body mass; N = 26 pairs). The fish within a pair were transferred to 40 L tanks supplied with flowing system water and were separated by a perforated, opaque divider for an overnight recovery period (day 0), following which the divider was removed to allow the fish to interact (day 1). Sham fish were handled in the same way but housed alone. Pairs of fish were fed 0.5% body weight per day, following the afternoon observation period, starting on observation day 2. Therefore, fish sampled after 1 d of interaction were not fed.

Behavioural observations were performed twice daily for 4 d pairs (morning and afternoon) or 3 times daily for 1 d pairs (morning, afternoon, and evening) to assess social status based on scoring of aggressive acts, position in the tank, and acquisition of a food pellet, with higher scores indicating more dominant behaviour. At the time of tissue collection, fin damage accrued because of social interactions was scored. The mean scores across all observation periods for each of these measurements were analysed using a principal component analysis (PCA), to determine an overall behaviour score (PC1) for each fish. The fish within a pair with the higher overall behaviour score was assigned dominant social status.

At the end of the 1 d or 4 d pairing period (i.e. on the morning of day 2 or 5, respectively), fish were euthanized by terminal anaesthesia (0.5 g L^{-1} benzocaine). Approximately 1 mL of blood was withdrawn from the caudal vasculature using a 23G needle and syringe rinsed with heparinized (Sigma-Aldrich H3393) 0.9% saline solution. Blood was centrifuged at 13,500 *g* for 3 min, and separated plasma was flash frozen in liquid nitrogen and stored at -80°C for later analysis of cortisol concentration. For molecular analyses, POA (see Bernier et al., 2008) was dissected out on ice, snap frozen in liquid nitrogen, and stored at -80°C until further processing.

4.2.3 Analytical Approaches

4.2.3.1 *In silico* prediction of miRNA-mRNA binding

To identify miRNAs that target the transcripts of interest, the 3' UTR sequence was used as input in the miRanda scanning algorithm (v 3.3a, Enright et al. 2003), as previously described for rainbow trout (Kostyniuk et al., 2019b). The 3'UTR sequences were obtained from the GenBank mRNA reference sequences for *crf* (accession no. NM_001124286.1, *crfb1*) and *11βhsd2* (accession no. NM_001124218.1) in rainbow trout. The database of rainbow trout miRNA with genomic and/or transcriptomic support was obtained from MicroTrout (http://www.mennigen-lab.com/microtrout.html, Mennigen and Zhang, 2016). The resulting miRNA hits were filtered to identify those with a pairing score threshold of >140 and a free-energy (ΔG) threshold of <-20 for *crf*, and <-15 for *11βhsd2* (the cutoff was relaxed somewhat for *11βhsd2* to obtain a reasonable number of results). This relatively stringent cutoff was used to reduce the risk of false positives because of the high sensitivity of the miRanda algorithm and for comparison with previous studies in trout (Cadonic et al., 2020; Ikert et al., 2021; Kostyniuk et al., 2019a; Kostyniuk et al., 2019b). Candidate miRNAs were selected based on a combination of high complementarity (pairing score) and more energetically favourable binding (ΔG), as well as reported involvement in any stress-related studies in fishes and mammals. *miR-210-3p* was selected as a potential regulator of *11βhsd2* mRNA abundance, while *miR-103a-3p* and *miR-139-5p* were selected as potential regulators of *crf* mRNA abundance.

4.2.3.2 Measurement of cortisol concentrations

A commercial radioimmunoassay kit (MP Biomedicals, Solon, OH, USA) was used to measure cortisol levels in plasma and media according to the manufacturer's instructions. This kit has been validated for use with rainbow trout (Gamperl et al., 1994). The detection limit for the kit is 0.17 pg dL^{-1} and the inter- and intra-assay variabilities (expressed as the coefficient of variation) averaged 5.4% and 5.7%, respectively.

4.2.3.3 Quantitative PCR (mRNA and miRNA)

Total RNA was extracted from either the entire POA (for miRNA experiment) or approximately half of it (for methylation experiment) after grinding the tissue to a powder on dry ice. Frozen tissue was sonicated in Trizol reagent on ice (Sonic Dismembrator Model 100; Thermo Fisher Scientific, Waltham, MA, USA), and total RNA extraction was performed as per the manufacturer's instructions (Trizol Reagent, Life Technologies, Carlsbad, CA, USA). The RNA was resuspended in 30 µL nuclease-free water and quantified using a Nanodrop 2000c UV-vis Spectrophotometer (Thermo Fisher Scientific). The resulting total RNA was stored at -80°C and used as template to generate cDNA for analysis of mRNA transcript abundance and/or miRNA abundance.

Synthesis of cDNA for mRNA abundance was performed using the QuantiTect Reverse Transcription Kit, according to the manufacturer's instructions (Qiagen, Hilden, Germany). Using 1 µg of total RNA as input, this kit includes an initial step to remove genomic DNA, which is followed by reverse transcription in a final reaction volume of 20 µL. A "no-RT"

control with water in place of reverse transcriptase was used to verify the absence of genomic DNA. Synthesized mRNA-cDNA was stored at -20°C until used in qPCR.

Synthesis of cDNA for miRNA abundance was performed using the miRCURY LNA RT Kit, according to the manufacturer's instructions (Qiagen). Using 10 ng of total RNA as input in a final volume of 10 µL, this reaction combines both polyadenylation and reverse transcription of mature miRNAs. The oligo-dT primers used in this reaction contain a proprietary 3' sequence required for amplification in qPCR using the LNA SYBR Green PCR Assay primer sets (Qiagen). A synthetic RNA spike-in template (UniSp6) was included in the reaction master mix to confirm reaction efficacy by later quantification of its cDNA abundance by qPCR, which was stable across groups (Fig. S4.1). Synthesized miRNA-cDNA was stored at -20°C until used in qPCR.

Quantification of mRNA transcript abundance was performed using the Rotor-Gene SYBR Green PCR Kit and a Rotor-Gene Q PCR cycler (Qiagen). Reactions were assembled according to the manufacturer's instructions, and scaled down to 10 uL. In each reaction, 1 µL of mRNA-cDNA was used as template with the exception of elongation factor 1a (*ef1α*) where 1 µL of a 50x dilution was used. A final primer concentration of 1 µM was used for all genes (Table 4.1). Cycling conditions were as per the manufacturer's instructions for the Rotor-Gene SYBR Green PCR Kit, with a combined annealing/extension temperature of 60°C except for *ef1α*, where 56°C was used. Primer efficiency was determined by serial dilution of a pooled cDNA sample and was 90-110% for all primer sets (Table 4.1). Melt curves confirmed amplification of a single product in all cases. The reference genes *ef1α* and *β-actin* were used for normalization (geometric mean), and stability across status within a time point (1d or 4d) was verified by one-way ANOVA.

Transcript abundance was analysed using the method of Pfaffl (2001), and expressed as fold-change relative to the sham group within a time point.

Quantification of miRNA abundance was performed using the miRCURY LNA SYBR Green PCR Kit and a Rotor-Gene Q PCR cycler (Qiagen). Reactions were assembled according to the manufacturer's instructions. Each reaction used 1 µL of miRNA-cDNA diluted based on miRNA-specific standard curves. All cDNA dilutions (standards and samples) were made fresh in nuclease-free water containing 50 ng mL^{-1} torula yeast RNA (Sigma, R6625) and tubes with low DNA binding (Eppendorf, DNA LoBind). Primer sets (miRCURY LNA miRNA PCR Assays) were obtained from Qiagen through the GeneGlobe database and 1 µL was used per 10 µL reaction. Primer efficiency was determined by serial dilution of a pooled cDNA sample and was 80-90% for all primer sets (Table 4.1). Cycling conditions were as per the manufacturer's instructions for the miRCURY LNA SYBR Green PCR Kit, with a combined annealing/extension temperature of 56°C. Melt curves confirmed amplification of a single product in all cases. Abundance of miRNA was quantified using NORMA-gene (Heckmann et al., 2011). The NORMA-gene algorithm does not require a stable reference gene but requires at least five targets to account for variance due to experimental bias, and has been previously used for miRNA analysis (Kostyniuk et al., 2019b). Our three miRNAs of interest, as well as the non-coding small nuclear RNA (snRNA) U6, a reference RNA previously used for miRNA normalization in rainbow trout (Ikert et al., 2021; Mennigen et al., 2014a), and UniSp6 were used for NORMA-gene analysis. Relative concentration was determined using the standard curve to account for primer efficiency, and relative concentrations for all five targets were normalized using NORMA-gene. Normalized concentrations were expressed relative to the mean of the sham values within each time point.

4.2.3.4 Methylation analysis by bisulphite sequencing

Preoptic area tissue ground to a powder on dry ice was divided between RNA extraction (see above) and genomic DNA (gDNA) extraction. The PureLink Genomic DNA Mini Kit (K1820, Invitrogen, Carlsbad, CA, USA) was used according to the manufacturer's instructions to digest the tissue and then isolate gDNA from the resulting lysate with a silica-based spin column. The gDNA was eluted in 50 µL elution buffer and quantified using a Nanodrop 2000c UV-vis Spectrophotometer (Thermo Fisher Scientific). Quality was verified by running a subset on a 1% agarose gel, where a single band >10 kb was observed. The gDNA was stored at -20°C until used in bisulphite conversion.

The EZ- DNA Methylation Lightning Kit (D5031, Zymo Research, Irvine, CA, USA) was used according to the manufacturer's instructions to treat gDNA with bisulphite, converting unmethylated cytosines into uracil (later amplified in PCR as thymine). Genomic DNA was diluted to 500 ng in 20 µL, and processed according to the manufacturer's instructions. The bisulphite-converted DNA was eluted in 10 µL elution buffer. A subset was quantified on a Nanodrop 2000c UV-vis Spectrophotometer (Thermo Fisher Scientific) and quality was verified by running a subset on a 1% agarose gel, where after chilling, the bisulphite-converted DNA appeared as a smear spanning 100-1500 bp. Bisulphite-DNA was stored at -20°C until used in PCR.

Bisulphite PCR primers were designed to target two regions upstream (1000 bp) of the *crf* gene, within the promoter region (Table 4.1). Primers were designed using the bisulphite primer seeker tool from Zymo (https://www.zymoresearch.com/pages/bisulfite-primer-seeker).

Specifically, two primer sets were designed to amplify a 167 bp region from position -669 to -503 bp (region 1) and a 199 bp region from -163 to +36 (region 2; Fig. 4.1). Region 1 (distal) is further upstream and contains two CpG sites. Region 2 (proximal) covers the transcription start site, and contains eight CpG sites. JASPAR 2020 was used to predict putative regulatory elements in the 1000 bp *crf* promoter region with a relative profile score threshold of 80% (Fornes et al., 2020). Specifically, glucocorticoid response elements (GRE), cAMP response elements (CRE), and TATA boxes were identified (Fig. 4.1).

PCR was carried out using ZymoTaq DNA Polymerase (E2002, Zymo Research) with primer-specific conditions. Region 1 reactions were set up according to the manufacturer's protocol, with 1 µM [primer pair] and 2 µL of bisulphite DNA as template in a 50 µL final volume. Region 1 cycling conditions were 95°C/10 min, followed by 40 cycles of 95°C/30 s, 50°C/35 s, 72°C/60 s, and a final extension of 72°C/7 min. Region 2 required two rounds of PCR for sufficient yield. Reactions were set up according to the manufacturer's protocol, with 0.5 µM [primer pair] and either 1 µL of bisulphite DNA (round 1) or 1 µL of the round 1 PCR product (round 2) in a 25 µL final volume. Region 2 cycling conditions were the same as those for region 1, except that annealing time was increased by 5 seconds, and 45°C was used instead of 50°C in round 1 only. In all cases, 10 µL of the final PCR products for all samples were run on a 2% agarose gel to confirm that a single product of the correct size was obtained. The remaining PCR reaction was purified using the PureLink PCR Micro Kit (K310050, Invitrogen) according to the manufacturer's instructions. The purified PCR product was eluted in 10 µL of the provided elution buffer and quantified on a Nanodrop 2000c UV-vis Spectrophotometer (Thermo Fisher Scientific).

For each fish, the purified PCR product was ligated into the pGEM T-vector by TA cloning (A3600, Promega, Madison, WI, USA) according to product instructions, with a 1:3 vector:insert ratio and overnight ligation incubation at 4°C to maximize the number of transformants. Ligations were stored at -20°C until transformation. Ligations (5 µL) were transformed into 50 µL NEB 5-alpha subcloning efficiency competent *Escherichia coli* (C2988J, New England BioLabs, Ipswich, MA, USA) according to the manufacturer's protocol and plated onto LB-agar plates containing 100 µg mL^{-1} ampicillin (Sigma A9518), 100 mM isopropyl β-d-1-thiogalactopyranoside (IPTG; IPT001, Bioshop, Burlington, ON, CA), and 80 µg mL^{-1} X-gal (XGA002, Bioshop). Plates were incubated overnight at 37°C. Twelve white colonies were chosen for each fish and inoculated into 3 mL of sterile LB medium consisting of 1% tryptone (Bioshop TRP402.1), 0.5% yeast extract (Fluka 70161), and 0.17 M NaCl (Fisher S271-3) supplemented with 100 µg mL^{-1} ampicillin. Cultures were incubated for 14-16 h at 37°C and plasmids then were extracted using a GeneJet plasmid miniprep kit (K0503, Thermo Fisher Scientific). Plasmids were sent to Genome Quebec for Sanger sequencing using their M13 forward primer. Sequences were aligned using Clustal Omega (Madeira et al., 2019) with the original reference sequence from GenBank and its bisulphite-converted counterpart to determine methylation status.

4.2.4 Statistical Analysis

Data are presented as means ± SEM, unless otherwise indicated. All statistical analyses were performed using Sigmaplot v13.0 (Systat Software, Inc., San Jose, CA, USA). Data were analysed by analysis of variance (ANOVA) to detect significant differences among groups. A Tukey post-hoc test was used to identify the source of significant differences. If necessary, data

were transformed to meet the assumptions of normality and equal variances of a parametric test, and when this was not possible, a non-parametric alternative was used. In all cases a significance level (α) of 0.05 was used.

4.3 Results

4.3.1 Plasma cortisol and behaviour within hierarchies

After four days of social interaction, clear hierarchies were established as evidenced by divergent behaviour scores (Table 4.2). Even after one day of social interaction, behaviour scores of pairs were divergent (Table 4.2). Plasma cortisol concentrations after 1 or 4 days of social interaction were higher in subordinate trout than in dominant and/or sham fish for all experiments (Table 4.2).

4.3.2 Abundance of avt *transcripts*

Transcript abundances of *crf* and *avt* were measured in the POA of sham, dominant and subordinate trout after 4 d of social interaction (Fig. 4.2). In this experiment, *crf* did not differ significantly among groups (Fig. 4.2a, ANOVA, $P = 0.354$), but in the same fish, dominants had significantly lower transcript abundance of *avt* than sham-treated fish (Fig. 4.2b, ANOVA, $P = 0.036$).

4.3.3 Abundance of miRNA and **crf** *or* **11ßhsd2** *transcripts*

In the miRNA experimental group, *crf* transcript abundance in the POA was significantly elevated after 4 d of social interaction in subordinate fish, relative to sham and dominant fish (Fig. 4.3b, ANOVA, $P < 0.001$), but not after 1 day of interaction (Fig. 4.3a, one-way ANOVA, $P = 0.384$). Although miRNA 139-5p is predicted to target the 3'UTR of *crf*, no significant effects of social status were present on the POA abundance of this miRNA after 1 d (Fig. 4.3c, one-way ANOVA, $P = 0.094$) or 4 d (Fig. 4.3d, one-way ANOVA, $P = 0.128$). However, miRNA 103a-3p is also predicted to target *crf*, and was significantly elevated in the POA of subordinate fish relative to both dominant and sham-treated fish after 1 d (Fig. 4.3e, one-way ANOVA, $P = 0.006$) but not 4 d of interaction (Fig. 4.3f, one-way ANOVA, $P = 0.257$). Transcript abundance of *11βhsd2* in the POA did not differ significantly across groups after 1 d of interaction (Fig. 4.4a, one-way ANOVA, $P = 0.710$), but after 4 d of social interaction, transcript abundance of this enzyme was significantly elevated in subordinates relative to sham-treated fish (Fig. 4.4b, one-way ANOVA, $P = 0.018$). The abundance of miRNA 210-3p, which is predicted to target the 3'UTR of the *11βhsd2* transcript, was stable across groups at both the earlier and later time points (Fig. 4.4c and d, one-way ANOVA, $P = 0.140$, 0.641).

Transcript abundance of U6 spliceosomal snRNA was measured initially as a reference gene for target miRNA expression, but its abundance in the POA was significantly elevated in subordinates relative to shams at both the 1 d and 4 d time points (Fig. 4.5a and b, one-way ANOVA, $P = 0.013$ on ranks and 0.015).

4.3.4 Methylation of the crf *promoter*

Methylation status of the *crf* promoter and *crf* transcript abundance were measured after 4 d of social interaction in POA from the same fish. A significant difference in *crf* transcript abundance was detected (Fig. 4.6, one-way ANOVA, $P = 0.042$). Although the Tukey post-hoc test failed to identify the source of this difference, subordinates tended to have higher *crf* transcript abundance than dominant fish ($p = 0.058$).

Methylation levels were assessed in two regions of the *crf* promoter: a 167 bp distal region (-669 to -503 bp relative to the transcription start site) containing two CpG sites, and a 199 bp proximal region (-163 to +36 bp) containing 8 CpG sites (see Fig. 4.1 for promoter structure and sequence with relevant features). Generally, the distal region (Fig. 4.7) had greater levels of methylation than the proximal region (Fig. 4.8). The two CpG sites in the distal region were highly methylated, with all fish exhibiting methylation at these sites (Fig. 4.7b), often at 100% (Fig. 4.7c). Notably, the CpG at position -590 is located within a putative glucocorticoid response element (GRE -591 to -575, Fig. 4.1). Non-CpG methylation of cytosine was present at lower levels in this distal region. However, methylation at non-CpG cytosine was markedly higher at positions -604 and -591 (Fig. 4.7), the latter of which is in the GRE site (Fig. 4.1). A significant effect of social status was observed at these two loci (Fig. 4.7c), with dominant fish having significantly lower methylation than subordinates at both sites (one-way ANOVA, $P = 0.007$ for -604 and 0.008 for -591). The region more proximal to the transcription start site had lower overall levels of methylation (Fig. 4.8). At many loci, none of the fish within a social status group exhibited methylation (sites that are missing bars in Fig. 4.8b), and 8 non-CpG cytosine sites were removed from analysis because no methylation was detected in any fish from any group (-115, -101, -94, -92, -91, -83, -70, -5). The highest % methylation for any fish at any

site in this region was 54.5% (a sham at CpG site -109). Assessment of differences among social groups was confounded by the frequency of 0% methylation, but no obvious effects of status on methylation were apparent.

4.4 Figures

Figure 4.1 The promoter region of *crf* in rainbow trout (*Oncorhynchus mykiss*). Panel A illustrates the promoter region 1000 base pairs (bp) upstream of the transcription start site (TSS) of the *crf* gene. The regions amplified for bisulphite sequencing are indicated in blue (region 1, distal) and green (region 2, proximal), and all CpG sites are indicated by red vertical lines. Panel B presents the corresponding sequence for the same target regions (blue and green highlight) and CpG sites (red highlight), as well as indicating primer binding sites (bold), and non-CpG cytosines within amplicons (red font). The TSS and response elements (CRE, GRE, TATA; see methods for details) are indicated in the sequence by underlining.

Figure 4.1

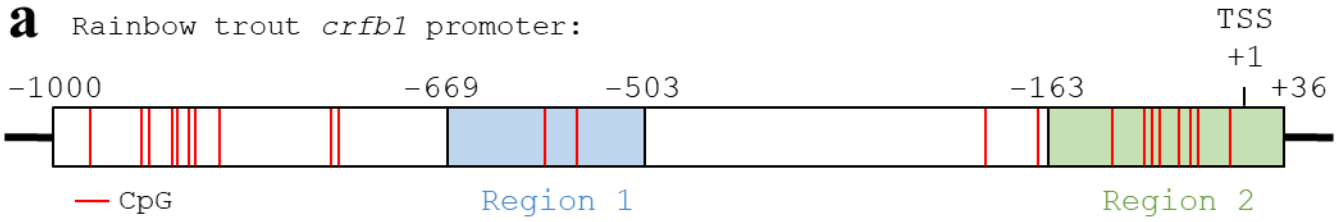

b

>*crfb1* promoter region

```
                                                                                PosTSS
CACTTTTTTT TTTGTCACAC CATTCTCGGT AAACCCTAGA CATTGTCATG TGTGAAAAGT     60 (-941)

CCAGGAGGTC GGACGTTTCT GAGATACTGG AACCAGCGCG CCTGCCACCG ACGATTATAC    120 (-881)

CACTCTCAAA GCCGTTTAGG TCACTGGTTT GCCCATTCTA ATGTTCAATC AAACAGTAAC    180 (-821)

TGAATGCCTT GGTGCCTGTC TGCCTGCTTT ATCTAGCAAG CCACGGCCAC GTGACTCACT    240 (-761)

GTCTTTTTGT GAATGGGGTG GTGTACCTAA TAAACTGGCC ATTCAGTGTA TGTTGGTGTG    300 (-701)

TAATCATGTT TAAGAAAAGT TGAGGAACTC TAATCAACAG ACAGTGCTTT AAAAGGGCCA    360 (-641)
 CRE
TATATTTGTA TTTAAAAAAA AAGTTGAGCT AGTAAGCTCC TATAGCATTC CGAACATTCT    420 (-581)
                                                          GRE
GTTCAAGACA TTTTAAGCGA TTGCCATTAA ATATTGGACA ATGCATTTCA GACCAATCTG    480 (-521)

TTGTTCTTGA AGTTGATTAG TACAATTATA TTAATTTAGA ATGTACTCTG AGGTAATCTG    540 (-461)
                                                    CRE
TTATAAATAT TCATCATGTC TCAGCAATAT TTTATTTCTA ATTTCTAATT CAGGGCACAA    600 (-401)

AGTCTGGCAT TTGATTGTCT GAGTGAGAAT CATTTTGAGA AGTGCACCAC CAAAATTACA    660 (-341)

ATTCTGCCCA TTTTCTGAAC AGGACTTGTG CATGACATAA TACAGGTCTC CTTTTTGTAG    720 (-281)
                                  CRE
AACAGACCAG CCACTGAGAT AAAGAACAAC TATAGACAAA TAATTATGTC TGCATCCAAG    780 (-221)

CCTGTGTGCG TGTTAGAAAA TATGTTGTAT TCTAAACACA CACACACACA CACGCACACA    840 (-161)

ACCAACATTT ATGACTCATC TCATTCAAAC TACCCCAGAC TTTCACAGAT GCGTTCATTC    900 (-101)

AAGTTACACC AATGTAACTC CGCGCATACG CAATCTCTGA GCTCAGAGCG TGACACTTGT    960  (-41)

CGCGGGTCTT GGCTATATAA ATCCAAACTG CCGTGCTTTA TTTGAAGAAC TCCTTATACA   1020  (+20)
                  TATA BOX                    TSS
CATTTCTTGA TCCATC                                                   1036  (+36)
```

Region 1
Region 2
CpG (all)
Non-CpG Cs (target regions only)
Primers
Response Elements (CRE, GRE, TATA)

Figure 4.2

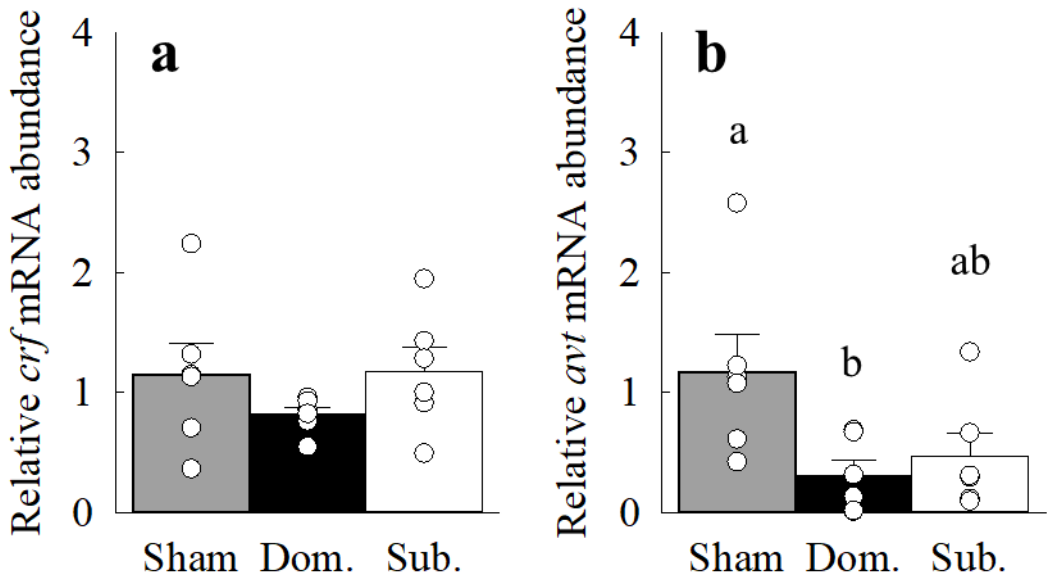

Figure 4.2 Transcript levels of *crf* (a) and *avt* (b) in the preoptic area (POA) of dominant (Dom.), subordinate (Sub.) and sham-treated rainbow trout (*Oncorhynchus mykiss*) after 4 days of social interaction. Transcript abundances were normalized to the geometric mean of the reference genes and expressed relative to the mean value for sham-treated fish. Data for *crf* in (a) also appear in Chapter 2 Fig. 2.8a and are included here for comparison to *avt.* Data are presented as means ± SEM ($N = 6$), with values for individuals shown as data points. Bars that share a letter are not significantly different from one another (ANOVA, $P = 0.354$, 0.036 for panels a and b, respectively).

Figure 4.3 Transcript levels of *crf* (a, b) and miRNAs targeting the *crf* 3'UTR (c-f) in the preoptic area (POA) of dominant (Dom.), subordinate (Sub.) and sham-treated rainbow trout (*Oncorhynchus mykiss*) after 1 day (a, c, e) or 4 days (b, d, f) of social interaction. Transcript abundance of *crf* was normalized to the geometric mean of the reference genes and expressed relative to the mean value for sham-treated fish. Transcript abundances of *miR-139-5p* (c, d) and *miR-103a-3p* (e, f) were normalized using the NORMA-Gene algorithm (see text for details). Data are presented as means ± SEM ($N = 6$), with values for individuals shown as data points. Bars that share a letter are not significantly different from one another (ANOVA, $P = 0.384$, <0.001, 0.094, 0.128, 0.006, 0.257 for panels a to f, respectively).

Figure 4.3

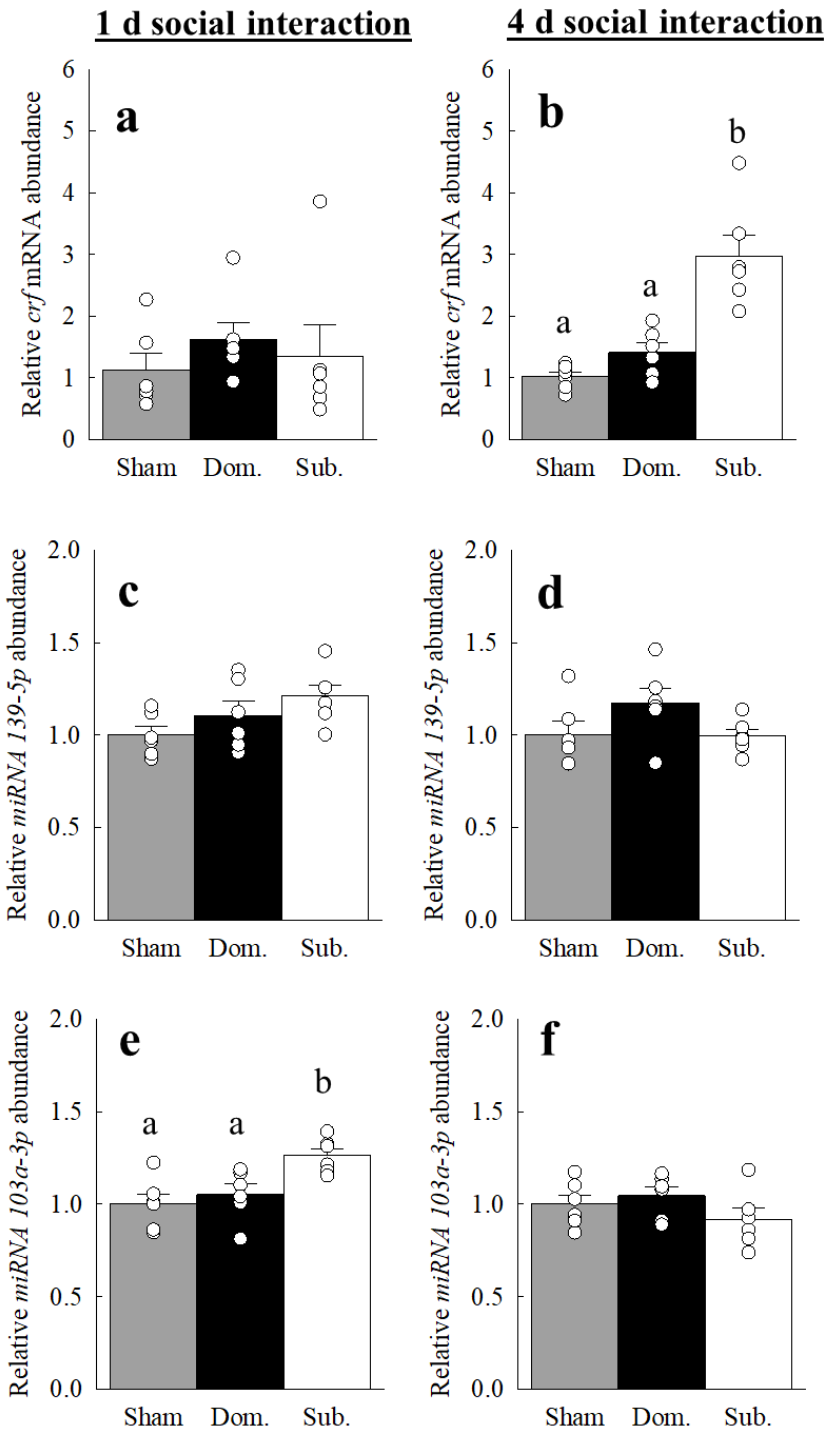
1 d social interaction
4 d social interaction
a
b
c
d
e
f
Relative crf mRNA abundance
Relative miRNA 139-5p abundance
Relative miRNA 103a-3p abundance
Sham
Dom.
Sub.

Figure 4.4 Transcript levels of *11βhsd2* (a, b) and *miR-210-3p*, which targets the *11βhsd2* 3'UTR (c, d) in the preoptic area (POA) of dominant (Dom.), subordinate (Sub.) and sham-treated rainbow trout (*Oncorhynchus mykiss*) after 1 day (a, c) or 4 days (b, d) of social interaction. Transcript abundance of *11βhsd2* was normalized to the geometric mean of the reference genes and expressed relative to the mean value for sham-treated fish. Transcript abundance of *miR-210-3p* was normalized using the NORMA-Gene algorithm (see text for details). Data are presented as means ± SEM ($N = 6$), with values for individuals shown as data points. Bars that share a letter are not significantly different from one another (ANOVA, $P =$ 0.710, 0.018, 0.140, 0.641 for panels a to d, respectively).

Figure 4.4

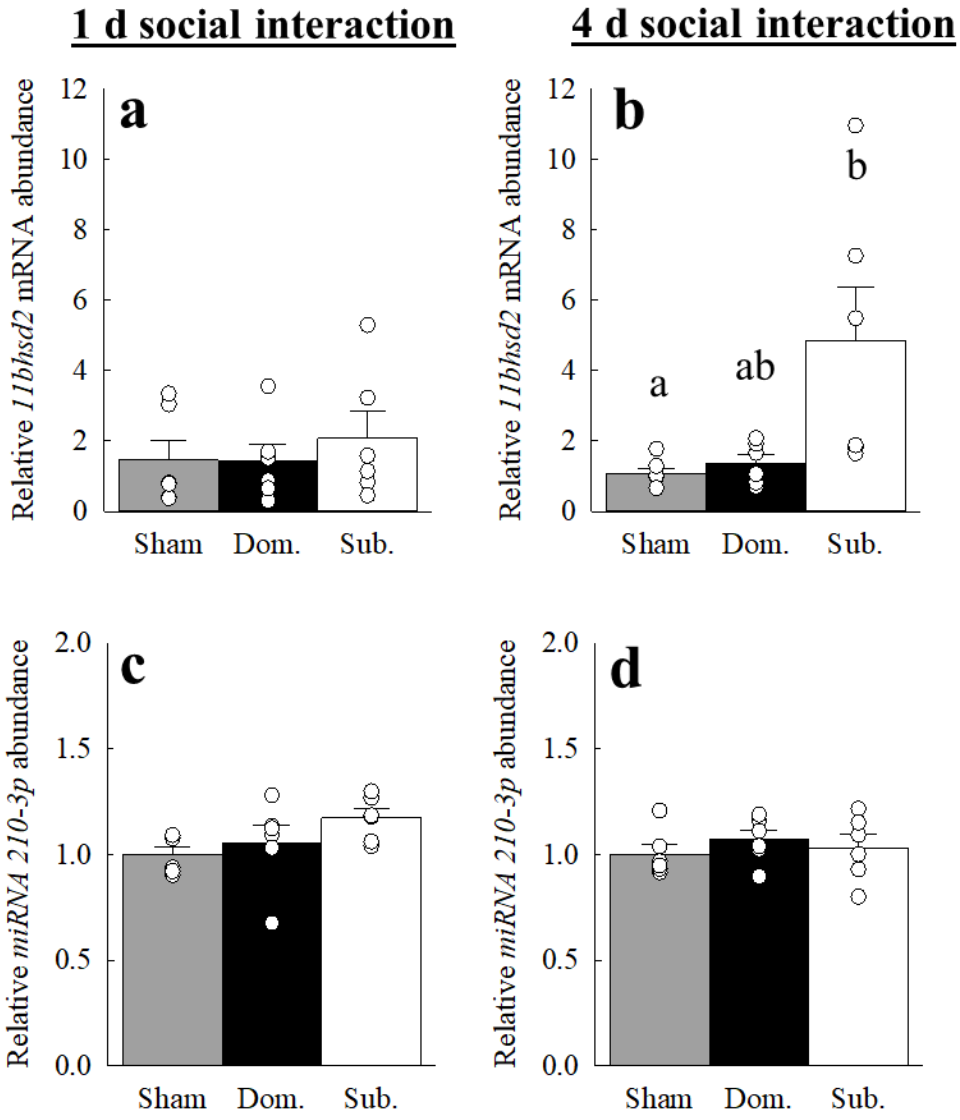
1 d social interaction
4 d social interaction
a
b
c
d
Relative 11bhsd2 mRNA abundance
Relative miRNA 210-3p abundance
0
2
4
6
8
10
12
0.0
0.5
1.0
1.5
2.0
Sham
Dom.
Sub.
a
ab
b

Figure 4.5

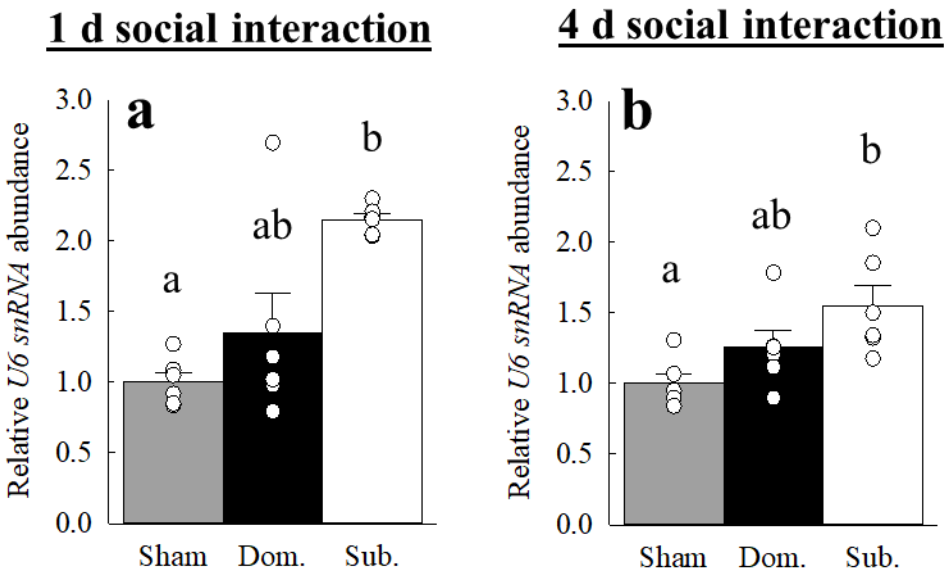

Figure 4.5 Transcript levels of *snRNA U6* miRNA in the preoptic area (POA) of dominant (Dom.), subordinate (Sub.) and sham-treated rainbow trout (*Oncorhynchus mykiss*) after 1 day (a) or 4 days (b) of social interaction. Transcript abundance was normalized using the NORMA-Gene algorithm (see text for details). Data are presented as means ± SEM ($N = 6$), with values for individuals shown as data points. Bars that share a letter are not significantly different from one another (ANOVA, $P = 0.013$ and 0.015 for panels a and b, respectively).

Figure 4.6

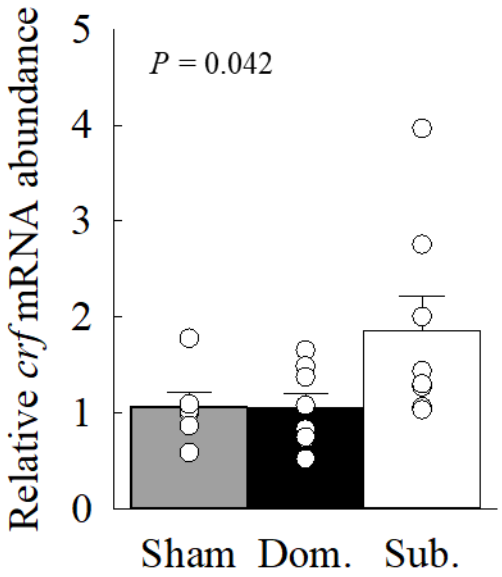

Figure 4.6 Transcript levels of *crf* after 4 days of social interaction in the preoptic area (POA) of dominant (Dom.), subordinate (Sub.) and sham-treated rainbow trout (*Oncorhynchus mykiss*) that were used to assess methylation of the *crf* promoter. Transcript abundance of *crf* was normalized to the geometric mean of the reference genes and expressed relative to the mean value for sham-treated fish. Data are presented as means ± SEM ($N = 6$), with values for individuals shown as data points.

Figure 4.7 Methylation status of cytosines in region 1 (distal) of the *crf* promoter in the preoptic area (POA) of dominant (Dom.), subordinate (Sub.), and sham-treated rainbow trout (*Oncorhynchus mykiss*). Grey shading indicates CpG sites. For each fish, 10-12 clones were sequenced to determine % C-methylation at each locus (a), and panel (c) presents mean values ± SEM for each locus. Panel (b) presents the percentage of fish (out of $N = 6$ sham or $N = 8$ pairs) that exhibited methylation within a given locus. Note that data for fish that exhibited % C-methylation of 0% were omitted from panel (a). In panel (c), bars at a given locus that share a letter are not significantly different from one another (see text for details).

Figure 4.7

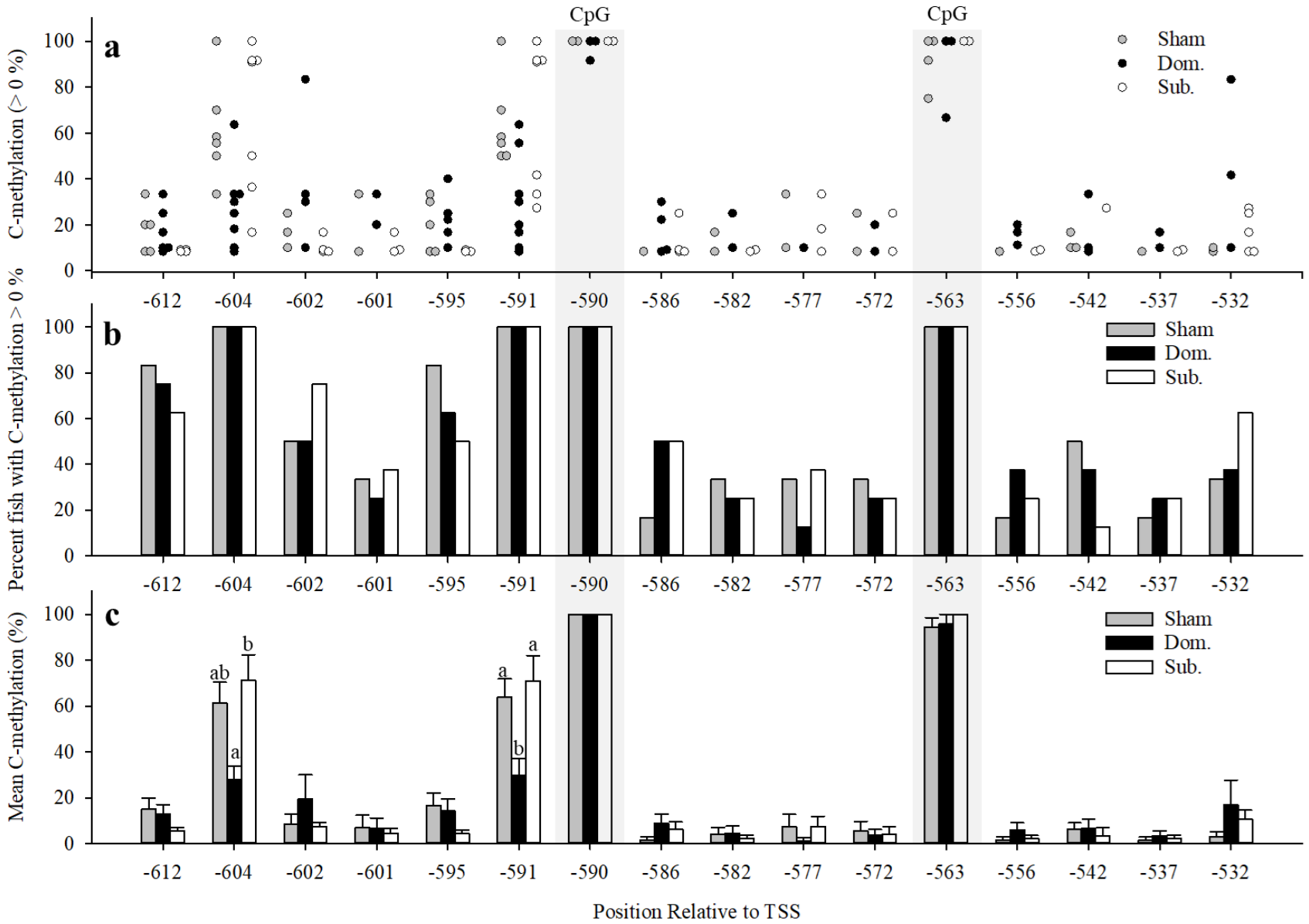
a
b
c
CpG
CpG
Sham
Dom.
Sub.
C-methylation (> 0 %)
Percent fish with C-methylation > 0 %
Mean C-methylation (%)
Position Relative to TSS
-612
-604
-602
-601
-595
-591
-590
-586
-582
-577
-572
-563
-556
-542
-537
-532
ab
a
b
a
b
a

Figure 4.8 Methylation status of cytosines in region 2 (proximal) of the *crf* promoter in the preoptic area (POA) of dominant (Dom.), subordinate (Sub.), and sham-treated rainbow trout (*Oncorhynchus mykiss*). Grey shading indicates CpG sites. For each fish, 8-12 clones were sequenced to determine % C-methylation at each locus (a), and panel (c) presents mean values ± SEM for each locus. Panel (b) presents the percentage of fish (out of $N = 6$ sham or $N = 8$ pairs) that exhibited methylation within a given locus. Note that data for fish that exhibited % C-methylation of 0% were omitted from panel (a).

Figure 4.8

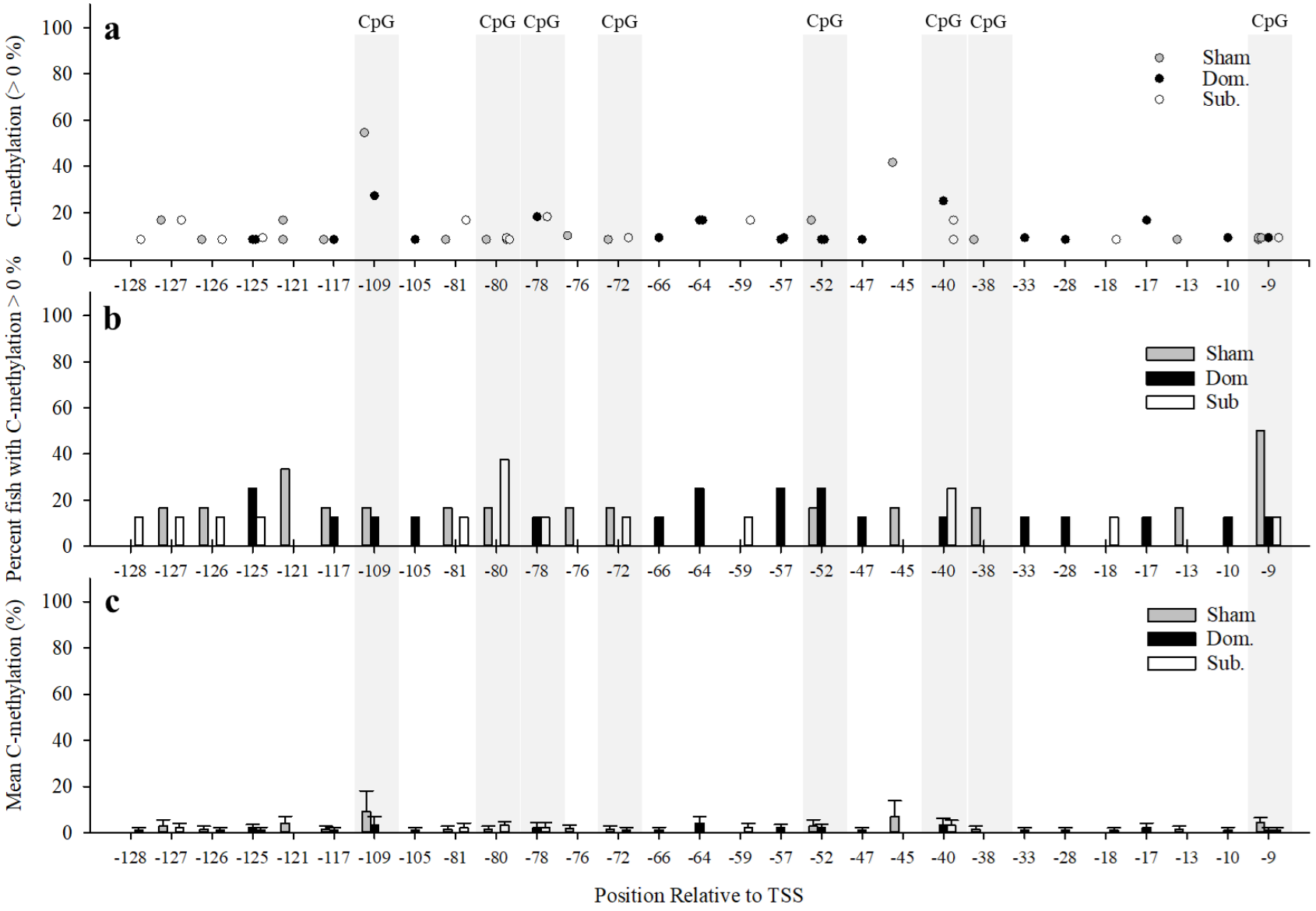
a
b
c
CpG
Sham
Dom.
Sub.
Dom
C-methylation (> 0 %)
Percent fish with C-methylation > 0 %
Mean C-methylation (%)
Position Relative to TSS
-128 -127 -126 -125 -121 -117 -109 -105 -81 -80 -78 -76 -72 -66 -64 -59 -57 -52 -47 -45 -40 -38 -33 -28 -18 -17 -13 -10 -9

4.5 Tables

Table 4.1 Primers used for mRNA and miRNA real-time RT-PCR (qPCR), and bisulphite PCR.

mRNA qPCR primers:

Gene	Primer sequence (5' to 3')	Amplicon size (bp)	Efficiency (%)	Accession number	Source
crf	F: ACAACGACTCAACTGAAGATCTCG	54	102	AF296672.1	(Bernier et al., 2008)
	R: AGGAAATTGAGCTTCATGTCAGG				
11βhsd2	F: AGGGCAAGGCTGTCTTCATC	117	106	NM_001124218.1	n/a
	R: CCTCCCCACACAGATCCAAC				
avt	F: TGAACACACCCAGAATAGAGC	96	110	XM_021590976.1	(Backström et al., 2011)
	R: TCTACTTCTGCTGTGTGTCTG				
β-actin	F: AGAGCTACGAGCTGCCTGAC	179	99	NM_001124235.1	(Moltesen et al., 2016)
	R: GTGTTGGCGTACAGGTCCTT				
ef1α	F: CATTGACAAGAGAACCATTGA	95	108	NM_001124339.1	(Birceanu et al., 2015)
	R: CCTTCAGCTTGTCCAGCAC				

miRNA/snRNA qPCR primers:

miRNA	Sequence (5' to 3')	Target	Eff. (%)	GeneGlobe ID	MIMAT
hsa-miR-139-5p	UCUACAGUGCACGUGUCUCCAGU	*crf*	87	YP00205874	MIMAT0000250
hsa-miR-103a-3p	AGCAGCAUUGUACAGGGCUAUGA	*crf*	80	YP00204063	MIMAT0000101
hsa-miR-210-3p	CUGUGCGUGUGACAGCGGCUGA	*11βhsd2*	81	YP00204333	MIMAT0000267
U6 snRNA	GUGCUCGCUUCGGCAGCACAUAUACUAAA AUUGGAACGAUACAGAGAAGAUUAGCAUG GCCCCUGCGCAAGGAUGACACGCAAAUUC GUGAAGCGUUCCAUAUUUUU	n/a	82	YP00203907	n/a

Bisulphite PCR primers:

Target	Sequence (5' to 3')	Pos. rel. to TSS	Amplicon Size (bp)
crf promoter (distal)	F: AATTAATAGATAGTGTTTTAAAAGGGTT	-590 to -563	167
	R: AATCAACTTCAAAAACAACAAATTAATC		
crf promoter (proximal)	F: ATAATTAATATTTATGATTTATTTTATTTAAATT	-163 to +36	199
	R: AATAAATCAAAAAATATATATAAAAAATTCT		

crf, corticotropin releasing factor; *11βhsd2*, 11β-hydroxysteroid dehydrogenase type 2, TSS, transcription start site (start of 5'UTR)

Table 4.2 Plasma cortisol concentrations (ng mL^{-1}) and behaviour scores for fish in all experiments.

		Plasma [cortisol] (ng mL^{-1})				Behaviour Score	
	N	**SHAM**	**DOM**	**SUB**	***P*-value**	**DOM**	**SUB**
AVT	6	4.14 ± 2.35^{a}	2.41 ± 0.46^{a}	170.51 ± 67.86^{b}	<0.001	1.89 ± 0.12	-1.50 ± 0.17
miRNA (1 d)	6	12.54 ± 5.93^{a}	9.72 ± 2.76^{a}	200.97 ± 42.71^{b}	<0.001	1.86 ± 0.29	-1.66 ± 0.11
miRNA (4 d)	6	10.08 ± 8.74^{a}	4.72 ± 2.03^{a}	260.67 ± 96.15^{b}	0.005	1.31 ± 0.15	-1.83 ± 0.23
methylation	6 sham, 8 pairs	3.17 ± 1.69^{a}	3.45 ± 0.67^{ab}	158.19 ± 51.01^{b}	0.016	1.33 ± 0.25	-1.39 ± 0.24
Overall (4 d only)	18 sham 20 pairs	5.80 ± 2.98^{a}	3.52 ± 0.67^{a}	192.63 ± 39.78^{b}	<0.001	1.58 ± 0.12	-1.58 ± 0.10

For cortisol, different superscript letters indicate significant differences. AVT and 1d miRNA, ANOVA on log-transformed data; 4d miRNA, methylation, and overall, ANOVA on ranks. Data are presented as means ± SEM.

4.6 Discussion

4.6.1 AVT as a potential regulator of the HPI axis during chronic social stress

AVT is a potential alternative to CRF as an ACTH secretatogue, based on functional evidence for this ability in fish (Baker et al., 1996; Bernier et al., 2009; Gesto et al., 2014). We hypothesized that AVT might serve as a key ACTH secretagogue in subordinate fish, maintaining stress axis activation and hence elevated circulating cortisol levels after several days of social stress, when *crf* transcript abundance is not elevated. Therefore, we predicted that subordinate trout would exhibit elevated *avt* mRNA abundance. Although subordinate trout in this experiment exhibited elevated cortisol, and *crf* transcript abundance that did not differ from that of dominant fish, *avt* transcript abundance was not significantly different between dominant and subordinate fish. These data suggest that social subordination does not upregulate *avt* transcript abundance to support activation of the stress axis. Similarly, whole brain *avt* transcript abundance was not elevated in subordinate rainbow trout held in groups of four fish for five days, although an interesting elevation of mRNA abundance of the AVT receptor was detected, potentially suggesting a role for AVT (Backström et al., 2021). Zebrafish subjected to 5 d of social subordination exhibited elevated *avt* but not *crf* transcript abundances (Pavlidis et al., 2011), suggesting that there may be species differences.

However, it is important to raise the issue of spatial distribution of these peptides in the teleost brain. CRF-producing neurons are located throughout the POA, which is a major site of CRF in the teleost brain (Cerdá-Reverter and Canosa, 2009). By contrast, AVT distribution is mainly restricted to the parvocellular and magnocellular neurons of the nucleus preopticus (NPO) within the POA (Bernier et al., 2009), and there is evidence that differences in *avt* expression between these two groups of neurons is functionally important. For example,

subordinate zebrafish displayed AVT-immunoreactive (AVT-ir) cells in the parvocellular group, but no staining in the magnocellular group, while the opposite was true in dominant individuals (Larson et al., 2006). The authors suggested that the magnocellular neurons may be involved in aggression, whereas the parvocellular neurons are associated with stress (Larson et al., 2006). In agreement with this observation, rainbow trout subjected to acute confinement stress showed increased *avt* mRNA levels in the parvocellular neurons of the NPO, but not in the magnocellular neurons (Gilchriest et al., 2000). When the stressor was repeated for several days, no difference in *avt* transcript abundance was present in either location, indicating some type of habituation response (Gilchriest et al., 2000). The specific localization of *avt* is clearly relevant for assessing its abundance in chronic social stress and could reveal subtle differences that were not evident using whole POA as in the present study.

4.6.2 miRNA as potential regulators of HPI axis activity during chronic social stress

Previous studies have reported elevated *crf* transcript abundance in subordinate relative to dominant trout after 8 h, 1 d or 3 d of social interaction (Bernier et al., 2008; Doyon et al., 2003), but not after 5 d of interaction (Jeffrey et al., 2012; Jeffrey et al., 2014). Similarly, *crf* transcript abundance was not elevated after 4 d of social interaction in the subordinates used in the present study to examine *avt* mRNA abundance. Unexpectedly, however, *crf* transcript abundance was elevated after 4 d of social interaction in subordinates used for miRNA and methylation analysis, and was not elevated after 1 d of social interaction in subordinates used for miRNA analysis. Given that cortisol levels were significantly elevated in all of these groups, it is clear that elevated cortisol is the more consistent trait among subordinate rainbow trout and does not always correspond to elevated *crf* transcript abundance. This apparent *crf*-cortisol disconnect

could exist because transcript abundance is not an ideal proxy for actual peptide signalling to the pituitary (for both *crf* and *avt*). What remain unclear, then, are the factors influencing regulation of *crf* transcript abundance during chronic activation of the stress axis. We explored two possibilities in the present study, miRNA and methylation.

In the group of fish used for miRNA analysis, transcript abundance of *crf* was unchanged by chronic social stress at 1 d, and elevated in subordinates at 4 d. Changes in abundance of miRNA are typically thought to be inversely related to their target mRNA by reducing the stability and translation of the mRNA molecule to which they are bound (Best et al., 2018; Huntzinger and Izaurralde, 2011). In 1 d subordinates we did not see an elevation in *crf* mRNA, and therefore we would not predict changes in the abundances of *miR-139-5p* and *miR-103a-3p*, which target *crf*. However, *miR-103a-3p* was unexpectedly upregulated in 1 d subordinates. In mammals, *miR-103a-3p* is expressed in many tissues with highest abundance in the brain, and the mRNA targets of this miRNA identified to date have mainly metabolic roles (Wilfred et al., 2007). Because a miRNA can have more than one target, it is possible that elevated *miR-103a-3p* in subordinate trout regulates a target other than *crf* (Mennigen and Zhang, 2016). Evidence supports the involvement of *miR-139-5p* during chronic stress. Chronic social defeat stress in rats activates the stress axis, including increasing *crf* mRNA abundance (Funk et al., 2006; Hostetler and Ryabinin, 2013; Wood et al., 2012). Abundance of *miR-139-5p* is elevated in the blood of rats that had a greater latency to defeat during chronic social defeat stress (Chen et al., 2015). In humans with major depressive disorder, and mice subjected to chronic unpredictable mild stress, *miR-139-5p* in the blood (and brain of mice) was upregulated (Wei et al., 2020). However, despite elevated *crf*, abundance, neither *miR-103a-3p* nor *miR-139-5p* were downregulated at 4 d

of social interaction in subordinate trout, and therefore are likely not involved in the regulation of *crf*.

Abundance of *11βhsd2* mRNA was also assessed, because mRNA expression of this cortisol-catabolizing enzyme was elevated in the subordinate POA, which may play a role in modulating negative feedback control of *crf* (Chapter 2). Consistent with the previous study (Chapter 2), *11βhsd2* mRNA was elevated in subordinate trout after 4 d of interaction. After 1 d of interaction, however, *11βhsd2* was not elevated. Given that this enzyme is cortisol-responsive (Alderman and Vijayan, 2012), it appears that several days of high cortisol levels are required to elicit increased *11βhsd2* transcript abundance. Abundance of *miR-210-3p*, which was predicted to target *11βhsd2*, was not altered at either 1 d or 4 d of social stress. This miRNA is involved in the hypoxia response in fish (Tse et al., 2015), but does not appear to play a role in social stress. It remains possible that another miRNA contributes to regulating *11βhsd2* transcript abundance in the POA; several other potential candidates were identified during the screening process. The approach used in the current study for selecting miRNA based on binding to specific 3'UTR sequences is not the only method available to identify candidate miRNA. Selection of miRNA in previous studies on rainbow trout was based on known function in mammals (Mennigen et al., 2012), on known roles in fishes (Kostyniuk et al., 2018), and on the results of small RNA next generation sequencing (Kostyniuk et al., 2019a). Assessment of miRNA is an active and novel area of research with a great deal of potential importance. The diversity of approaches in candidate miRNA selection perhaps reflects the novelty of the field. Although changes in miRNA were not observed in the current study, continued development of tools and knowledge for fish could reveal miRNA that play key roles during chronic stress.

The strongest effect in the miRNA analysis was perhaps also the least expected. The short non-coding RNA U6 is a component of the spliceosome (Lou et al., 2015; Wilkinson et al., 2020) and was screened for potential use as a reference gene in the current study because it was used successfully in other studies on rainbow trout (Ikert et al., 2021; Mennigen et al., 2014b). Although we were not the first to report instability of this particular RNA (Lou et al., 2015; Schwarzenbach et al., 2015), why snRNA U6 was elevated in subordinate fish in the current study was unclear. The functional relevance of this change may warrant investigation.

4.6.3 Methylation as a potential regulator of HPI axis activity during chronic social stress

Analysis of the *crf* promoter revealed some subtle but intriguing differences in methylation status. Changes in DNA methylation can alter access to gene regulatory elements in the promoter region, either increasing or decreasing transcription depending on the nature of the regulatory element (Zannas and West, 2014). Overall, methylation was higher in the distal region than the proximal region, which is consistent with general methylation patterns across gene elements in the zebrafish genome (McGaughey et al., 2014). Differential methylation was not apparent at any of the CpG loci, which tend to be the predominant targets of DNA methylation (de Mendoza et al., 2021). However, two non-CpG cytosines had significantly lower methylation levels in dominant fish. Originally, non-CpG methylation (or CpH using base degeneracy codes) was thought to be restricted to stem cells and absent in most other tissues, but more recent evidence suggests a functional role for this epigenetic mark in vertebrates (de Mendoza et al., 2021; Guo et al., 2014; Schultz et al., 2015). For example, 17β-estradiol (E2) reduces muscle growth and the gene expression of *myod,* a transcription factor essential for muscle growth, in rainbow trout (Koganti et al., 2017). It was found that E2 treatment also resulted in differential

non-CpG methylation of the *myod* promoter, supporting a functional role for non-CpG methylation in the skeletal muscle of rainbow trout (Koganti et al., 2017). Because promoter methylation is often associated with repression of transcription of the target gene, the methylation pattern observed in the present study would imply increased transcript abundance of *crf* in dominant fish. However, measurement of *crf* transcript abundance in the same set of fish suggested elevated abundance in subordinate rather than dominant fish. Of the two differentially methylated non-CpG sites in the current study, one is CpG-adjacent, and within a putative GRE (-591 to -575). Putative GRE sites must be functionally characterized to determine whether they are positive or negative (Schoneveld et al., 2004). However, altered methylation at a GRE could impact how this gene responds to circulating cortisol levels. Functional relevance is speculative at this point, but future studies could help determine a role for the differential methylation observed in the *crf* promoter.

4.6.4 Summary and conclusions

Overall, the current study explored several avenues through which *crf* signalling and/or HPI axis regulation could be modulated during chronic social stress. Measurement of *avt* transcript abundance in the POA did not support a role for AVT in supplementing or replacing CRF during chronic social stress, although analysis of specific nuclei within the POA may be necessary to uncover a role for AVT. Analysis of several selected miRNAs did not reveal changes in abundance caused by social stress, but additional screening of candidate microRNAs and/or a miRNA transcriptomic analysis could be useful in this respect. Methylation analysis of the *crf* promoter revealed significant changes at two loci, one of which is within a putative regulatory element, which may modulate transcription of *crf*. These studies highlight the

challenges of exploring epigenetic mechanisms in a non-model species like the rainbow trout. Prediction of *in silico* miRNA candidates does not guarantee success, and changes observed in mammals do not always translate to fishes. To understand the mismatch between the observed patterns of *crf* regulation and circulating cortisol levels during chronic social stress, further study is needed.

4.7 Supplementary information

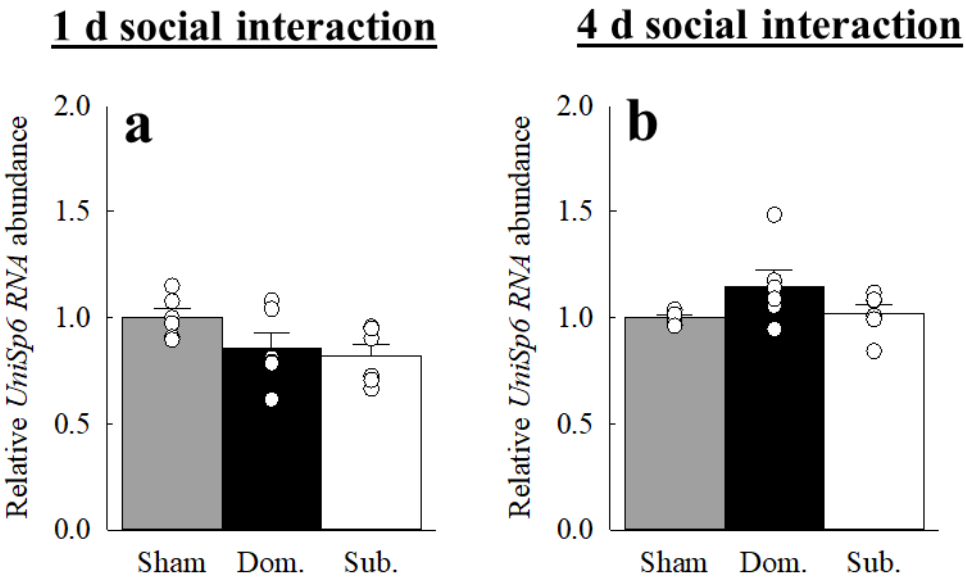

Figure S4.1 Transcript levels of *UniSp6* RNA in the preoptic area (POA) of dominant (Dom.), subordinate (Sub.) and sham-treated rainbow trout (*Oncorhynchus mykiss*) after 1 day (a) or 4 days (b) of social interaction. Transcript abundance was normalized using the NORMA-Gene algorithm (see text for details). Data are presented as means ± SEM (N = 6), with values for individuals shown as data points. Bars that share a letter are not significantly different from one another (ANOVA, $P = 0.086$ and 0.111 for panels a and b, respectively).

Chapter 5. General Discussion

5.1 Overview

The present thesis investigated how the HPI axis is regulated when plasma cortisol levels are sustained at an elevated level during chronic social stress. Multiple mechanisms act to lower cortisol levels following an acute stressor. Therefore, a key question is why these mechanisms fail to lower cortisol levels during chronic stress. Are these mechanisms less effective during chronic stress, or does activation of the stress axis overwhelm the capacity to lower cortisol levels? To address this question, aspects of both negative feedback/cortisol clearance and HPI axis activation were measured to determine their relative contributions to circulating cortisol levels during chronic social stress. The data suggest that negative feedback and cortisol clearance are largely intact in socially subordinate trout. This conclusion is supported by plasma cortisol dynamics *in vivo* in response to an exogenous cortisol load and during recovery from social stress; in both cases, subordinate fish were able to rapidly lower circulating cortisol levels. Intact negative feedback was also supported by the stable transcript and protein abundances of corticosteroid receptors in the HPI axis tissues. Transcript abundance of *11βhsd2*, the enzyme that inactivates cortisol, was elevated in the POA and pituitary, suggesting a role for this enzyme in modulating cortisol signalling in these tissues during chronic social stress.

The force opposing negative feedback/cortisol clearance is HPI axis activation, and evidence for continuous activation of the HPI axis during chronic social stress was mixed. We would predict elevated mRNA abundances of *crf* and *pomc* if the HPI axis is continuously activated. However, transcript abundance of *crf* in the POA was largely unaffected by subordinate status and only occasionally mildly elevated, while transcript abundances of the three paralogues of *pomc* in the pituitary were not elevated. This variation in *crf* transcript abundance seems typical of chronic social stress (Bernier et al., 2008; Doyon et al., 2006; Jeffrey

et al., 2012; Jeffrey et al., 2014) and indeed, of stressors in general (Faught et al., 2016), raising questions about the value of *crf* transcript abundance as an indicator of HPI axis activation. Chapter 4 probed alternative modes of *crf* regulation, and uncovered a difference in methylation of the *crf* promoter that warrants further study, particularly because *crf* promoter methylation was implicated in responses to chronic stress in mammals (Elliott et al., 2010). The candidate miRNAs targeting *crf* or *11βhsd2* in the POA did not differ with social status, but further targeted or global (transcriptomic) screening of other miRNA candidates could reveal yet another layer of fine-tuning of *crf* transcript abundance. Collectively, the impact of chronic social stress at the level of the preoptic area is not straightforward, with transcript abundances of *crf* and *avt* not showing consistent upregulation, cortisol signalling capacity being modified through *11βhsd2* transcript abundance but apparently not by alteration of the corticosteroid receptors (at either the transcript or protein levels), and the presence of methylation changes in the *crf* promoter.

In contrast to the equivocal findings for the POA and pituitary, the present thesis revealed a key role for the head kidney during chronic social stress. Under basal conditions (i.e. without stimulation by ACTH or db-cAMP), most endpoints measured in Chapter 3 supported a finding of increased cortisol synthesis by the head kidney in subordinates. Increased basal cortisol production makes sense in the context of Chapter 2, where no impairment in cortisol clearance or negative feedback was identified, leaving cortisol production as the obvious mechanism to maintain elevated plasma cortisol levels. A novel finding was the increased abundance of two paralogues of SF-1, a transcription factor known to regulate steroidogenesis in mammals (Ruggiero and Lalli, 2016). The head kidney was the only HPI axis tissue that did not show an elevation of *11βhsd2* transcript abundance. Coupled with stable transcript abundances of

corticosteroid receptors, this observation suggests that cortisol signalling in this tissue was not altered by chronic social stress. Despite increases in unstimulated steroidogenic capacity, chronic social stress clearly attenuates the production of cortisol in response to stimulation of the MC2R signalling pathway. Although this phenomenon of attenuated acute cortisol production during chronic stress was reported previously (Jeffrey et al., 2014; Sloman et al., 2002b), the underlying mechanism had not been established. The data of the current thesis places constraints on steroidogenesis downstream of cAMP in the signalling pathway. The constraints exist despite the elevated basal capacity for steroidogenesis provided by increased transcript abundances of *star*, *p450*scc, and *ff1*, and also despite an apparent elevation in ACTH signalling capacity via the MC2R provided by increased transcript abundances of *mrap1* and *mrap2*. Further, the constraint is unlikely to involve negative feedback, the capacity for which appeared to be unchanged in the head kidney. Although further study is needed to pin down the mechanism underlying this attenuation, the present study provided substantial insight into the "tug-of-war" between activation and negative feedback during regulation of the HPI axis during chronic social stress.

5.2 Limitations

Despite the advances reported in the present thesis, the work was not without limitations. The choice of rainbow trout as a study system has advantages, such as clear relevance to aquaculture and the formation of strong social hierarchies to elicit chronic stress reliably. Genomic and transcriptomic resources for rainbow trout (and other salmonids) have increased in recent years (Berthelot et al., 2014; Juanchich et al., 2016; Lien et al., 2016; Mennigen and Zhang, 2016; Salem et al., 2015), and these advances have led to the discovery of novel gene paralogues resulting from the teleost and salmonid whole genome duplications (Volff, 2005). For

instance, there appear to be four paralogues of *crf* in Atlantic salmon *(Salmo salar*, Grone and Maruska, 2015). Rainbow trout similarly appear to have four paralogues of *crf* (Lai et al., 2021), with the *crfb1* paralogue being assessed most often in stress research (including in the current thesis) as it appears to be the only paralogue that was identified prior to 2015 (Alderman et al., 2012; Backström et al., 2011; Bernier et al., 2008; Craig et al., 2005; Jeffrey et al., 2012; Jeffrey et al., 2014; Madison et al., 2013). A recent study in Atlantic salmon demonstrated abundant transcript abundance of this paralogue in the brain relative to the other three, and while all paralogues responded to their stressor regimes to some extent, effects were more pronounced in *crfb1* and *b2* (Lai et al., 2021). A similar characterization of *crf* paralogues has not been done in rainbow trout, but is warranted. The fate of duplicated genes may be subfunctionalization (partitioning ancestral functions among duplicate genes), neofunctionalization (acquisition of a novel function), or nonfunctionalization and conversion into a pseudogene (Volff, 2005). As paralogues are discovered, they will require characterization (e.g. Marandel et al., 2019) and rainbow trout are only in the early stages of this process.

Another area in which advances in teleosts have been made recently is the measurement of miRNA (Best et al., 2018; Bizuayehu and Babiak, 2014). The genome and transcriptome (mRNA and miRNA) studies cited above have expanded miRNA and 3'UTR sequences and hugely advanced the ability to screen for candidate miRNA using predictive binding tools. However, the novelty of the field as a whole means that best practices for miRNA studies remain a work in progress. In the present thesis, miRNA candidates were chosen based on their predicted binding to genes of interest, and unfortunately, the candidates chosen did not appear to be differentially regulated by chronic social stress. An alternative approach adopted in other studies involves selecting miRNA based on previous studies or transcriptomic analysis, and then

predicting the mRNA targets of these miRNA (Kostyniuk et al., 2018; Kostyniuk et al., 2019a). A diversity of approaches is perhaps unavoidable in a field that is relatively novel, and as this body of research grows, the success of screening methods should improve.

A limitation of the present study that is shared with many in the field is the reliance on transcript abundance data, because increased transcript abundance does not always correspond to increased protein abundance or activity. Autoregulation of the glucocorticoid receptor in rainbow trout hepatocytes provides a classic example, with cortisol treatment significantly elevating *gr* transcript abundance but decreasing Gr protein content over the same period (Sathiyaa and Vijayan, 2003). Transcript abundance is invaluable when assessing transcriptional regulation, which was a common theme throughout the present thesis. Classically, cortisol exerts its effect though transcriptional regulation mediated by the corticosteroid receptors, and the data reported here suggest that increased cortisol production in the head kidney is due in large part to transcriptional upregulation of proteins involved in key steps in steroidogenesis (Chapter 3). Similarly, the epigenetic mechanisms examined in Chapter 4 generally target transcription. Although we aimed to assess protein levels where possible, robust antibodies for rainbow trout are not always readily available. Indeed, we invested in the production of a custom antibody for 11βHSD2 to overcome this problem (Chapter 2). We also diversified our experimental approaches, when possible, to go beyond transcript abundances alone (e.g. flow cytometry and *in vitro* head kidney preparations in Chapter 3). However, reliance on transcript abundance as a physiologically-meaningful experimental end-point remains a limitation of the present work.

A final point of note is the issue of tissue heterogeneity. Most of our measurements were made on POA, pituitary or head kidney, tissues in which the cells of interest (CRF-releasing neurons, corticotropes and interrenal cells, respectively) are found together with other cell types

(Bernier et al., 2009; Cerdá-Reverter and Canosa, 2009; Gallo and Civinini, 2003; Hontela et al., 2008). This challenge is particularly important for the head kidney, where steroidogenic cells are rare (1:8,000; Hontela et al., 2008) and measurement of endpoints, like cAMP, that are ubiquitous in all head kidney cells may be hampered by dilution of the signal of interest. Additionally, differences in AVT expression are region-specific within the POA of dominant and subordinate zebrafish (Larson et al., 2006). This limitation exists in many studies, for example in measurements done using whole brain as opposed to brain regions, and warrants greater discussion and consideration than it typically receives.

5.3 Significance

The physiological response to chronic stressors tends to be less clear-cut than the response to acute stressors, and correspondingly it has received less research attention. Nevertheless, chronic stress warrants attention for both its basic and applied significance. The stress response is often described as being adaptive, but typically with the caveat that if the stressor is maintained for an undefined amount of time that is "too long", the stress response can become maladaptive (Barton, 2002; Charmandari et al., 2005; Wendelaar Bonga, 1997). Boonstra (2013) eloquently argues the case that chronic activation of the stress axis is not maladaptive in a natural environment. Although juvenile salmonids form hierarchies in the natural environment (Bachman, 1984; Jenkins, 1969; Nakano, 1995) the lab setting of the present thesis did not allow subordinate trout to escape the environment of the dominant fish and therefore chronic social stress likely resides in a grey area between adaptive and maladaptive. Moreover, whether a response is adaptive requires measuring fitness, which has not been well established during chronic social stress, especially in salmonid fish. The data of the present thesis

provide insight into the regulation of the HPI axis in this grey area, which is important in terms of understanding basic endocrine function. Moreover, the findings reported in the present thesis may guide future research to mitigate the maladaptive aspects of chronic social stress, which is of relevance for poor quality environments and aquaculture stressors.

Social stress in juvenile rainbow trout provides an excellent model to study chronic stress responses because it elicits a robust and sustained elevation in endogenous circulating cortisol. In addition, longstanding use of rainbow trout for stress research provides a body of work for context and comparison. Much of this literature targeted HPI axis activity, with relatively few studies having set out to assess negative feedback function and clearance of cortisol in a specific fashion, despite the importance of these processes to plasma cortisol concentrations and hence the physiology of the fish. The present thesis addresses this knowledge gap and provides a comprehensive picture of the suite of forces acting on the HPI axis during a chronic stressor. Although several endpoints did not change as anticipated, such as corticosteroid receptor abundance throughout the HPI axis, there is value in ruling out these mechanisms to guide future research. Importantly, the thesis adds novel members to the suite of forces regulating HPI axis activity, including *ff1* in the head kidney, *11βhsd2* in the POA and pituitary, and altered methylation of the *crf* promoter. Finally, the thesis brings to light the importance of changes at the level of the head kidney during chronic stress.

List of References

Abou-Samra, A.-B., Harwood, J. P., Catt, K. J. and Aguilera, G. (1987). Mechanisms of Action of CRF and Other Regulators of ACTH Release in Pituitary Corticotrophs. *Ann. N. Y. Acad. Sci.* **512**, 67–84.

Aerts, J. (2018). Quantification of a Glucocorticoid Profile in Non-pooled Samples Is Pivotal in Stress Research Across Vertebrates. *Front. Endocrinol. (Lausanne).* **9**, 1–9.

Aerts, J., Metz, J. R., Ampe, B., Decostere, A., Flik, G. and De Saeger, S. (2015). Scales tell a story on the stress history of fish. *PLoS One* **10**, 1–17.

Aguilera, G. (1994). Regulation of pituitary ACTH secretion during chronic stress. *Front. Neuroendocrinol.* **15**, 321–350.

Aguilera, G. and Liu, Y. (2012). The Molecular Physiology of CRH Neurons. *Front. Neuroendocrinol.* **33**, 67–84.

Aguilera, G. and Rabadan-Diehl, C. (2000). Vasopressinergic regulation of the hypothalamic-pituitary-adrenal axis: Implications for stress adaptation. *Regul. Pept.* **96**, 23–29.

Agulleiro, M. J., Roy, S., Sánchez, E., Puchol, S., Gallo-Payet, N. and Cerdá-Reverter, J. M. (2010). Role of melanocortin receptor accessory proteins in the function of zebrafish melanocortin receptor type 2. *Mol. Cell. Endocrinol.* **320**, 145–52.

Alderman, S. L. and Vijayan, M. M. (2012). 11β-Hydroxysteroid dehydrogenase type 2 in zebrafish brain: a functional role in hypothalamus-pituitary-interrenal axis regulation. *J. Endocrinol.* **215**, 393–402.

Alderman, S. L., McGuire, A., Bernier, N. J. and Vijayan, M. M. (2012). Central and peripheral glucocorticoid receptors are involved in the plasma cortisol response to an acute stressor in rainbow trout. *Gen. Comp. Endocrinol.* **176**, 79–85.

Allis, C. D. and Jenuwein, T. (2016). The molecular hallmarks of epigenetic control. *Nat. Rev. Genet.* **17**, 487–500.

Aluru, N. and Vijayan, M. M. (2006). Aryl hydrocarbon receptor activation impairs cortisol response to stress in rainbow trout by disrupting the rate-limiting steps in steroidogenesis. *Endocrinology* **147**, 1895–1903.

Aluru, N. and Vijayan, M. M. (2008). Molecular characterization, tissue-specific expression, and regulation of melanocortin 2 receptor in rainbow trout. *Endocrinology* **149**, 4577–4588.

Ambrosi, C., Manzo, M. and Baubec, T. (2017). Dynamics and Context-Dependent Roles of DNA Methylation. *J. Mol. Biol.* **429**, 1459–1475.

Arukwe, A. (2008). Steroidogenic acute regulatory (StAR) protein and cholesterol side-chain cleavage (P450scc)-regulated steroidogenesis as an organ-specific molecular and cellular target for endocrine disrupting chemicals in fish. *Cell Biol. Toxicol.* **24**, 527–40.

Bachman, R. A. (1984). Foraging Behavior of Free-Ranging Wild and Hatchery Brown Trout in a Stream. *Trans. Am. Fish. Soc.* **113**, 1–32.

Backström, T., Schjolden, J., Øverli, Ø., Thörnqvist, P. O. and Winberg, S. (2011). Stress effects on AVT and CRF systems in two strains of rainbow trout (Oncorhynchus mykiss) divergent in stress responsiveness. *Horm. Behav.* **59**, 180–186.

Backström, T., Thörnqvist, P. O. and Winberg, S. (2021). Social effects on AVT and CRF

systems. *Fish Physiol. Biochem.*

Baduy, F., Guerreiro, P. M., Canário, A. V. and Saraiva, J. L. (2017). Social organization and endocrine profiles of Australoheros facetus, an exotic freshwater fish in southern Portugal. *Acta Ethol.* **20**, 263–277.

Baker, M. E. (2010). Evolution of 11beta-hydroxysteroid dehydrogenase-type 1 and 11beta-hydroxysteroid dehydrogenase-type 3. *FEBS Lett.* **584**, 2279–2284.

Baker, B. I., Bird, D. J. and Buckingham, J. C. (1996). In the trout, CRH and AVT synergize to stimulate ACTH release. *Regul. Pept.* **67**, 207–210.

Balm, P. H. M. and Pottinger, T. G. (1995). Corticotrope and Melanotrope POMC-Derived Peptides in Relation to Interrenal Function during Stress in Rainbow Trout (Oncorhynchus mykiss). *Gen. Comp. Endocrinol.* **98**, 279–288.

Barcellos, L. J. G., Nicolaiewsky, S., De Souza, S. M. G. and Lulhier, F. (1999a). The effects of stocking density and social interaction on acute stress response in Nile tilapia Oreochromis niloticus (L.) fingerlings. *Aquac. Res.* **30**, 887–892.

Barcellos, L. J. G., Nicolaiewsky, S., De Souza, S. M. G. and Lulhier, F. (1999b). Plasmatic levels of cortisol in the response to acute stress in Nile tilapia, Oreochromis niloticus (L.), previously exposed to chronic stress. *Aquac. Res.* **30**, 437–444.

Barton, B. A. (2002). Stress in fishes: a diversity of responses with particular reference to changes in circulating corticosteroids. *Integr. Comp. Biol.* **42**, 517–525.

Barton, B. A., Schreck, C. B. and Barton, L. D. (1987). Effects of chronic cortisol administration and daily acute stress on growth, physiological conditions, and stress

responses in juvenile rainbow trout. *Dis. Aquat. Organ.* **2**, 173–185.

Basu, R., Singh, R. J., Basu, A., Chittilapilly, E. G., Johnson, C. M., Toffolo, G., Cobelli, C. and Rizza, R. A. (2004). Splanchnic Cortisol Production Occurs in Humans. *Diabetes* **53**, 2051–2059.

Baubec, T., Colombo, D. F., Wirbelauer, C., Schmidt, J., Burger, L., Krebs, A. R., Akalin, A. and Schübeler, D. (2015). Genomic profiling of DNA methyltransferases reveals a role for DNMT3B in genic methylation. *Nature* **520**, 243–7.

Beery, A. K. and Kaufer, D. (2015). Stress, social behavior, and resilience: Insights from rodents. *Neurobiol. Stress* **1**, 116–127.

Bélair-Bambrick, M.-È. (2016). Regulation of cortisol production by serotonin and negative feedback in the head kidney of rainbow trout (Oncorhynchus mykiss) - M.Sc. Thesis.

Bentz, A. B., George, E. M., Wolf, S. E., Rusch, D. B., Podicheti, R., Buechlein, A., Nephew, K. P. and Rosvall, K. A. (2021). Experimental competition induces immediate and lasting effects on the neurogenome in free-living female birds. *Proc. Natl. Acad. Sci. U. S. A.* **118**, 1–9.

Bernier, N. J., Lin, X. and Peter, R. E. (1999). Differential expression of corticotropin-releasing factor (CRF) and urotensin I precursor genes, and evidence of CRF gene expression regulated by cortisol in goldfish brain. *Gen. Comp. Endocrinol.* **116**, 461–77.

Bernier, N. J., Alderman, S. L. and Bristow, E. N. (2008). Heads or tails ? Stressor-specific expression of corticotropin-releasing factor and urotensin I in the preoptic area and caudal neurosecretory system of rainbow trout. *J. Endocrinol.* **196**, 637–48.

Bernier, N. J., Flik, G. and Klaren, P. H. M. (2009). Regulation And Contribution Of The Corticotropic, Melanotropic And Thyrotropic Axes To The Stress Response In Fishes. In *Fish Physiology Vol. 28 Fish Neuroendocrinology*, pp. 235–311. Elsevier Inc.

Berthelot, C., Brunet, F., Chalopin, D., Juanchich, A., Bernard, M., Noël, B., Bento, P., Da Silva, C., Labadie, K., Alberti, A., et al. (2014). The rainbow trout genome provides novel insights into evolution after whole-genome duplication in vertebrates. *Nat. Commun.* **5**, 1–10.

Bessa, E., Sadoul, B., Mckenzie, D. J. and Geffroy, B. (2021). Group size, temperature and body size modulate the effects of social hierarchy on basal cortisol levels in fishes. *Horm. Behav.* **136**, 105077.

Best, C. and Vijayan, M. M. (2017). Cortisol elevation post-hatch affects behavioural performance in zebrafish larvae. *Gen. Comp. Endocrinol.* **257**, 220–226.

Best, C., Ikert, H., Kostyniuk, D. J., Craig, P. M., Navarro-Martin, L., Marandel, L. and Mennigen, J. A. (2018). Epigenetics in teleost fish: From molecular mechanisms to physiological phenotypes. *Comp. Biochem. Physiol. Part - B Biochem. Mol. Biol.* **224**, 210–244.

Beuschlein, F., Mutch, C., Bayers, D. L., Ulrich-Lai, Y. M., Engeland, W. C., Keegan, C. and Hammer, G. D. (2002). Steroidogenic factor-1 is essential for compensatory adrenal growth following unilateral adrenalectomy. *Endocrinology* **143**, 3122–3135.

Birceanu, O., Mai, T. and Vijayan, M. M. (2015). Maternal transfer of bisphenol A impacts the ontogeny of cortisol stress response in rainbow trout. *Aquat. Toxicol.* **168**, 11–18.

Bizuayehu, T. and Babiak, I. (2014). MicroRNA in teleost fish. *Genome Biol. Evol.* **6**, 1911–1937.

Bland, M. L., Jamieson, C. A. M., Akana, S. F., Bornstein, S. R., Eisenhofer, G., Dallman, M. F. and Ingraham, H. A. (2000). Haploinsufficiency of steroidogenic factor-1 in mice disrupts adrenal development leading to an impaired stress response. *Proc. Natl. Acad. Sci. U. S. A.* **97**, 14488–14493.

Boonstra, R. (2013). Reality as the leading cause of stress: Rethinking the impact of chronic stress in nature. *Funct. Ecol.* **27**, 11–23.

Bradford, C. S., Fitzpatrick, M. S. and Schreck, C. B. (1992). Evidence for ultra-short-loop feedback in ACTH-induced interrenal steroidogenesis in coho salmon: Acute self-suppression of cortisol secretion in vitro. *Gen. Comp. Endocrinol.* **87**, 292–299.

Bremer, A. A. and Miller, W. L. (2014). Regulation of Steroidogenesis. In *Cellular Endocrinology in Health and Disease*, pp. 207–227. Elsevier Inc.

Breuner, C. W. and Orchinik, M. (2002). Plasma binding proteins as mediators of corticosteroid action in vertebrates. *J. Endocrinol.* **175**, 99–112.

Bury, N. R., Sturm, A., Le Rouzic, P., Lethimonier, C., Ducouret, B., Guiguen, Y., Robinson-Rechavi, M., Laudet, V., Rafestin-Oblin, M. E. and Prunet, P. (2003). Evidence for two distinct functional glucocorticoid receptors in teleost fish. *J. Mol. Endocrinol.* **31**, 141–156.

Cadonic, I. G., Ikert, H. and Craig, P. M. (2020). Acute air exposure modulates the microRNA abundance in stress responsive tissues and circulating extracellular vesicles in

rainbow trout (Oncorhynchus mykiss). *Comp. Biochem. Physiol. - Part D Genomics Proteomics* **34**, 100661.

Carbonara, P., Dioguardi, M., Cammarata, M., Zupa, W., Vazzana, M., Spedicato, M. T. and Lembo, G. (2019). Basic knowledge of social hierarchies and physiological profile of reared sea bass Dicentrarchus labrax (L.). *PLoS One* **14**, 1–16.

Carpenter, R. E., Maruska, K. P., Becker, L. and Fernald, R. D. (2014). Social opportunity rapidly regulates expression of CRF and CRF receptors in the brain during social ascent of a teleost fish, Astatotilapia burtoni. *PLoS One* **9**, e96632.

Carter, R. N., Paterson, J. M., Tworowska, U., Stenvers, D. J., Mullins, J. J., Seckl, J. R. and Holmes, M. C. (2009). Hypothalamic-pituitary-adrenal axis abnormalities in response to deletion of 11β-HSD1 is strain-dependent. *J. Neuroendocrinol.* **21**, 879–887.

Castillo, J., Castellana, B., Acerete, L., Planas, J. V, Goetz, F. W., Mackenzie, S. and Tort, L. (2008). Stress-induced regulation of steroidogenic acute regulatory protein expression in head kidney of Gilthead seabream (Sparus aurata). *J. Endocrinol.* **196**, 313–322.

Cawley, N. X., Li, Z. and Loh, Y. P. (2016). Biosynthesis, trafficking, and secretion of pro-opiomelanocortin-derived peptides. *J. Mol. Endocrinol.* **56**, T77–T97.

Cerdá-Reverter, J. M. and Canosa, L. F. (2009). Chapter 1 Neuroendocrine Systems of the Fish Brain. *Fish Physiol.* **28**, 3–74.

Chai, C., Liu, Y. and Chan, W.-K. (2003). Ff1b is required for the development of steroidogenic component of the zebrafish interrenal organ. *Dev. Biol.* **260**, 226–244.

Chapman, K., Holmes, M. and Seckl, J. (2013). 11B-Hydroxysteroid Dehydrogenases:

Intracellular Gate-Keepers of Tissue Glucocorticoid Action. *Physiol. Rev.* **93**, 1139–1206.

Charmandari, E., Tsigos, C. and Chrousos, G. (2005). Endocrinology of the stress response. *Annu. Rev. Physiol.* **67**, 259–84.

Chen, J., Evans, A. N., Liu, Y., Saavedra, J. M. and Aguilera, G. (2012). Maternal deprivation in rats is associated with corticotropin releasing hormone (CRH) promoter hypomethylation and enhances CRH transcriptional responses to stress in adulthood. *J. Neuroendocrinol.* **24**, 1055–1064.

Chen, R. J., Kelly, G., Sengupta, A., Heydendael, W., Nicholas, B., Beltrami, S., Luz, S., Peixoto, L., Abel, T. and Bhatnagar, S. (2015). MicroRNAs as biomarkers of resilience or vulnerability to stress. *Neuroscience* **305**, 36–48.

Chrétien, M. and Mbikay, M. (2016). From the prohormone theory to pro-opiomelanocortin and to proprotein convertases (PCSK1 to PCSK9). *J. Mol. Endocrinol.* **56**, T49–T62.

Craig, P. M., Al-Timimi, H. and Bernier, N. J. (2005). Differential increase in forebrain and caudal neurosecretory system CRF and urotensin I gene expression associated with seawater transfer in rainbow trout. *Endocrinology* **146**, 3851–3860.

Culbert, B. M. and Gilmour, K. M. (2016). Rapid recovery of the cortisol response following social subordination in rainbow trout. *Physiol. Behav.* **164**, 306–313.

Culbert, B. M., Gilmour, K. M. and Balshine, S. (2018). Stress axis regulation during social ascension in a group-living cichlid fish. *Horm. Behav.* **103**, 121–128.

Das, C., Thraya, M. and Vijayan, M. M. (2018). Nongenomic cortisol signaling in fish. *Gen. Comp. Endocrinol.* **265**, 121–127.

de Mendoza, A., Poppe, D., Buckberry, S., Pflueger, J., Albertin, C. B., Daish, T., Bertrand, S., de la Calle-Mustienes, E., Gómez-Skarmeta, J. L., Nery, J. R., et al. (2021). The emergence of the brain non-CpG methylation system in vertebrates. *Nat. Ecol. Evol.* **5**, 369–378.

DiBattista, J. D., Levesque, H. M., Moon, T. W. and Gilmour, K. M. (2006). Growth depression in socially subordinate rainbow trout Oncorhynchus mykiss: more than a fasting effect. *Physiol. Biochem. Zool.* **79**, 675–687.

Donaldson, E. M. and Fagerlund, U. H. M. (1972). Corticosteroid dynamics in Pacific salmon. *Gen. Comp. Endocrinol.* **3**, 254–265.

Dores, R. M. and Garcia, Y. (2015). Views on the co-evolution of the melanocortin-2 receptor, MRAPs, and the hypothalamus/pituitary/adrenal-interrenal axis. *Mol. Cell. Endocrinol.* **408**, 12–22.

Dores, R. M., Liang, L., Hollmann, R. E., Sandhu, N. and Vijayan, M. M. (2016). Identifying the activation motif in the N-terminal of rainbow trout and zebrafish melanocortin-2 receptor accessory protein 1 (MRAP1) orthologs. *Gen. Comp. Endocrinol.* **234**, 117–122.

Doyon, C., Gilmour, K. M., Trudeau, V. L. and Moon, T. W. (2003). Corticotropin-releasing factor and neuropeptide Y mRNA levels are elevated in the preoptic area of socially subordinate rainbow trout. *Gen. Comp. Endocrinol.* **133**, 260–271.

Doyon, C., Leclair, J., Trudeau, V. L. and Moon, T. W. (2006). Corticotropin-releasing factor and neuropeptide Y mRNA levels are modified by glucocorticoids in rainbow trout, Oncorhynchus mykiss. *Gen. Comp. Endocrinol.* **146**, 126–135.

Du, J., Li, M., Huang, Q., Liu, W., Li, W., Li, Y. and Gong, Z. (2019). The critical role of microRNAs in stress response: Therapeutic prospect and limitation. *Pharmacol. Res.* **142**, 294–302.

Ejike, C. and Schreck, C. B. (1980). Stress and Social Hierarchy Rank in Coho Salmon. *Trans. Am. Fish. Soc.* **109**, 423–426.

Elliott, E., Ezra-Nevo, G., Regev, L., Neufeld-Cohen, A. and Chen, A. (2010). Resilience to social stress coincides with functional DNA methylation of the Crf gene in adult mice. *Nat. Neurosci.* **13**, 1351–1353.

Erickson, J. G. (1967). Social Hierarchy, Territoriality, and Stress Reactions in Sunfish. *Physiol. Zool.* **40**, 40–48.

Fabbri, E., Capuzzo, A. and Moon, T. W. (1998). The role of circulating catecholamines in the regulation of fish metabolism: an overview. *Comp. Biochem. Physiol. C. Pharmacol. Toxicol. Endocrinol.* **120**, 177–92.

Faught, E. and Vijayan, M. M. (2018). The mineralocorticoid receptor is essential for stress axis regulation in zebrafish larvae. *Sci. Rep.* **8**, 18081.

Faught, E. and Vijayan, M. M. (2019). Loss of the glucocorticoid receptor in zebrafish improves muscle glucose availability and increases growth. *Am. J. Physiol. Endocrinol. Metab.* **316**, E1093–E1104.

Faught, E. and Vijayan, M. M. (2020). Glucocorticoid and mineralocorticoid receptor activation modulates postnatal growth. *J. Endocrinol.* **244**, 261–271.

Faught, E., Aluru, N. and Vijayan, M. M. (2016). The Molecular Stress Response. In *Fish*

Physiology Vol. 35 Biology of Stress in Fish, pp. 113–166. Elsevier Inc.

Fierro-Castro, C., Santa-Cruz, M. C., Hernández-Sánchez, M., Teles, M. and Tort, L. (2015). Analysis of steroidogenic pathway key transcripts in interrenal cells isolated by laser microdissection (LMD) in stressed rainbow trout. *Comp. Biochem. Physiol. -Part A Mol. Integr. Physiol.* **190**, 39–46.

Fornes, O., Castro-Mondragon, J. A., Khan, A., Van Der Lee, R., Zhang, X., Richmond, P. A., Modi, B. P., Correard, S., Gheorghe, M., Baranašić, D., et al. (2020). JASPAR 2020: Update of the open-Access database of transcription factor binding profiles. *Nucleic Acids Res.* **48**, D87–D92.

Fryer, J. N. and Peter, R. E. (1977). Hypothalamic control of ACTH secretion in goldfish. III. Hypothalamic Cortisol Implant Studies. *Gen. Comp. Endocrinol.* **33**, 215–225.

Fryer, J., Lederis, K. and Rivier, J. (1984). Cortisol inhibits the ACTH-releasing activity of urotensin I, CRF and sauvagine observed with superfused goldfish pituitary cells. *Peptides* **5**, 925–930.

Funk, D., Li, Z. and Lê, A. D. (2006). Effects of environmental and pharmacological stressors on c-fos and corticotropin-releasing factor mRNA in rat brain: Relationship to the reinstatement of alcohol seeking. *Neuroscience* **138**, 235–243.

Fuzzen, M. L. M., Van Der Kraak, G. and Bernier, N. J. (2010). Stirring Up New Ideas About the Regulation of the Hypothalamic-Pituitary-Interrenal Axis in Zebrafish (Danio rerio). *Zebrafish* **7**, 349–358.

Gallo, V. P. and Civinini, A. (2003). Survey of the Adrenal Homolog in Teleosts. *Int. Rev.*

Cytol. **230**, 89–187.

Gamperl, A. K., Vijayan, M. M. and Boutilier, R. G. (1994). Experimental control of stress hormone levels in fishes: techniques and applications. *Rev. Fish Biol. Fish.* **4**, 215–255.

Geslin, M. and Auperin, B. (2004). Relationship between changes in mRNAs of the genes encoding steroidogenic acute regulatory protein and P450 cholesterol side chain cleavage in head kidney and plasma levels of cortisol in response to different kinds of acute stress in the rainbow trout. *Gen. Comp. Endocrinol.* **135**, 70–80.

Gesto, M., Soengas, J. L., Rodríguez-Illamola, A. and Míguez, J. M. (2014). Arginine vasotocin treatment induces a stress response and exerts a potent anorexigenic effect in rainbow trout, oncorhynchus mykiss. *J. Neuroendocrinol.* **26**, 89–99.

Gilchriest, B. J., Tipping, D. R., Hake, L., Levy, A. and Baker, B. I. (2000). The effects of acute and chronic stresses on vasotocin gene transcripts in the brain of the rainbow trout (Oncorhynchus mykiss). *J. Neuroendocrinol.* **12**, 795–801.

Gilmour, K. M. (2005). Mineralocorticoid receptors and hormones: Fishing for answers. *Endocrinology* **146**, 44–46.

Gilmour, K. M., Dibattista, J. D. and Thomas, J. B. (2005). Physiological causes and consequences of social status in salmonid fish. *Integr. Comp. Biol.* **45**, 263–273.

Gilmour, K. M., Kirkpatrick, S., Massarsky, A., Pearce, B., Saliba, S., Stephany, C.-É. and Moon, T. W. (2012). The influence of social status on hepatic glucose metabolism in rainbow trout Oncorhynchus mykiss. *Physiol. Biochem. Zool.* **85**, 309–320.

Gilmour, K. M., Craig, P. M., Dhillon, R. S., Lau, G. Y. and Richards, J. G. (2017).

Regulation of energy metabolism during social interactions in rainbow trout : a role for AMP-activated protein kinase. *Am. J. Physiol. Regul. Integr. Comp. Physiol.* **313**, 549–559.

Godwin, J. and Thompson, R. (2012). Hormones and Behavior Nonapeptides and Social Behavior in Fishes. *Horm. Behav.* **61**, 230–238.

Gorissen, M. and Flik, G. (2016). The Endocrinology of the Stress Response in Fish - An Adaptation-Physiological View. In *Fish Physiology Vol. 35 Biology of Stress in Fish*, pp. 75–111. Elsevier Inc.

Grone, B. P. and Maruska, K. P. (2015). Divergent evolution of two corticotropin-releasing hormone (CRH) genes in teleost fishes. *Front. Neurosci.* **9**, 1–13.

Guo, J. U., Su, Y., Shin, J. H., Shin, J., Li, H., Xie, B., Zhong, C., Hu, S., Le, T., Fan, G., et al. (2014). Distribution, recognition and regulation of non-CpG methylation in the adult mammalian brain. *Nat. Neurosci.* **17**, 215–222.

Ha, M. and Kim, V. N. (2014). Regulation of microRNA biogenesis. *Nat. Rev. Mol. Cell Biol.* **15**, 509–524.

Hammond, G. L. (2016). Plasma steroid-binding proteins: Primary gatekeepers of steroid hormone action. *J. Endocrinol.* **230**, R13–R25.

Han, L. and Zhao, Z. (2008). Comparative analysis of CpG Islands in four fish genomes. *Comp. Funct. Genomics* **2008**, 1–6.

Harris, A. P., Holmes, M. C., De Kloet, E. R., Chapman, K. E. and Seckl, J. R. (2012). Mineralocorticoid and glucocorticoid receptor balance in control of HPA axis and behaviour. *Psychoneuroendocrinology* **38**, 648–658.

He, L. and Hannon, G. J. (2004). MicroRNAs: small RNAs with a big role in gene regulation. *Nat. Rev. Genet.* **5**, 522–531.

Heckmann, L. H., Sørensen, P. B., Krogh, P. H. and Sørensen, J. G. (2011). NORMA-Gene: A simple and robust method for qPCR normalization based on target gene data. *BMC Bioinformatics* **12**, 1–7.

Herget, U. and Ryu, S. (2015). Coexpression analysis of nine neuropeptides in the neurosecretory preoptic area of larval zebrafish. *Front. Neuroanat.* **9**, 1–11.

Hill, M. N. and Tasker, J. G. (2012). Endocannabinoid signaling, glucocorticoid-mediated negative feedback, and regulation of the hypothalamic-pituitary-adrenal axis. *Neuroscience* **204**, 5–16.

Höglund, E., Balm, P. H. M. and Winberg, S. (2002). Behavioural and neuroendocrine effects of environmental background colour and social interaction in Arctic charr (Salvelinus alpinus). *J. Exp. Biol.* **205**, 2535–2543.

Hontela, A. and Vijayan, M. M. (2008). Adrenocortical Toxicology in Fishes. In *Adrenal Toxicology*, pp. 233–256. CRC Press.

Hontela, A., Leblond, V. S. and Chang, J. P. (2008). Purification and isolation of corticosteroidogenic cells from head kidney of rainbow trout (Oncorhynchus mykiss) for testing cell-specific effects of a pesticide. *Comp. Biochem. Physiol. - C Toxicol. Pharmacol.* **147**, 52–60.

Hostetler, C. M. and Ryabinin, A. E. (2013). The crf system and social behavior: A review. *Front. Neurosci.* **7**, 1–15.

Hsu, H. J., Lin, G. and Chung, B. C. (2003). Parallel early development of zebrafish interrenal glands and pronephros: Differential control by wt1 and ff1b. *Development* **130**, 2107–2116.

Huising, M. O., Metz, J. R., van Schooten, C., Taverne-Thiele, A. J., Hermsen, T., Kemenade, B. M. L. V. and Flik, G. (2004). Structural characterisation of a cyprinid (Cyprinus carpio L.) CRH, CRH-BP and CRH-R1, and the role of these proteins in the acute stress response. *J. Mol. Endocrinol.* **32**, 627–648.

Huising, M. O., van der Aa, L. M., Metz, J. R., de Fátima Mazon, A., Kemenade, B. M. L. V. and Flik, G. (2007). Corticotropin-releasing factor (CRF) and CRF-binding protein expression in and release from the head kidney of common carp: Evolutionary conservation of the adrenal CRF system. *J. Endocrinol.* **193**, 349–357.

Huntzinger, E. and Izaurralde, E. (2011). Gene silencing by microRNAs: Contributions of translational repression and mRNA decay. *Nat. Rev. Genet.* **12**, 99–110.

Idler, D. R. and Truscott, B. (1972). Corticosteroids in fish. In *Steroids in Nonmammalian Vertebrates* (ed. Idler, D.), pp. 127–211. New York: Academic Press.

Ikert, H., Lynch, M. D. J., Doxey, A. C., Giesy, J. P., Servos, M. R., Katzenback, B. A. and Craig, P. M. (2021). High Throughput Sequencing of MicroRNA in Rainbow Trout Plasma, Mucus, and Surrounding Water Following Acute Stress. *Front. Physiol.* **11**, 1–17.

Ings, J. S., Servos, M. R. and Vijayan, M. M. (2011). Hepatic transcriptomics and protein expression in rainbow trout exposed to municipal wastewater effluent. *Environ. Sci. Technol.* **45**, 2368–2376.

Ivy, C. M., Robertson, C. E., Bernier, N. J. and Bernier, N. J. (2017). Acute embryonic

anoxia exposure favours the development of a dominant and aggressive phenotype in adult zebrafish. *Proc. R. Soc. B Biol. Sci.* **284**, 20161868.

Iwama, G. K. (1998). Stress in Fish. *Ann. N. Y. Acad. Sci.* **851**, 304–310.

Iwata, E. and Suzuki, N. (2020). Steroidal regulation of the aromatase gene and dominant behavior in the false clown anemonefish Amphiprion ocellaris. *Fish. Sci.* **86**, 457–463.

Iwata, E., Suzuki, N. and Ohno, S. (2019). Influence of social stability on the sex determination process in false clown anemonefish (Amphiprion ocellaris). *Mar. Freshw. Behav. Physiol.* **52**, 107–119.

Jeffrey, J. D., Esbaugh, A. J., Vijayan, M. M. and Gilmour, K. M. (2012). Modulation of hypothalamic-pituitary-interrenal axis function by social status in rainbow trout. *Gen. Comp. Endocrinol.* **176**, 201–210.

Jeffrey, J. D., Gollock, M. J. and Gilmour, K. M. (2014). Social stress modulates the cortisol response to an acute stressor in rainbow trout (Oncorhynchus mykiss). *Gen. Comp. Endocrinol.* **196**, 8–16.

Jenkins, T. M. (1969). Social Structure, Position Choice and Micro-distribution of Two Trout Species (Salmo trutta and Salmo gairdneri) Resident in Mountain Streams. *Anim. Behav. Monogr.* **2**, 55–123.

Johnsson, J. I., Winberg, S. and Sloman, K. A. (2006). Social interactions. In *Fish Physiology Vol. 24 Behaviour and Physiology of Fish*, pp. 151–196. Elsevier Inc.

Johnstone, H. A., Wigger, A., Douglas, A. J., Neumann, I. D., Landgraf, R., Seckl, J. R. and Russell, J. A. (2000). Attenuation of hypothalamic-pituitary-adrenal axis stress responses in

late pregnancy: Changes in feedforward and feedback mechanisms. *J. Neuroendocrinol.* **12**, 811–822.

Jones, P. A. (2012). Functions of DNA methylation: islands, start sites, gene bodies and beyond. *Nat. Rev. Genet.* **13**, 484–492.

Juanchich, A., Bardou, P., Rué, O., Gabillard, J.-C., Gaspin, C., Bobe, J. and Guiguen, Y. (2016). Characterization of an extensive rainbow trout miRNA transcriptome by next generation sequencing. *BMC Genomics* **17**, 1–12.

Keller-Wood, M. (2015). Hypothalamic-Pituitary-Adrenal Axis-Feedback Control. *Compr. Physiol.* **5**, 1161–1182.

Khor, Y. M., Soga, T. and Parhar, I. S. (2016). Early-life stress changes expression of GnRH and kisspeptin genes and DNA methylation of GnRH3 promoter in the adult zebrafish brain. *Gen. Comp. Endocrinol.* **227**, 84–93.

Kiilerich, P., Servili, A., Péron, S., Valotaire, C., Goardon, L., Leguen, I. and Prunet, P. (2018). Regulation of the corticosteroid signalling system in rainbow trout HPI axis during confinement stress. *Gen. Comp. Endocrinol.* **258**, 184–193.

Kobayashi, T., Nakamura, M., Kajiura-Kobayashi, H., Young, G. and Nagahama, Y. (1998). Immunolocalization of steroidogenic enzymes (P450scc, P450c17, P450arom, and 3B-HSD) in immature and mature testes of rainbow trout (Oncorhynchus mykiss). *Cell Tissue Res.* **292**, 573–577.

Koganti, P. P., Wang, J., Cleveland, B. and Yao, J. (2017). 17β-Estradiol Increases Non-CpG Methylation in Exon 1 of the Rainbow Trout (Oncorhynchus mykiss) MyoD Gene. *Mar.*

Biotechnol. **19**, 321–327.

Kostyniuk, D. J., Culbert, B. M., Mennigen, J. A. and Gilmour, K. M. (2018). Social status affects lipid metabolism in rainbow trout, Oncorhynchus mykiss. *Am. J. Physiol. Regul. Integr. Comp. Physiol.* **315**, R241–R255.

Kostyniuk, D. J., Zhang, D., Martyniuk, C. J., Gilmour, K. M. and Mennigen, J. A. (2019a). Social status regulates the hepatic miRNAome in rainbow trout : Implications for posttranscriptional regulation of metabolic pathways. *PLoS One* **14**, e0217978.

Kostyniuk, D. J., Marandel, L., Jubouri, M., Dias, K., de Souza, R. F., Zhang, D., Martyniuk, C. J., Panserat, S. and Mennigen, J. A. (2019b). Profiling the rainbow trout hepatic mirnaome under diet-induced hyperglycemia. *Physiol. Genomics* **51**, 411–431.

Kuo, M.-W., Postlethwait, J., Lee, W.-C., Lou, S.-W., Chan, W.-K. and Chung, B. (2005). Gene duplication, gene loss and evolution of expression domains in the vertebrate nuclear receptor NR5A (Ftz-F1) family. *Biochem. J.* **389**, 19–26.

Kusakabe, M., Nakamura, I. and Young, G. (2003). 11B-Hydroxysteroid dehydrogenase complementary deoxyribonucleic acid in rainbow trout: Cloning, sites of expression, and seasonal changes in gonads. *Endocrinology* **144**, 2534–2545.

Laberge, F., Yin-Liao, I. and Bernier, N. J. (2019). Temporal profiles of cortisol accumulation and clearance support scale cortisol content as an indicator of chronic stress in fish. *Conserv. Physiol.* **7**, 1–13.

Lacroix, M. and Hontela, A. (2001). Regulation of acute cortisol synthesis by cAMP-dependent protein kinase and protein kinase C in a teleost species, the rainbow trout (Oncorhynchus

mykiss). *J. Endocrinol.* **169**, 71–78.

Lai, F., Royan, M. R., Gomes, A. S., Espe, M., Aksnes, A., Norberg, B., Gelebart, V. and Rønnestad, I. (2021). The stress response in Atlantic salmon (Salmo salar L.): identification and functional characterization of the corticotropin-releasing factor (crf) paralogs. *Gen. Comp. Endocrinol.* **313**, 113894.

Laidley, C. W. and Leatherland, J. F. (1988). Cohort sampling, anaesthesia and stocking-density effects on plasma cortisol, thyroid hormone, metabolite and ion levels in rainbow trout, Salmo gairdneri Richardson. *J. Fish Biol.* **33**, 73–88.

Larson, E. T., Malley, D. M. O., Melloni, R. H., Hall, M. and Ave, H. (2006). Aggression and vasotocin are associated with dominant – subordinate relationships in zebrafish. **167**, 94–102.

Leder, E. H. and Silverstein, J. T. (2006). The pro-opiomelanocortin genes in rainbow trout (Oncorhynchus mykiss): Duplications, splice variants, and differential expression. *J. Endocrinol.* **188**, 355–363.

Lee, R. C., Feinbaum, R. and Ambros, V. (1993). The C . elegans Heterochronic Gene lin-4 Encodes Small RNAs with Antisense Complementarity to lin-14. *Cell* **75**, 843–854.

Lenkov, K., Lee, M. H., Lenkov, O. D., Swafford, A. and Fernald, R. D. (2015). Epigenetic DNA Methylation Linked to Social Dominance. *PLoS One* **10**, 1–11.

Liang, L., Schmid, K., Sandhu, N., Angleson, J. K., Vijayan, M. M. and Dores, R. M. (2015). Structure/function studies on the activation of the rainbow trout melanocortin-2 receptor. *Gen. Comp. Endocrinol.* **210**, 145–151.

Lien, S., Koop, B. F., Sandve, S. R., Miller, J. R., Matthew, P., Leong, J. S., Minkley, D. R., Zimin, A., Grammes, F., Grove, H., et al. (2016). The Atlantic salmon genome provides insights into rediploidization. *Nature* **533**, 200–205.

Lou, G., Ma, N., Xu, Y., Jiang, L., Yang, J., Wang, C., Jiao, Y. and Gao, X. (2015). Differential distribution of U6 (RNU6-1) expression in human carcinoma tissues demonstrates the requirement for caution in the internal control gene selection for microRNA quantification. *Int. J. Mol. Med.* **36**, 1400–1408.

Madaro, A., Olsen, R. E., Kristiansen, T. S., Ebbesson, L. O. E., Nilsen, T. O., Flik, G. and Gorissen, M. (2015). Stress in Atlantic salmon: response to unpredictable chronic stress. *J. Exp. Biol.* **218**, 2538–2550.

Madeira, F., Park, Y. M., Lee, J., Buso, N., Gur, T., Madhusoodanan, N., Basutkar, P., Tivey, A. R. N., Potter, S. C., Finn, R. D., et al. (2019). The EMBL-EBI search and sequence analysis tools APIs in 2019. *Nucleic Acids Res.* **47**, W636–W641.

Madison, B. N., Woo, P. T. K. and Bernier, N. J. (2013). Duress without stress: Cryptobia infection results in HPI axis dysfunction in rainbow trout. *J. Endocrinol.* **218**, 287–297.

Madison, B. N., Tavakoli, S., Kramer, S. and Bernier, N. J. (2015). Chronic cortisol and the regulation of food intake and the endocrine growth axis in rainbow trout. *J. Endocrinol.* **226**, 103–119.

Manuel, R., Metz, J. R., Flik, G., Vale, W. W. and Huising, M. O. (2014). Corticotropin-releasing factor-binding protein (CRF-BP) inhibits CRF- and urotensin-I-mediated activation of CRF receptor-1 and -2 in common carp. *Gen. Comp. Endocrinol.* **202**, 69–75.

Marandel, L., Kostyniuk, D. J., Best, C., Forbes, J. L. I., Liu, J., Panserat, S. and Mennigen, J. A. (2019). Pck-ing up steam: Widening the salmonid gluconeogenic gene duplication trail. *Gene* **698**, 129–140.

McCarthy, I. D., Carter, C. G. and Houlihan, D. F. (1992). The effect of feeding hierarchy on individual variability in daily feeding of rainbow trout, Oncorhynchus mykiss (Walbaum). *J. Fish Biol.* **41**, 257–263.

McCormick, S. D., Regish, A., O'Dea, M. F. and Shrimpton, J. M. (2008). Are we missing a mineralocorticoid in teleost fish? Effects of cortisol, deoxycorticosterone and aldosterone on osmoregulation, gill Na+,K+-ATPase activity and isoform mRNA levels in Atlantic salmon. *Gen. Comp. Endocrinol.* **157**, 35–40.

McGaughey, D. M., Abaan, H. O., Miller, R. M., Kropp, P. A. and Brody, L. C. (2014). Genomics of CpG Methylation in Developing and Developed Zebrafish. *G3* **4**, 861–869.

McGhee, K. E. and Bell, A. M. (2014). Paternal care in a fish: Epigenetics and fitness enhancing effects on offspring anxiety. *Proc. R. Soc. B Biol. Sci.* **281**, 2–7.

McKittrick, C. R., Blanchard, D. C., Hardy, M. P. and Blanchard, R. J. (2009). Social stress effects on hormones, brain, and behavior. *Horm. Brain Behav. Online* 333–367.

McQuillan, H. J., Kusakabe, M. and Young, G. (2011). Effects of chronic manipulation of adrenocorticotropic hormone levels in Chinook salmon on expression of interrenal steroidogenic acute regulatory protein and steroidogenic enzymes. *Gen. Comp. Endocrinol.* **174**, 156–65.

Mennigen, J. A. and Zhang, D. (2016). MicroTrout: A comprehensive, genome-wide miRNA

target prediction framework for rainbow trout, Oncorhynchus mykiss. *Comp. Biochem. Physiol. Part D Genomics Proteomics* **20**, 19–26.

Mennigen, J. A., Panserat, S., Larquier, M., Plagnes-Juan, E., Medale, F., Seiliez, I. and Skiba-Cassy, S. (2012). Postprandial regulation of hepatic microRNAs predicted to target the insulin pathway in rainbow trout. *PLoS One* **7**, e38604.

Mennigen, J. A., Martyniuk, C. J., Seiliez, I., Panserat, S. and Skiba-Cassy, S. (2014a). Metabolic consequences of microRNA-122 inhibition in rainbow trout, Oncorhynchus mykiss. *BMC Genomics* **15**, 1–20.

Mennigen, J. A., Plagnes-Juan, E., Figueredo-Silva, C. A., Seiliez, I., Panserat, S. and Skiba-Cassy, S. (2014b). Acute endocrine and nutritional co-regulation of the hepatic omy-miRNA-122b and the lipogenic gene fas in rainbow trout, Oncorhynchus mykiss. *Comp. Biochem. Physiol. - B Biochem. Mol. Biol.* **169**, 16–24.

Metcalfe, A. N. B., Huntingford, F. A., Graham, W. D., Thorpe, J. E., Metcalfe, N. B., Huntingford, F. A., Graham, W. D., Thorpe, J. E. and Metcalfe, A. N. B. (1989). Early social status and the development of life-history strategies in Atlantic salmon. *Proc. R. Soc. London. Ser. B, Biol. Sci.* **236**, 7–19.

Moltesen, M., Laursen, D. C., Thörnqvist, P., Andersson, M. Å., Winberg, S. and Höglund, E. (2016). Effects of acute and chronic stress on telencephalic neurochemistry and gene expression in rainbow trout (Oncorhynchus mykiss). *J. Exp. Biol.* **219**, 3907–3914.

Mommsen, T. P., Vijayan, M. M. and Moon, T. W. (1999). Cortisol in teleosts: dynamics, mechanisms of action, and metabolic regulation. *Rev. Fish Biol. Fish.* **9**, 211–268.

Morandini, L., Honji, R. M., Ramallo, M. R., Moreira, R. G. and Pandolfi, M. (2014). The interrenal gland in males of the cichlid fish Cichlasoma dimerus: Relationship with stress and the establishment of social hierarchies. *Gen. Comp. Endocrinol.* **195**, 88–98.

Mullins, M., Postlethwait, J. and Westerfield, M. (1998). Genetic Nomenclature Guide for Zebrafish. *Trends Genet.* **14**, S.32-S.33.

Nakano, S. (1995). Individual Differences in Resource Use, Growth and Emigration Under the Influence of a Dominance Hierarchy in Fluvial Red-Spotted Masu Salmon in a Natural Habitat. *J. Anim. Ecol.* **64**, 75–84.

Nematollahi, M. A., van Pelt-Heerschap, H. and Komen, J. (2009). Transcript levels of five enzymes involved in cortisol synthesis and regulation during the stress response in common carp: Relationship with cortisol. *Gen. Comp. Endocrinol.* **164**, 85–90.

Nichols, D., Weisbart, M. and Quinn, J. (1985). Cortisol kinetics and fluid distribution in brook trout (Salvelinus fontinalis). *J. Endocrinol.* **107**, 57–69.

Noakes, D. L. G. and Leatherland, J. F. (1977). Social dominance and interrenal cell activity in rainbow trout, Salmo gairneri (Pisces, Salmonidae). *Environ. Biol. Fish* **2**, 131–136.

Øverli, Ø., Harris, C. A. and Winberg, S. (1999a). Short-term effects of fights for social dominance and the establishment of dominant-subordinate relationships on brain monoamines and cortisol in rainbow trout. *Brain. Behav. Evol.* **54**, 263–275.

Øverli, Olsen, R. E., Løvik, F. and Ringø, E. (1999b). Dominance hierarchies in Arctic charr, Salvelinus alpinus L.: Differential cortisol profiles of dominant and subordinate individuals after handling stress. *Aquac. Res.* **30**, 259–264.

Owen, W. and Idler, D. (1972). Identification and metabolic clearance of cortisol and cortisone in a marine teleost, the sea raven Hemitripterus americanus Gmelin (family Scorpaenidae). *J. Endocrinol.* **53**, 101–112.

Patiño, R., Bradford, C. S. and Schreck, C. B. (1986). Adenylate cyclase activators and inhibitors, cyclic nucleotide analogs, and phosphatidylinositol: Effects on interrenal function of coho salmon (Oncorhynchus kisutch) in vitro. *Gen. Comp. Endocrinol.* **63**, 230–235.

Pavlidis, M., Sundvik, M., Chen, Y.-C. and Panula, P. (2011). Adaptive changes in zebrafish brain in dominant-subordinate behavioral context. *Behav. Brain Res.* **225**, 529–37.

Peters, G., Delventhal, H. and Klinger, H. (1980). Physiological and Morphological Effects of Social Stress on the Eel, Anguilla anguilla L.pp. 225–227.

Pfaffl, M. W. (2001). A new mathematical model for relative quantification in real-time RT-PCR. *Nucleic Acids Res.* **29**, 2002–2007.

Pottinger, T. G. and Carrick, T. R. (2001). ACTH does not mediate divergent stress responsiveness in rainbow trout. *Comp. Biochem. Physiol. - Part A Mol. Integr. Physiol.* **129**, 399–404.

Pottinger, T. G., Moran, T. A. and Cranwell, P. A. (1992). The biliary accumulation of corticosteroids in rainbow trout, Oncorhynchus mykiss, during acute and chronic stress. *Fish Physiol. Biochem.* **10**, 55–66.

Quek, S. I. and Chan, W. K. (2009). Transcriptional activation of zebrafish cyp11a1 promoter is dependent on the nuclear receptor Ff1b. *J. Mol. Endocrinol.* **43**, 121–130.

Redding, J. M., Patiño, R. and Schreck, C. B. (1984). Clearance of corticosteroids in yearling coho salmon, Oncorhynchus kisutch, in fresh water and seawater and after stress. *Gen. Comp. Endocrinol.* **54**, 433–443.

Reid, S. G., Bernier, N. J. and Perry, S. F. (1998). The adrenergic stress response in fish: control of catecholamine storage and release. *Comp. Biochem. Physiol. C. Pharmacol. Toxicol. Endocrinol.* **120**, 1–27.

Romero, L. M., Dickens, M. J. and Cyr, N. E. (2009). The reactive scope model - A new model integrating homeostasis, allostasis, and stress. *Horm. Behav.* **55**, 375–389.

Rotllant, J., Arends, R. J., Mancera, J. M., Flik, G., Wendelaar Bonga, S. E. and Tort, L. (2000). Inhibition of HPI axis response to stress in gilthead sea bream (Sparus aurata) with physiological plasma levels of cortisol. *Fish Physiol. Biochem.* **23**, 13–22.

Ruggiero, C. and Lalli, E. (2016). Impact of ACTH signaling on transcriptional regulation of steroidogenic genes. *Front. Endocrinol. (Lausanne).* **7**, 1–14.

Sadoul, B. and Vijayan, M. M. (2016). Stress and Growth. In *Fish Physiology Vol. 35 Biology of Stress in Fish*, pp. 167–205. Elsevier Inc.

Sakamoto, T., Yoshiki, M., Takahashi, H., Yoshida, M., Ogino, Y., Ikeuchi, T., Nakamachi, T., Konno, N., Matsuda, K. and Sakamoto, H. (2016). Principal function of mineralocorticoid signaling suggested by constitutive knockout of the mineralocorticoid receptor in medaka fish. *Sci. Rep.* **6**, 37991.

Salem, M., Paneru, B., Al-Tobasei, R., Abdouni, F., Thorgaard, G. H., Rexroad, C. E. and Yao, J. (2015). Transcriptome assembly, gene annotation and tissue gene expression atlas

of the rainbow trout. *PLoS One* **10**, 1–27.

Samaras, A., Santo, C. E., Papandroulakis, N., Mitrizakis, N., Pavlidis, M., Höglund, E., Pelgrim, T. N. M., Zethof, J., Spanings, F. A. T., Vindas, M. A., et al. (2018). Allostatic load and stress physiology in European seabass (Dicentrarchus labrax L.) and gilthead seabream (Sparus aurata L.). *Front. Endocrinol. (Lausanne).* **9**, 1–13.

Samaras, A., Dimitroglou, A., Kollias, S., Skouradakis, G., Papadakis, I. E. and Pavlidis, M. (2021). Cortisol concentration in scales is a valid indicator for the assessment of chronic stress in European sea bass, Dicentrarchus labrax L. *Aquaculture* **545**, 737257.

Sandhu, N., Liang, L., McGeer, J., Dores, R. M. and Vijayan, M. M. (2019). Cadmium disrupts melanocortin 2 receptor signaling in rainbow trout. *Aquat. Toxicol.* **209**, 26–33.

Sathiyaa, R. and Vijayan, M. M. (2003). Autoregulation of glucocorticoid receptor by cortisol in rainbow trout hepatocytes. *Am. J. Physiol. Cell Physiol.* **284**, 1508–1515.

Schimmer, B. P. and White, P. C. (2010). Minireview: Steroidogenic Factor 1: Its Roles in Differentiation, Development, and Disease. *Mol. Endocrinol.* **24**, 1322–1337.

Schoneveld, O. J. L. M., Gaemers, I. C. and Lamers, W. H. (2004). Mechanisms of glucocorticoid signalling. *Biochim. Biophys. Acta - Gene Struct. Expr.* **1680**, 114–128.

Schreck, C. B. and Tort, L. (2016). The Concept of Stress in Fish. In *Fish Physiology Vol. 35 Biology of Stress in Fish*, pp. 1–34. Elsevier Inc.

Schulte, P. M. (2014). What is environmental stress? Insights from fish living in a variable environment. *J. Exp. Biol.* **217**, 23–34.

Schultz, M. D., He, Y., Whitaker, J. W., Hariharan, M., Mukamel, E. A., Leung, D.,

Rajagopal, N., Nery, J. R., Urich, M. A., Chen, H., et al. (2015). Human Body Epigenome Maps Reveal Noncanonical DNA Methylation Variation. *Nature* **523**, 212–216.

Schwarzenbach, H., Da Silva, A. M., Calin, G. and Pantel, K. (2015). Data normalization strategies for microRNA quantification. *Clin. Chem.* **61**, 1333–1342.

Scott, D. B. C. and Currie, C. E. (1980). Social hierarchy in relation to adrenocortical activity in Xiphophorus helleri Heckel. *J. Fish Biol.* **16**, 265–277.

Scott, D. B. C. and Rennie, S. E. (1980). Nuclear diameter as a criterion of adrenocortical activity in a teleost fish Coregonus lavaretus (L.). *J. Fish Biol.* **17**, 83–90.

Seebacher, F. and Krause, J. (2019). Epigenetics of Social Behaviour. *Trends Ecol. Evol.* **34**, 818–830.

Sewer, M. B. and Waterman, M. R. (2003). ACTH modulation of transcription factors responsible for steroid hydroxylase gene expression in the adrenal cortex. *Microsc. Res. Tech.* **61**, 300–307.

Sheu-Gruttadauria, J. and MacRae, I. J. (2017). Structural Foundations of RNA Silencing by Argonaute. *J. Mol. Biol.* **429**, 2619–2639.

Sloman, K. A. and Armstrong, J. D. (2002). Physiological effects of dominance hierarchies: Laboratory artefacts or natural phenomena? *J. Fish Biol.* **61**, 1–23.

Sloman, K. A., Metcalfe, N. B., Taylor, A. C. and Gilmour, K. M. (2001). Plasma cortisol concentrations before and after social stress in rainbow trout and brown trout. *Physiol. Biochem. Zool.* **74**, 383–389.

Sloman, K. A., Montpetit, C. J. and Gilmour, K. M. (2002a). Modulation of catecholamine

release and cortisol secretion by social interactions in the rainbow trout, Oncorhynchus mykiss. *Gen. Comp. Endocrinol.* **127**, 136–146.

Sloman, K. A., Wilson, L., Freel, J. A., Taylor, A. C., Metcalfe, N. B. and Gilmour, K. M. (2002b). The effects of increased flow rates on linear dominance hierarchies and physiological function in brown trout, Salmo trutta. *Can. J. Zool.* **80**, 1221–1227.

Sloman, K. A., McDonald, M. D., Barimo, J. F., Lepage, O., Winberg, S., Wood, C. M. and Walsh, P. J. (2005). Does pulsatile urea excretion serve as a social signal in the gulf toadfish Opsanus beta? *Physiol. Biochem. Zool.* **78**, 724–735.

Sørensen, C., Nilsson, G. E., Summers, C. H., Overli, O., Sorensen, C., Nilsson, G. E., Summers, C. H. and Overli, O. (2011). Social stress reduces forebrain cell proliferation in rainbow trout (Oncorhynchus mykiss). *Behav. Brain Res.*

Sørensen, C., Johansen, I. B. and Øverli, Ø. (2013). Physiology of Social Stress in Fishes. In *The Physiology of Fishes, Fourth Edition*, pp. 288–326. CRC Press.

Stankiewicz, A. M., Swiergiel, A. H. and Lisowski, P. (2013). Epigenetics of stress adaptations in the brain. *Brain Res. Bull.* **98**, 76–92.

Sterrenburg, L., Gaszner, B., Boerrigter, J., Santbergen, L., Bramini, M., Elliott, E., Chen, A., Peeters, B. W. M. M., Roubos, E. W. and Kozicz, T. (2011). Chronic stress induces sex-specific alterations in methylation and expression of corticotropin-releasing factor gene in the rat. *PLoS One* **6**, 1–14.

Stocco, D. M. (2000). The role of the StAR protein in steroidogenesis: Challenges for the future. *J. Endocrinol.* **164**, 247–253.

Stringer, G. and Hoar, W. (1955). Aggressive behaviour of underyearling kamloops trout. *Can. J. Zool.* **33**, 148–160.

Sturm, A., Bury, N., Dengreville, L., Fagart, J., Flouriot, G., Rafestin-Oblin, M. E. and Prunet, P. (2005). 11-Deoxycorticosterone is a potent agonist of the rainbow trout (Oncorhynchus mykiss) mineralocorticoid receptor. *Endocrinology* **146**, 47–55.

Takahashi, H. and Sakamoto, T. (2013). The role of "mineralocorticoids" in teleost fish: Relative importance of glucocorticoid signaling in the osmoregulation and "central" actions of mineralocorticoid receptor. *Gen. Comp. Endocrinol.* **181**, 223–228.

Takei, Y. and Hwang, P. P. (2016). Homeostatic Responses to Osmotic Stress. In *Fish Physiology Vol. 35 Biology of Stress in Fish*, pp. 207–249. Elsevier Inc.

Taylor, S. C. and Posch, A. (2014). The Design of a Quantitative Western Blot Experiment, The Design of a Quantitative Western Blot Experiment. *Biomed Res. Int.* **2014**, e361590.

Tea, J., Alderman, S. L. and Gilmour, K. M. (2019). Social stress increases plasma cortisol and reduces forebrain cell proliferation in subordinate male zebrafish (Danio rerio). *J. Exp. Biol.* **222**, jeb194894.

Teitsma, C. A., Anglade, I., Lethimonier, C., Le Dréan, G., Saligaut, D., Ducouret, B. and Kah, O. (1999). Glucocorticoid receptor immunoreactivity in neurons and pituitary cells implicated in reproductive functions in rainbow trout: a double immunohistochemical study. *Biol. Reprod.* **60**, 642–650.

Teles, M., Tridico, R., Callol, A., Fierro-Castro, C. and Tort, L. (2013). Differential expression of the corticosteroid receptors GR1, GR2 and MR in rainbow trout organs with

slow release cortisol implants. *Comp. Biochem. Physiol. - A Mol. Integr. Physiol.* **164**, 506–511.

Tokarz, J., Norton, W., Möller, G., Hrabé de Angelis, M., Adamski, J., Hrabe, M. and Mo, G. (2013). Zebrafish 20β-hydroxysteroid dehydrogenase type 2 is important for glucocorticoid catabolism in stress response. *PLoS One* **8**, e54851.

Tokarz, J., Möller, G., Hrabé de Angelis, M. and Adamski, J. (2015). Steroids in teleost fishes: A functional point of view. *Steroids* **103**, 123–144.

Truscott, B. (1979). Steroid metabolism in fish. *Gen. Comp. Endocrinol.* **38**, 196–206.

Tsachaki, M., Meyer, A., Weger, B., Kratschmar, D. V., Tokarz, J., Adamski, J., Belting, H. G., Affolter, M., Dickmeis, T. and Odermatt, A. (2017). Absence of 11-keto reduction of cortisone and 11-ketotestosterone in the model organism zebrafish. *J. Endocrinol.* **232**, 323–335.

Tse, A. C. K., Li, J. W., Chan, T. F., Wu, R. S. S. and Lai, K. P. (2015). Hypoxia induces miR-210, leading to anti-apoptosis in ovarian follicular cells of marine medaka Oryzias melastigma. *Aquat. Toxicol.* **165**, 189–196.

Tujague, M., Saligaut, D., Teitsma, C., Kah, O., Valotaire, Y. and Ducouret, B. (1998). Rainbow Trout Glucocorticoid Receptor Overexpression in Escherichia coli: Production of Antibodies for Western Blotting and Immunohistochemistry. *Gen. Comp. Endocrinol.* **211**, 201–211.

Ulrich-Lai, Y. M., Figueiredo, H. F., Ostrander, M. M., Choi, D. C., Engeland, W. C. and Herman, J. P. (2006). Chronic stress induces adrenal hyperplasia and hypertrophy in a

subregion-specific manner. *Am. J. Physiol. Endocrinol. Metab.* **291**, 965–973.

Urs, A. N., Dammer, E., Kelly, S., Wang, E., Merrill, A. H. and Sewer, M. B. (2007). Steroidogenic factor-1 is a sphingolipid binding protein. *Mol. Cell. Endocrinol.* **265**–**266**, 174–178.

Val, P., Lefrançois-Martinez, A. M., Veyssière, G. and Martinez, A. (2003). SF-1 a key player in the development and differentiation of steroidogenic tissues. *Nucl. Recept.* **1**, 1–23.

Valen, R., Jordal, A. E. O., Murashita, K. and Rønnestad, I. (2011). Postprandial effects on appetite-related neuropeptide expression in the brain of Atlantic salmon, Salmo salar. *Gen. Comp. Endocrinol.* **171**, 359–366.

Vijayan, M. M. and Leatherland, J. F. (1990). High stocking density affects cortisol secretion and tissue distribution in brook charr, Salvelinus fontinalis. *J. Endocrinol.* **124**, 311–318.

Vijayan, M. M. and Moon, T. W. (1994). The stress response and the plasma disappearance of corticosteroid and glucose in a marine teleost, the sea raven. *Can. J. Zool.* **72**, 379–386.

Vijayan, M. M., Aluru, N. and Leatherland, J. F. (2010). Stress Response and the Role of Cortisol. In *Fish Diseases and Disorders Vol. 2: Non-infectious Disorders*, pp. 182–201. CAB International.

Volff, J.-N. (2005). Genome evolution and biodiversity in teleost fish. *Heredity (Edinb).* **94**, 280–294.

Von Hofsten, J., Karlsson, J. and Olsson, P. E. (2003). Fushi tarazu factor-1 mRNA and protein is expressed in steroidogenic and cholesterol metabolising tissues during different

life stages in Arctic char (Salvelinus alpinus). *Gen. Comp. Endocrinol.* **132**, 96–102.

Weaver, I. C. G., Cervoni, N., Champagne, F. A., D'Alessio, A. C., Sharma, S., Seckl, J. R., Dymov, S., Szyf, M. and Meaney, M. J. (2004). Epigenetic programming by maternal behavior. *Nat. Neurosci.* **7**, 847–54.

Wei, Z. X., Xie, G. J., Mao, X., Zou, X. P., Liao, Y. J., Liu, Q. S., Wang, H. and Cheng, Y. (2020). Exosomes from patients with major depression cause depressive-like behaviors in mice with involvement of miR-139-5p-regulated neurogenesis. *Neuropsychopharmacology* **45**, 1050–1058.

Wendelaar Bonga, S. E. (1997). The Stress Response in Fish. *Physiol. Rev.* **77**, 591–625.

Wheeler, B. M., Heimberg, A. M., Moy, V. N., Sperling, E. A., Holstein, T. W., Heber, S. and Peterson, K. J. (2009). The deep evolution of metazoan microRNAs. *Evol. Dev.* **11**, 50–68.

Wilfred, B. R., Wang, W. X. and Nelson, P. T. (2007). Energizing miRNA research: A review of the role of miRNAs in lipid metabolism, with a prediction that miR-103/107 regulates human metabolic pathways. *Mol. Genet. Metab.* **91**, 209–217.

Wilkinson, M. E., Charenton, C. and Nagai, K. (2020). RNA Splicing by the Spliceosome. *Annu. Rev. Biochem.* **89**, 359–388.

Williams, T. and Bernier, N. (2017). CRF and urocortin 3 protect the heart from hypoxia/reoxygenation-induced apoptosis in zebrafish. *Am. J. Physiol. Regul. Integr. Comp. Physiol.* **313**, 1–5.

Wilson, J. M., Vijayan, M. M., Kennedy, C. J., Iwama, G. K. and Moon, T. W. (1998). beta-

Naphthoflavone abolishes interrenal sensitivity to ACTH stimulation in rainbow trout. *J. Endocrinol.* **157**, 63–70.

Winberg, S. and Lepage, O. (1998). Elevation of brain 5-HT activity, POMC expression, and plasma cortisol in socially subordinate rainbow trout. *Am. J. Physiol.* **274**, R645–R654.

Winberg, S. and Nilsson, G. E. (1993). Roles of brain monoamine neurotransmitters in agonistic behaviour and stress reactions, with particular reference to fish. *Comp. Biochem. Physiol. - C Pharmacol. Toxicol. Endocrinol.* **106**, 597–614.

Winberg, S., Höglund, E. and Øverli, Ø. (2016). Variation in the Neuroendocrine Stress Response. In *Fish Physiology Vol. 35 Biology of Stress in Fish*, pp. 35–74. Elsevier Inc.

Winter, J., Jung, S., Keller, S., Gregory, R. I. and Diederichs, S. (2009). Many roads to maturity: microRNA biogenesis pathways and their regulation. *Nat. Cell Biol.* **11**, 228–234.

Wood, S. K., McFadden, K. V., Grigoriadis, D., Bhatnagar, S. and Valentino, R. J. (2012). Depressive and cardiovascular disease comorbidity in a rat model of social stress: A putative role for corticotropin-releasing factor. *Psychopharmacology (Berl).* **222**, 325–336.

Wunderink, Y. S., Engels, S., Halm, S., Yúfera, M., Martínez-Rodríguez, G., Flik, G., Klaren, P. H. M. and Mancera, J. M. (2011). Chronic and acute stress responses in Senegalese sole (Solea senegalensis): The involvement of cortisol, CRH and CRH-BP. *Gen. Comp. Endocrinol.* **171**, 203–210.

Zannas, A. and West, A. (2014). Epigenetics and the regulation of stress vulnerability and resilience. *Neuroscience* **264**, 157–170.

Ziv, L., Muto, A., Schoonheim, P. J., Meijsing, S. H., Strasser, D., Ingraham, H. A., Schaaf,

M. J. M., Yamamoto, K. R. and Baier, H. (2012). An affective disorder in zebrafish with mutation of the glucocorticoid receptor. *Mol. Psychiatry* **2012**, 1–11.

Zou, H., Shi, M., He, F., Guan, C. and Lu, W. (2021). Expression of corticotropin releasing hormone in olive flounder (Paralichthys olivaceus) and its transcriptional regulation by c-Fos and the methylation of promoter. *Comp. Biochem. Physiol. Part - B Biochem. Mol. Biol.* **251**, 110523.